UNIVERSITY OF CALIFORNIA,
IRVINE

Regulation of Regenerative Responses by Factors in the Extracellular Matrix during Axolotl (*Ambystoma mexicanum*) Limb Regeneration

DISSERTATION

submitted in partial satisfaction of the requirements
for the degree of

DOCTOR OF PHILOSOPHY

in Biological Sciences

by

Anne Quy Phan

Dissertation Committee:
Professor David M. Gardiner, Chair
Professor Susan V. Bryant
Professor Marian L. Waterman
Professor Thomas F. Schilling
Associate Professor Rahul Warrior

2014

DEDICATION

This dissertation is dedicated to my family.

To my mother, Nu Iris Dinh, who fought vehemently against the notion that educating a female is not equivalent to pouring good wine into your best shoes.

To my father, Bao Quy Phan who has instilled a value of intelligence, and plotted and worked to ensure I had the highest probability of developing intellect.

To my sister, April Ai Han Phan, who learned at a very early age how to aspirate cancer cells, while other kids got to play outside.

To my brothers, Andy Khai Phan and Dat Hy Phan, who always made it a challenge to keep it up academically. I am always proud to call you family.

To the Phan clan who always accepted and supported their ‘mad scientist’ cousin.

To the Dinh family, it is an honor.

To the Frys and Hamils, thank you for welcoming me and being my family away from home.

To Alexander Hamil, I would not be anywhere without you.

TABLE OF CONTENTS

LIST OF FIGURES

LIST OF TABLES

ACKNOWLEDGEMENTS

David M. Gardiner my mentor in research has guided and supported me through my transformation into a scientist. I could not have imagined a more supportive, open, enthusiastic, and encouraging mentor. Dave was always willing to go where the science (and I) led us, whether into mammals or to a glycobiology conference. There will never be another PI like you.

Susan V. Bryant, our co-PI in the lab, always had her door open for questions, ideas, advice and suggestions so I always had twice the mentorship and support.

My doctoral committee members: Thomas Schilling, Rahul Warrior, and Marian Waterman were committed to my growth and success. They gave extensive feedback and guidance inside and outside of committee meetings. Your investment in me was greatly appreciated and I hope to pay it back as a colleague.

Gardiner laboratory members past and present have all contributed in their own way. Gillian Cummings, the master surgeon under whom I apprenticed. Veronica Aguilar, Kimberly Lank, Ryan Lank, Danielle Leone, Evan Lister, Crystal Shimauchi and countless undergraduate workers who kept the lab running. My fellow graduate students, Jeffrey Lehrberg and Cristian Aguilar who journeyed with me. The postdocs who took their time to share their knowledge and experience, Catherine McCusker, Jason Lee, and Katrina Llewellyn. I will never forget Henrik Lauridsen's passion and enthusiasm for science, nor his amazing surgical skills. Jim Mondo, Warren Vieira, and Don Ferris always kept lab interesting.

My numerous but unique undergraduate research mentees who all contributed to the science, and helped me grow into an experienced mentor: Ekaterina Perminov, Andrew Dinh, Caitlyn Hwe, Michelle Oei, Craig Flath, Cynthia Shu, Tiffany Vu and Rachele Mariano.

The Ken Cho laboratory, including Rebekah Le, William Chu, Mui Luong, Kitt Paraiso, Anna Javier, Soledad Mochel, Jin Cho, provided access to a surgical camera and qPCR machine as well as friendship, snacks and comradery.

My collaborators: Maksim Plikus and Raul Ramos, Jennifer Simkin and Ken Muneoka, Roger Lawrence and Jeffrey Esko who all provided expertise, materials, and advice.

And of course, Alexander Hamil, who supported me in every way possible including but not limited to: helping change animals, making Holtfreter's, bouncing experimental ideas, reading and correcting my proposals and manuscripts, sitting through all my practice talks. I honestly do not know how you do it all.

CURRICULUM VITAE

Anne Quy Phan
Laboratory of D.M. Gardiner & S.V. Bryant
University of California, Irvine
Developmental and Cell Biology

Education

Doctor of Philosophy in Biological Sciences — University of California, Irvine
Graduated: Summer 2014 — Developmental & Cell Biology

Bachelor of Science: Biological Sciences, Molecular Biology — San Jose State University
Minors: Mathematics, Chemistry
Graduated: Winter 2007

Honors and Awards

2013 - 2014	TLTC Pedagogical Fellow	University of California, Irvine
2013	Edward Steinhaus Teaching Award	University of California, Irvine
2009 - 2012	HHMI-UCI Graduate Teaching Fellow	University of California, Irvine
2008	Center for Virus Research Summer Trainee	University of California, Irvine
2007	Dean's Scholar	San Jose State University

Research Experience

2009 – 2014 — University of California, Irvine
Principal Investigator: David M. Gardiner — **Doctoral Student**
Discovered the role of heparan sulfates of the ECM to mediate positional information by regulating growth factor signaling to induce limb patterning during salamander limb regeneration
Conservation of the role of heparan sulfate in mammalian ECM to regulate growth and pattern during regeneration
Development of exogenous mammalian factors to synthetically induce limb regeneration

Winter 2009 — University of California, Irvine
Principal Investigator: Andrej Luptak — **Rotating Graduate Student**
Determine biological activity of human ribozyme located in intron of CPEB3 gene to understand biological role of CPEB3 ribozyme and possibly other ribozymes

Fall 2008 — University of California, Irvine
Principal Investigator: Charles Glabe — **Rotating Graduate Student**
Real-time visualization of aggregation and localization of Amyloid β in neurons to determine cytotoxic form and mechanism of cytotoxicity in development of Alzheimer's Disease

Summer 2008 — University of California, Irvine
Principal Investigator: Hung Fan — **Rotating Graduate Student**
Optimization of Ligation-Dependent PCR assay for detection of low copy number virus XMRV in patient samples to determine prevalence and role in the development of prostate cancer

2008 — University of California, San Francisco
Principal Investigator: Gabrielle Bergers — **Intern**
Discover down stream signaling targets of VEGF and HIF in mouse glioblastoma model and their effects on cell migration and angiogenesis

2007 San Jose State University
Principal Investigator: J. Brandon White **Undergraduate Researcher**
Ascertain effect of Bioactive compounds: Apigenin, Curcumin, DAPT, EGCG, and Genistein on cell growth, viability, and Notch signaling pathway in human breast cancer cells

Publications

Anne Q. Phan, Jangwoo Lee, Michelle Oei, Craig Flath, Caitlyn Hwe, Rachele Mariano, Tiffany Vu, Cynthia Shu, Andrew Dinh, Ken Muneoka, Susan V. Bryant and David M. Gardiner. Heparan sulfates mediate positional information by regulating growth factor signaling in axolotl (*Ambystoma mexicanum*) limb regeneration. (*in revision*) (2014).

Catherine D. McCusker, Anne Q. Phan, David M. Gardiner. Tissue-specific induction of growth and pattern during ectopic limb regeneration in *Ambystoma mexicanum. (in preparation)* (2014).

Lectures and Conferences

2014 San Diego Glycobiology Symposium: Poster Presenter
2013 Frontiers in Stems Cells & Regeneration: Invited Speaker
2013 San Diego Glycobiology Symposium: Speaker
2013 UC Irvine Developmental & Cell Biology Department Retreat: Poster Presenter
2012 San Diego Glycobiology Symposium: Participant
2011 UC Irvine Developmental & Cell Biology Department Retreat: Poster Presenter
2011 West Coast Developmental Biology Meeting: Poster Presenter
2009 Future of Science Conference: Workshop Leader
2009 UC Irvine Developmental & Cell Biology Department Retreat: Poster Presenter
2009 DARPA Restorative Injury Repair (RIR)/MURI Workshop: Participant
2008 CSU Biotechnology Symposium: Participant & Volunteer

Teaching Experience

Summer 2009 – Present University of California Irvine
Biological Sciences 199: Undergraduate Research **Graduate Student Mentor**
Independent Study in Biological Sciences Research: Train, mentor and direct individual experimental laboratory undergraduate research. Guide students through undergraduate education to future careers

Mentees

2013 – 2014 Andrew Dinh
2012 – 2013 Sunit Shah, Currently: UCI Medical Center
2011 – 2013 Michelle Oei, Currently: USC, School of Pharmacy
2012 – 2013 Caitlyn Hwe, Currently: UC Davis, School of Veterinary Medicine
2010 – 2012 Craig Flath, Currently: Vanderbilt University, School of Medicine
2010 – 2011 Dawoud Abdulmalek: UCLA
2009 – 2010 Rachele Mariano, Currently: UCLA, School of Dentistry
2009 – 2010 Tiffany Vu, Currently: Western University, College of Dental Medicine
2009 – 2010 Cynthia Shu, Currently: UCLA, Access/BSP

Spring 2014 University of California, Irvine
Biological Sciences D140: How to Read a Science Paper
Upper division course integrating seminars, journal club and class discussions developed to train undergraduate researchers how to read and critically evaluate primary scientific literature
Course Developer/Instructor of Record: Create and develop all course materials, obtain course approval from department and school, coordinate all logistics for course set up, sole instructor

2013 – 2014 University of California, Irvine
TA Professional Development Program
Series of discipline-specific interactive workshops designed to provide new TAs with skills and information that will help them begin their new instructional careers.
Pedagogical Fellow: Mentor new graduate student TAs through department and teaching. After receiving advanced pedagogical training, develop and lead a series of discipline-specific TA training workshops such as: Enhancing Student Learning, Balancing Teaching & Research, Effective Exam Writing, FERPA Regulations, TA Roles & Responsibilities

Summer 2013 Marine Biological Laboratory, Woods Hole, MA
Frontiers in Stem Cells and Regeneration
NIH-sponsored course for advanced researchers seeking comprehensive and sophisticated training in research strategies & approaches for advancing stem cell and regeneration research.
Laboratory TA: Develop lab exercise, manage logistics of lab setup, give lab introduction and directions, conduct lab exercise, and ensure health and welfare of experimental animals

Fall 2009, 2010*, 2012 University of California, Irvine
Biological Sciences 93: DNA to Organisms
Introductory biology course, first course of core curriculum for biology majors
Discussion Leader: Design materials focused on active learning and group work for 3 sections of 30 students, lead discussion, grade, gradebook and website, assist in creating lecture exams
***Head TA:** In addition to my own 3 sections, assign and manage 10 other discussion leaders for 2 sections of 500 students, mentor new discussion leaders, liaison between professor and TAs

Winter 2012 University of California, Irvine
Biological Sciences D104: Developmental Biology
Upper division course with emphasis on key processes of development and regeneration
Administrative TA: Mange all administrative duties for 2 sections of 250 students including gradebook, website, exams, message board, emails, course materials, student concerns

Professional Development

2013-2014	TLTC Pedagogical Fellow Program
2013	Becoming an Effective Mentor Workshop
2009-2012	HHMI-UCI Professor Program – *In Situ* Discussion Leader Training
2009	TLTC TA Professional Development Program

Professional Activities & Service

2013	Graduate Student Seminar Speaker Search Committee	University of California, Irvine
2013	Graduate Student Rep on Faculty Search Committee	University of California, Irvine
2007	College of Science Dean's Student Advisory Board	San Jose State University

Community Outreach & Service

2012 – 2014	Intel International Science and Engineering Qualifying Fair – Organizer
2009 – 2014	Intel International Science and Engineering Qualifying Fair – Judge
2010	Pacific Links Foundation: ADAPT Benefit to Stop Human Trafficking – Organizer
2010	Cornelia Connelly School Science Fair – Judge
2009 – 2011	Orange County Science and Engineering Fair – Judge
2009 – 2010	Orange County Science and Engineering Fair Workshop – Mentor
1997 – 2003	St. Patrick's Vietnamese Catholic Association – Vietnamese Teacher

ABSTRACT OF THE DISSERTATION

Regulation of Regenerative Responses by Factors in the Extracellular Matrix during Axolotl (*Ambystoma mexicanum*) Limb Regeneration

by

Anne Q. Phan

Doctor of Philosophy in the Biological Sciences
University of California, Irvine, 2014
Professor David M. Gardiner

Salamanders are unique among adult vertebrates in their ability to regenerate complex body structures after traumatic injury. Axolotl limb regeneration is a stepwise sequence of three requisite processes: (1) scarless wound healing to generate a regenerative wound epithelium, (2) blastema formation by migration, proliferation and dedifferentiation to create a mass of multipotent regeneration-competent progenitor cells, and (3) induction of pattern formation by interaction of cells with opposing positional information. The challenge to understanding how to induce and enhance regenerative ability in humans is to discover which of these processes fail in humans and why they fail.

In axolotl regeneration, cells maintain a memory of their original position and use this 'positional information' to accurately regenerate the lost pattern. The goal of this project was to elucidate the molecular mechanism of positional information in axolotl limb regeneration and determine if it is conserved in mammals.

I used an *in vivo* gain-of-function assay for the requisite processes of axolotl limb regeneration (Accessory Limb Model) to determine the minimal components required to mediate positional information and induce *de novo* limb pattern.

I found that cell-free anterior and posterior extracellular matrix (ECM) have position-specific signaling properties that either inhibit regeneration or induce *de novo* limb pattern. The position-specific functionality of the ECM is established by differential expression of heparan sulfate sulfotransferases during regeneration resulting in position-specific growth factor regulation. My findings indicate that heparan sulfates are both necessary and sufficient to mediate positional information in axolotl limb regeneration. Similarly, mouse ECM was also capable of inducing limb pattern in a position-specific, heparan sulfate-dependent, age-dependent manner. Using mammalian-derived, commercially available factors, I synthetically induced axolotl limb regeneration, thus demonstrating that the factors required for regeneration are not salamander-specific.

This study demonstrates a specific novel mechanism for positional information in axolotl limb regeneration and establishes a crucial functional link between salamander regeneration and mammals. The ability to regulate axolotl regeneration with mammalian ECM has allowed identification of target mechanisms to induce regeneration in humans. In addition to the fields of regeneration, development, and glycobiology, this novel mechanism of positional information has implications to the fields of cancer biology and aging.

CHAPTER 1: Introduction

Regeneration

Regeneration is the process by which biological organisms maintain, renew or restore body parts that have been lost or damaged. Regeneration can be classified into different hierarchal biological levels (Figure 1.1). At the cellular level, cells can regenerate some of their structures such as the regeneration of damaged axons by neuronal cells. Tissues are also capable of regeneration, for example the epithelial tissues of the skin and gut are constantly being renewed and can be regenerated upon damage. Many organisms can repair damage to internal organs such as the heart or liver, although with variable fidelity. Some organisms (amphibians, reptiles, fish) can regenerate entire body structures after amputation. Planarians and hydra can regenerate an entirely separate organism from relatively small portions of the original body (Figure 1.1).

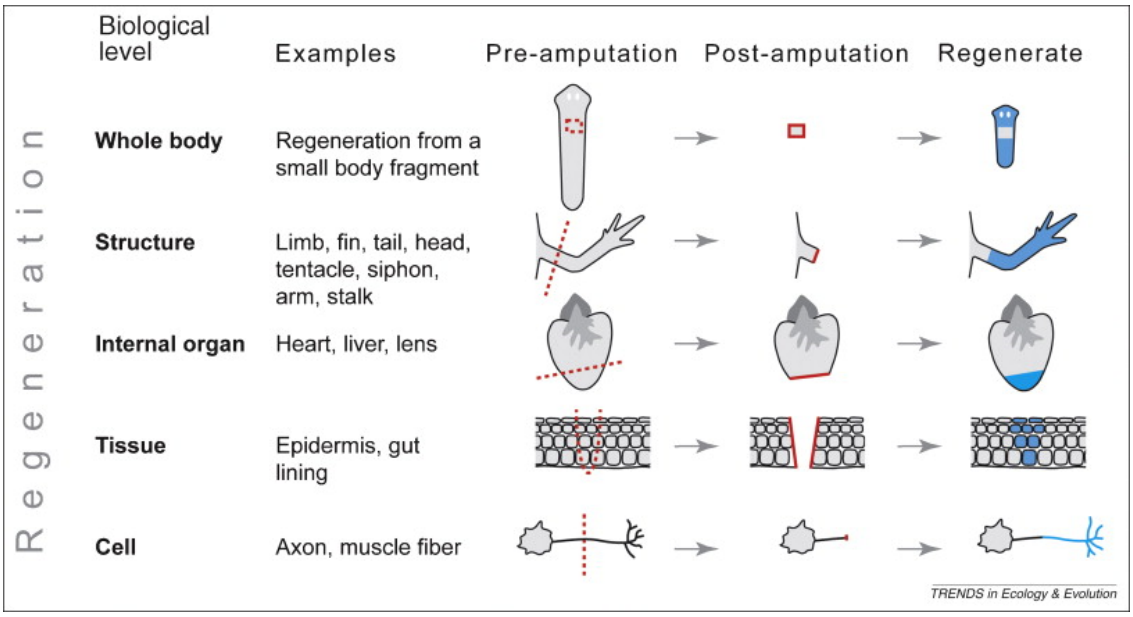

Figure 1.1. Regeneration can occur at Different Biological Levels.
Some organisms can regenerate at all biological levels (hydra, planarian). Salamanders can regenerate structures (limbs), whereas mammals seem to be limited to partial internal organ regeneration. Dashed red lines indicate amputation planes; solid red lines indicate wound surfaces; and blue fill indicates regenerated body parts. (Bely and Nyberg, 2010)

The earliest documented experimental studies of regeneration began with Abraham Trembly with hydra in the 1700s (Morgan, 1901). Since then, the experimental study of regeneration has expanded to a range of organisms with variable abilities to regenerate including but not limited to worms, lampreys, fish, lizards, salamanders frogs, and mice.

There have been many recent advances in our understanding of regeneration, Lineage-restricted cells contribute to regeneration in salamanders (Kragl et al., 2009) frogs (Gargioli and Slack, 2004), zebrafish (Stewart and Stankunas, 2012), and mice (Rinkevich et al., 2011). Molecules have been identified that may be responsible for nerve dependence and can induce or rescue regeneration (Kumar et al., 2007a, 2011; Makanae et al., 2013; Yu et al., 2012). The previously conceived limits of mammalian regenerative ability have been expanded (Ito et al., 2007; Muneoka et al., 2008a; Seifert et al., 2012a). There are now novel insights from zebrafish into mechanisms on how regenerative ability may be lost during evolution (Kang et al., 2013; Nachtrab et al., 2011)

Although the term ‘regeneration’ is used for diverse phenomena, each may have arisen independently, proceed through nonhomologous mechanisms, and result in variable fidelity. The elaborate hierarchy and classification of regeneration encompasses disparate views.

Physiological regeneration refers to cyclic replacement of tissues such as blood, hair or deer antlers. Regeneration in response to traumatic injury such as amputation can be through two modes: epimorphosis or morphallaxis (Morgan, 1901). Epimorphosis involves the migration, proliferation and dedifferentiation of adult cells at

the site of injury to form a blastema, a mass of multipotent progenitor cells that eventually redifferentiatiate to create the missing body part. Relative organism size is maintained during epimorphic regeneration. During morphallaxis, all the remaining cells of the organism reorganize to reconstruct a complete but smaller animal (Agata et al., 2007; Gilbert, 2013; Figure 1.2).

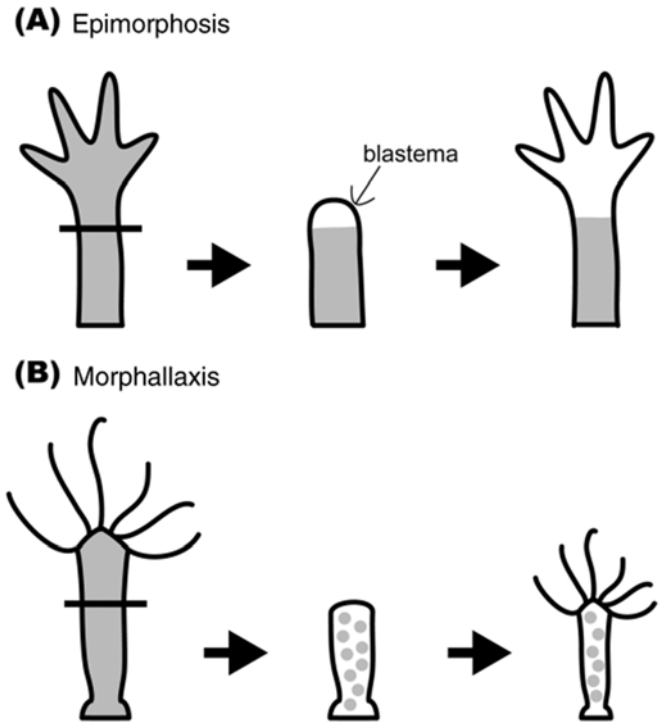

Figure 1.2. Epimorphosis and Morphallaxis Modes of Regeneration. (A) Salamander Limb Regeneration, as an example of epimorphosis, involves formation of a blastema, a mass of undifferentiated cells. The blastema grows to eventually recreate the lost portion of the limb. (B) Hydra Regeneration, as an example of morphallaxis, involves direct remodeling of remaining cells to recreate a complete organism. (Agata et al., 2007)

In mammals, hypertrophy may be considered a type of regeneration where there is a compensatory increase in size in response to organ damage or removal (liver, kidneys) (Gilbert, 2013). However, hypertrophy may restore metabolic function but it does not result in restoration of the original pattern and structure. This is often referred to as compensatory regeneration (Hata et al., 2007).

Regeneration can be also classified as complete, after which the organism has healed scar-free, or incomplete, after which there is fibrosis and scarring.

As considered in this dissertation, regeneration is initiated specifically by an unpredictable sublethal injury that severs a piece of the body, leaving a wounded, multicellular stump. To prevent complications, for the remainder of this dissertation, I will focus on a model of complete epimorphic regeneration, salamander limb regeneration.

Axolotl Limb Regeneration

With the rapid advancement of stem cell biology and the development of induced-pluripotent cells (iPS), one of the major hurdles of regenerative medicine is understanding how to coordinate and organize these competent cells to regenerate complex functioning pattern. Salamander limb regeneration is a model system in which complex pattern regeneration can be studied.

Birds cannot regenerate limbs at any stage of development. Mammals have slightly better regenerative ability compared to birds. Mice can regenerate digit tips amputated through the most distal phalanx (Borgens, 1982; Reginelli et al., 1995). Similar digit tip regeneration occurs in humans (Douglas, 1972; Illingworth, 1974). Frogs have intermediate ability to regenerate limbs. Hindlimb buds can regenerate completely but regenerative capacity declines as metamorphosis proceeds (Beck et al., 2009; Dent, 1962; Muneoka et al., 1986; Suzuki et al., 2006)

Salamanders are unique among adult vertebrates in their ability to regenerate complex body structures after traumatic injury. The Mexican salamander (*Ambystoma mexicanum*), referred to as the axolotl, is a powerful model for limb regeneration because it can regenerate exactly what was lost following amputation, and it does not

form scars. Axolotl limb regeneration occurs through 3 required steps: 1) wound healing, 2) blastema formation (dedifferentiation), and 3) pattern formation (redifferentiation) (Figure 1.3).

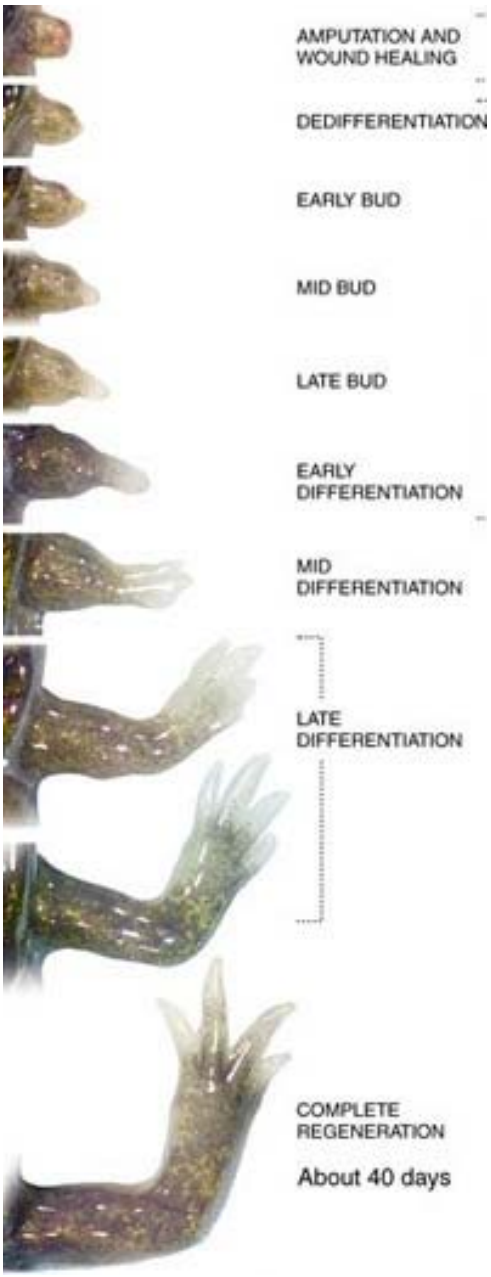

Figure 1.3. Stages of Axolotl Limb Regeneration. (Images by D.M.Gardiner)

After amputation, the keratinocytes migrate to close the wound and create a specialized tissue known as the wound epithelium (Campbell and Crews, 2008; Ferris et al., 2010; Shimokawa et al., 2012). This specialized wound epithelium is required for regeneration. If a wound is allowed to close without formation of a wound epithelium, there will not be a regenerative response (Mescher, 1976; Shimokawa et al., 2012).

After wound healing, the wound epithelium (WE) interacts with the end of the nerve to induce neurotrophic signaling between the nerve and WE. The signaling results in a thickened apical epithelial cap (AEC) that is functionally equivalent to the apical ectodermal ridge (AER) of a developing limb bud in the embryo (Summerbell, 1974; Thornton, 1960). In response to nerve-WE signaling, cells in the amputation stump migrate to the site of injury, proliferate, and dedifferentiate to form the mass of multipotent progenitor cells known as the blastema. The nerve is required for regeneration to progress from wound healing to blastema formation (Peadon and Singer, 1965; Singer, 1946, 1947; Wallace, 1981).

The last step of axolotl limb regeneration is pattern formation during which the dedifferentiated blastema cells redifferentiate to reform the original pattern and structure of the injured limb. Cells of the limb retain a memory of their original position on the limb, and use this ‘positional information’ to regenerate exactly what was lost.

Much of limb regeneration research has focused on neurotrophic signaling from the nerve to induce blastema formation (Kumar et al., 2007a; Makanae et al., 2013). Mechanisms of scarless wound healing have been of interest to those within and outside the field (Denis et al., 2013; Murawala et al., 2012; Seifert et al., 2012a; Yokoyama et al., 2011). There have been some recent studies into the mechanisms of

cellular positional identity/memory/information, however these have focused on where the cells contribute to the regenerate, rather than how they induce pattern. Regenerative therapies to regenerate pattern will require pattern formation.

This dissertation will focus on how the axolotl uses positional information to accurately regenerate pattern and structure during limb regeneration.

Polar Coordinate Model of Positional Information

The Polar Coordinate Model proposes that cells have positional information in a spatial pattern around the circumference of the limb (1-12, Figure 1.4A) and along the proximal-distal axis (Figure 1.4A-E). Cells maintain memory of this positional information upon amputation and interactions between cells with different positional values in order to drive regeneration and pattern formation in the axolotl, as well as in the cockroach and fruit fly (Bryant et al., 1981; French et al., 1976).

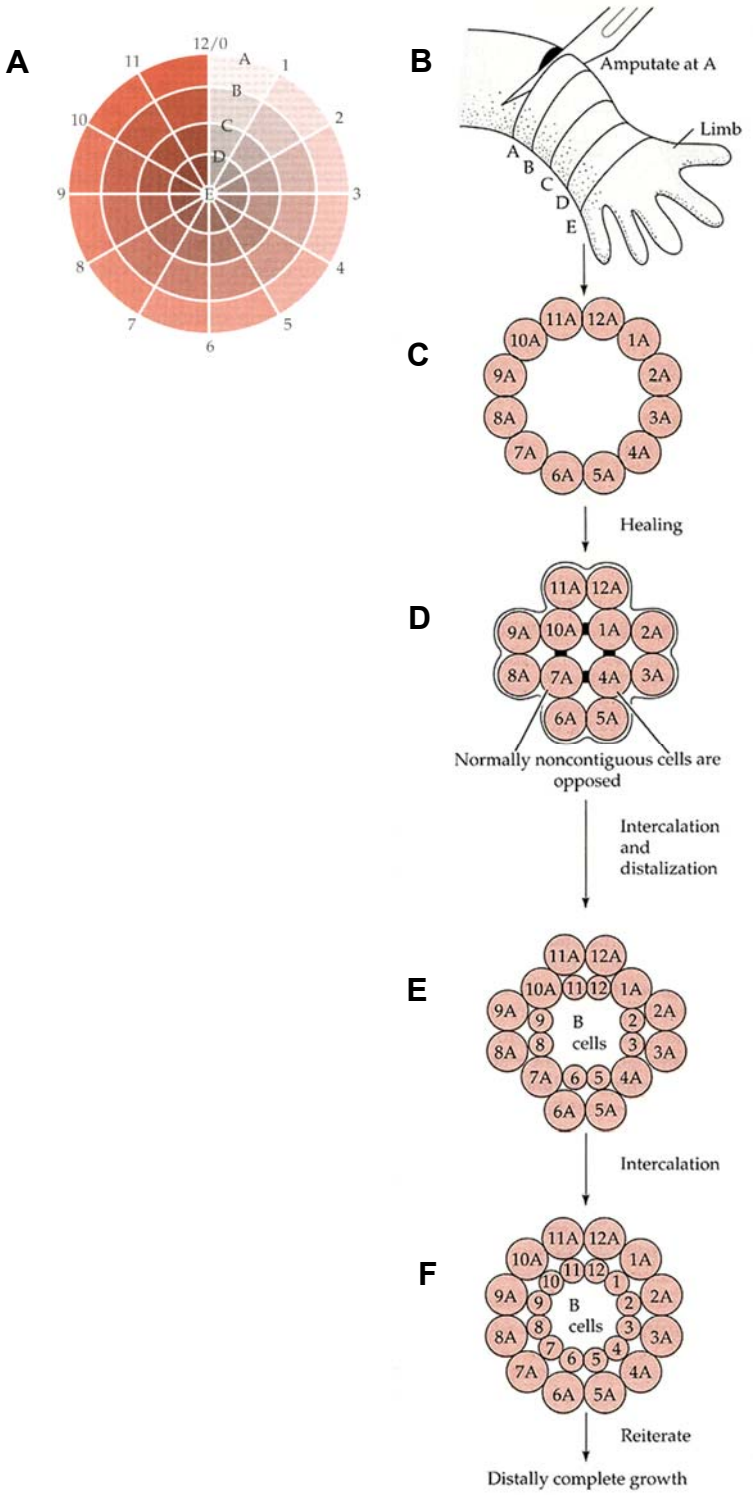

Figure 1.4. Polar Coordinate Model of Positional Information: Distal Outgrowth from Wound Surfaces. (A,B) Cells of the limb have positional information in polar coordinate 'values.' A-E across the proximal-distal axis, and 1-12 around the circumference of the limb, encompassing the anterior-posterior and dorsal-ventral axes. (B) If the limb is amputated at position A, proximal to B-E, the amputated limb stump will have exposed circumferential information at level A. (C) During wound healing, cells from opposite sides of the limb will migrate to close the wound. As a result, normally nonadjacent cells interact with each other by short-range cell-cell communication (D, 10A and 1A). The cells proliferate and intercalate the missing, intermediate circumferential values (11A and 12A) to resolve the disparity in positional values (E). Since these new cells are adjacent to A cells, by the 'distalization rule' such cells will acquire the next more distal B identity. (F) Intercalation reiterates until distal outgrowth is complete. Based on Bryant et al 1981, adapted from Gilbert 2013

According to the Polar Coordinate Model of positional information, pattern formation is induced when cells with opposing positional information interact. This was experimentally demonstrated by a series of supernumerary induction studies in the salamander limb, as well as in *Drosophila* imaginal discs and cockroach limbs (Bryant et al., 1981; French et al., 1976). In the case of a right/left limb contralateral graft (Figure 1.5A), anterior and posterior cells that are not normally adjacent to each other (Figure 1.5A-B, 3 and 9) interact to induce intercalation of the intermediate values. Therefore, at each point of anterior/posterior confrontation, an ectopic limb is induced and three limbs are regenerated (Figure 1.5C) (French et al., 1976).

Intercalary regeneration was observed with all the body axes (anterior/posterior, dorsal/ventral, proximal/distal) in fruit flies and grasshoppers in addition to salamanders (Bryant et al., 1981; French et al., 1976).

The phenomena of intercalary regeneration has also been found in planarians (Agata et al., 2003; Kato et al., 2001; Romero and Bueno, 2001), crickets (Nakamura et al., 2007), and frogs (Yokoyama et al., 2002). This model of pattern formation has become increasingly popular (Bénazet and Zeller, 2009; Kerszberg and Wolpert, 2007; Wolpert, 2011). There is evidence of a similar model of limb pattern during mouse limb development (Mariani, 2010; Mariani et al., 2008) and during incomplete in utero human regeneration (Gardiner and Holmes, 2012).

Subsequent contribution and grafting studies have identified the loose connective tissue fibroblasts as the cells that carry positional information (Bryant et al., 2002; Endo et al., 2004; Maden and Mustafa, 1982; Nacu et al., 2013; Reynolds et al., 1983; Rollman-Dinsmore and Bryant, 1984).

In addition to finding that juxtaposition of opposing positional values induces regeneration, lack of positional disparity can actually inhibit regeneration (Bryant and Baca, 1978; Carlson, 1974, 1975; Holder et al., 1980; Slack, 1980; Tank, 1978; Tank and Holder, 1978; Wigmore and Holder, 1985).

A number of possible molecular mechanisms for positional information have been proposed. Retinoic acid (RA) can convert positional identity of regeneration blastemas into more proximal/posterior/ventral values (Bryant and Gardiner, 1992; Crawford and Stocum, 1988; Kim and Stocum, 1986; Ludolph et al., 1990; Maden, 1982; McCusker et al., 2014; Pecorino et al., 1996; Romero and Bueno, 2001; Thoms and Stocum, 1984; Wanek et al., 1991). Through RA based experimental screens, Prod1 (some homology to CD59) was identified as a candidate for proximal/distal positional identity (Kumar et al., 2007b; da Silva et al., 2002). Prod1 is expressed in a proximal to distal gradient, upregulated by RA and is present at the cell surface. It has been proposed that nAG (newt anterior gradient) is a ligand for Prod1 and induces nerve-dependent blastema cell proliferation. However, proliferation does not equate to pattern formation. Manipulation of Prod1 does not induce pattern formation and intercalary regeneration. Intriguingly, the Dachous/Fat signalling pathway has been shown to be involved in leg size and shape during cricket leg regeneration through the proximal/distal axis (Bando et al., 2009). Endogenous bioelectrical networks have been proposed to store non-genetic pattering information, but it has yet to be proven with pattern induction rather than simply loss of cellular function (Levin, 2014).
However, a molecular mechanism capable of mediating positional information to induce patttern formation during intercalary regeneration has not been identified.

The goal of this project was to elucidate the molecular mechanism of positional information in axolotl limb regeneration and determine if it is conserved in mammals.

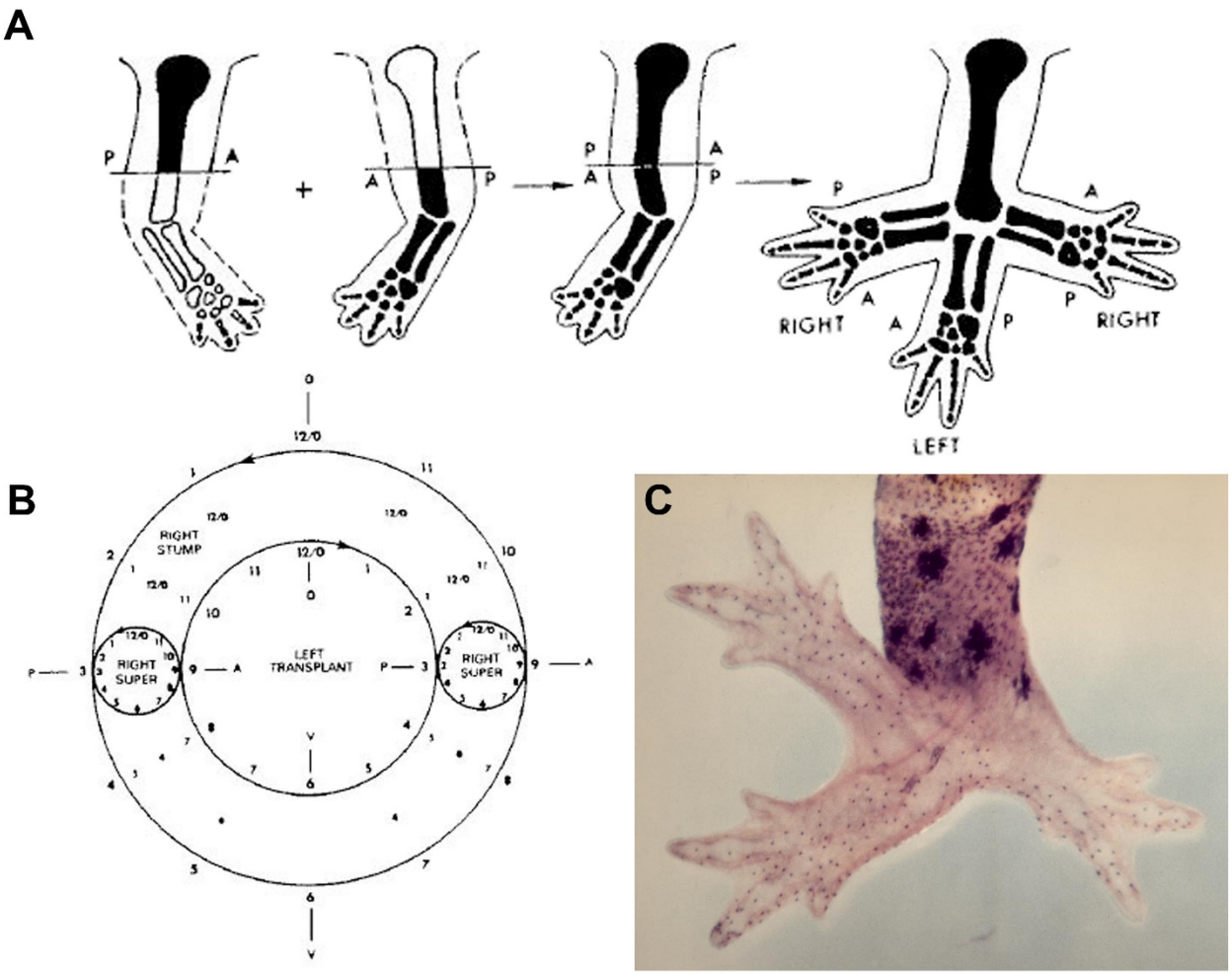

Figure 1.5. Application of the Polar Coordinate Model to the Production of Supernumerary Amphibian Limbs following Contralateral Transplantations. The Polar Coordinate Model proposes that cells have positional information based on their original position. A-C shows how short-range interaction between cells of opposing positional information can induce formation of two supernumerary limbs. (A) Experiment diagram of anterior/posterior contralateral graft inducing the formation of supernumerary limbs at each confrontation. (B) Schematic cross section of graft-host junction from a distal view in which the outer circle represents the host circumference and the inner circle represents the graft circumference. (C) Result of a left/right contralateral graft. A, Anterior; P, Posterior; D, Dorsal; V, Ventral (French et al., 1976)

Accessory Limb Model

Surgical induction of ectopic limb formation was documented by Bodemer in 1958 and expanded by later studies (Bodemer, 1958, 1959; Lheureux, 1977; Maden and Mustafa, 1982; Reynolds et al., 1983) Based on these observations, the Gardiner Lab developed a step-wise *in vivo* gain-of-function assay known as the Accessory Limb Model (ALM) to study the three requirements of limb regeneration; 1) a wound, 2) nerve signaling from a deviated nerve and 3) opposing positional information from a skin graft from the opposite side of the limb (Figure 1.5) (Endo et al., 2004). When a nerve is deviated into the wound, a symmetrical mass of multipotent cells known as a blastema forms (98% N=40) (Figure 1.6A,B). Without further signaling, the blastema regresses and is reintegrated into the arm (Figure 1.6C). If a piece of skin from the opposing side of the arm (posterior into anterior) is grafted adjacent to the deviated nerve (Figure 1.6D), then the blastema is patterned into an ectopic limb (75%, N=15) (Figure 1.6E, 1.6F). Nerve-induced ectopic limb blastemas are equivalent to amputation-induced blastemas (Satoh et al., 2007). The ALM has been adapted to Xenopus (Mitogawa et al., 2014) and other body parts (Hirata et al., 2013)and has been used repeatedly to identify regeneration specific signals during wound healing and blastema formation (Hirata et al., 2010; Makanae et al., 2013; Satoh et al., 2008a, 2010a). As the surgical technique becomes disseminated, the ALM is gaining adoption as a gain-of-function assay for the steps required for axolotl limb regeneration.

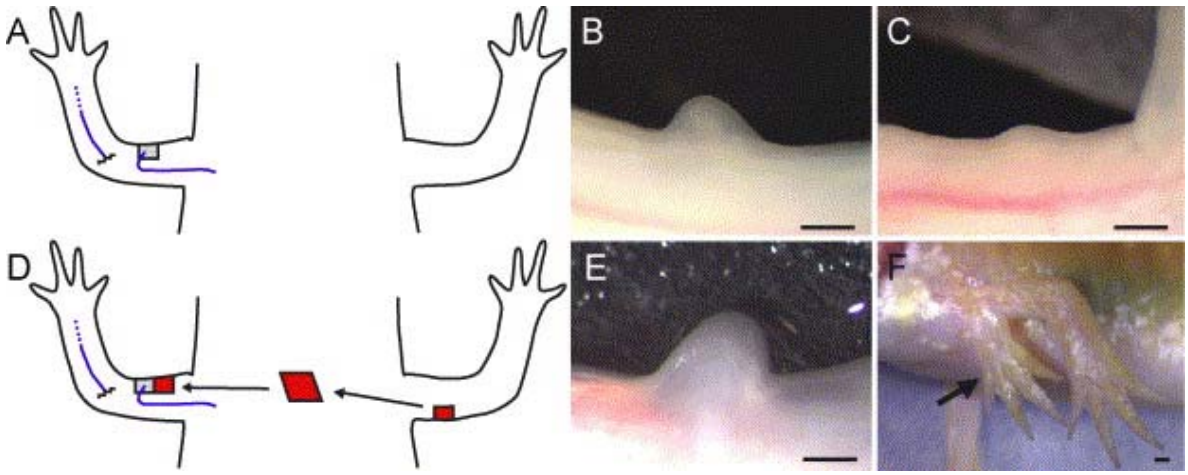

Figure 1.6. Accessory Limb Model (ALM) to Study Blastema Formation and Pattern Formation during Axolotl Limb Regeneration. (A) A nerve is surgically deviated into skin wound on the anterior of mid-stylopod. This surgery leads to the formation of an ectopic blastema (B; 13 days) that eventually regresses (C; 20 days). (D) If a piece of skin from the opposite of the limb (posterior) is grafted adjacent to the deviated nerve, a blastema is formed (E; 14 days) that continues to growth and undergo pattern formation to generate an ectopic limb (F; 5 months). (Endo et al., 2004)

This Accessory Limb Model demonstrates a contralateral skin graft is sufficient to mediate positional information and induce limb pattern formation.

It has been suggested that intercalary regeneration may be an experimentally induced phenomenon (Roensch et al., 2013) that may not be homologous with the mechanisms that occur during regeneration that is not experimentally manipulated. It seems unlikely that there would exist in one organism, two different mechanisms to illicit the same uncommon result, limb regeneration. Vastly different processes in divergent organisms often use conserved mechanisms. Regardless, the study of salamander limb regeneration using the ALM as a model of intercalary regeneration is a tool to eventually develop regenerative therapies to surgically/experimentally induce similar responses in humans.

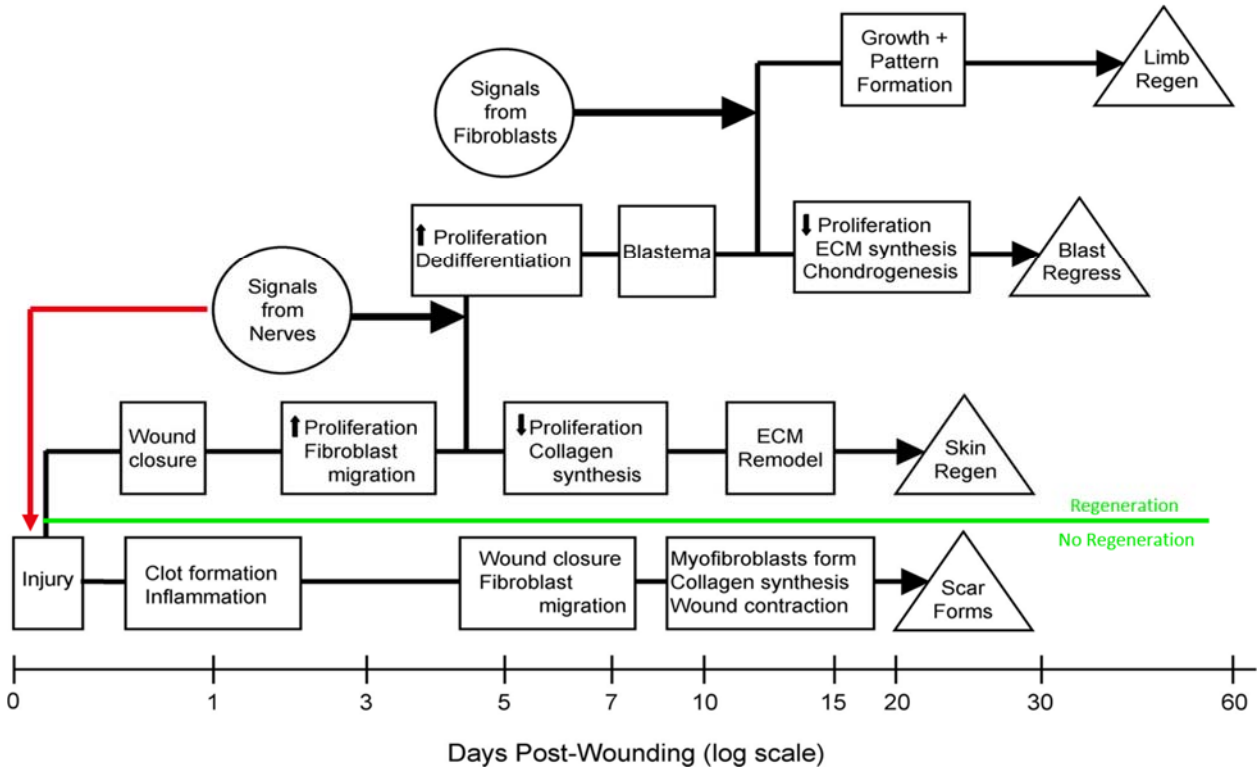

Figure 1.7. The Stepwise Model for Limb Regeneration. The points of divergence of the three developmental pathways (wound healing, blastema formation, and pattern formation) are represented by vertical lines. The stepwise experimental system allows for the parsing of the overtly complex developmental process of limb regeneration so that each part can be studied independently of the others. Regen, regeneration; Dediff; dedifferentiation; Synth, synthesis; Form; formation (Endo et al., 2004)

The ALM can be used to discover the molecular nature of positional information by assaying the ability of factors grafted into a wound with a deviated nerve (ND) to affect blastema formation and pattern formation. In this dissertation, ALM experiments in which the skin graft was experimentally substituted were conducted to determine the minimal factors required to mediate positional information and induce axolotl limb regeneration.

Heparan Sulfate Glycosaminoglycans

The skin grafts used to mediate positional information in the ALM contained cells and extracellular matrix (ECM). Studies in which posterior mouse limb bud cells were grafted into the chick limb bud suggest that ZPA signaling ability (posterior positional

information) is maintained in the ECM rather than by the cells and is mediated by heparan sulfates in the ECM (Schaller and Muneoka, 2001). Therefore, the studies that are the basis for this dissertation are focused on the ability of heparan sulfates in the ECM to mediate positional information.

Cells exist embedded in an ECM composed of fibrous proteins that provide tensile strength and elasticity (collagens, elastins), adhesive glycoproteins (fibronectin, laminin, tenascin) and proteoglycans that interact with other extracellular components. Together, the various ECM components create an instructive extracellular environment that regulates cell proliferation, migration, and differentiation, thereby dictating the physical and biological properties of cells and tissues (Esko et al., 2009).

Heparan sulfate proteoglycans (HSPGs) are a major bioactive component of the ECM that can regulate growth factor signaling by 1) sequestering growth factors in the ECM, 2) protecting growth factors against proteolysis and 3) acting as a necessary co-receptor for signaling (Esko et al., 2009; Sarrazin et al., 2011) (Figure 1.8).

HSPGs consist of a core protein with one or more covalently attached heparan sulfate chains. Heparan sulfates (HS), a type of glycosaminoglycan (GAG), are linear polysaccharide chains of repeating disaccharides of glucosamine and uronic acid. Unlike heparin that is exclusively expressed in mast cells, heparan sulfate is larger, less sulfated, and synthesized by all cell types (Esko et al., 2009).

HSPGs can be grouped by their location: membrane HSPGs (syndecans and glypicans), or extracellular HSPGs (agrin, perlecan, type XVIII collagen). Typical HS GAG chains are extensive (~40-300 sugar residues, 7–80 kD, ~20-150 nm) and therefore tend to dominate the biological activity of HSPGs. These sugar residues are

extensively modified by N-deacetylase-N-sulfotransferases (NDSTs), epimerases, and O-sulfotransferases (HS2STs, HS6STs, HS3STs) to generate unique HS fine structure (Bishop et al., 2007; Esko et al., 2009; Sarrazin et al., 2011)(Figure 1.9)

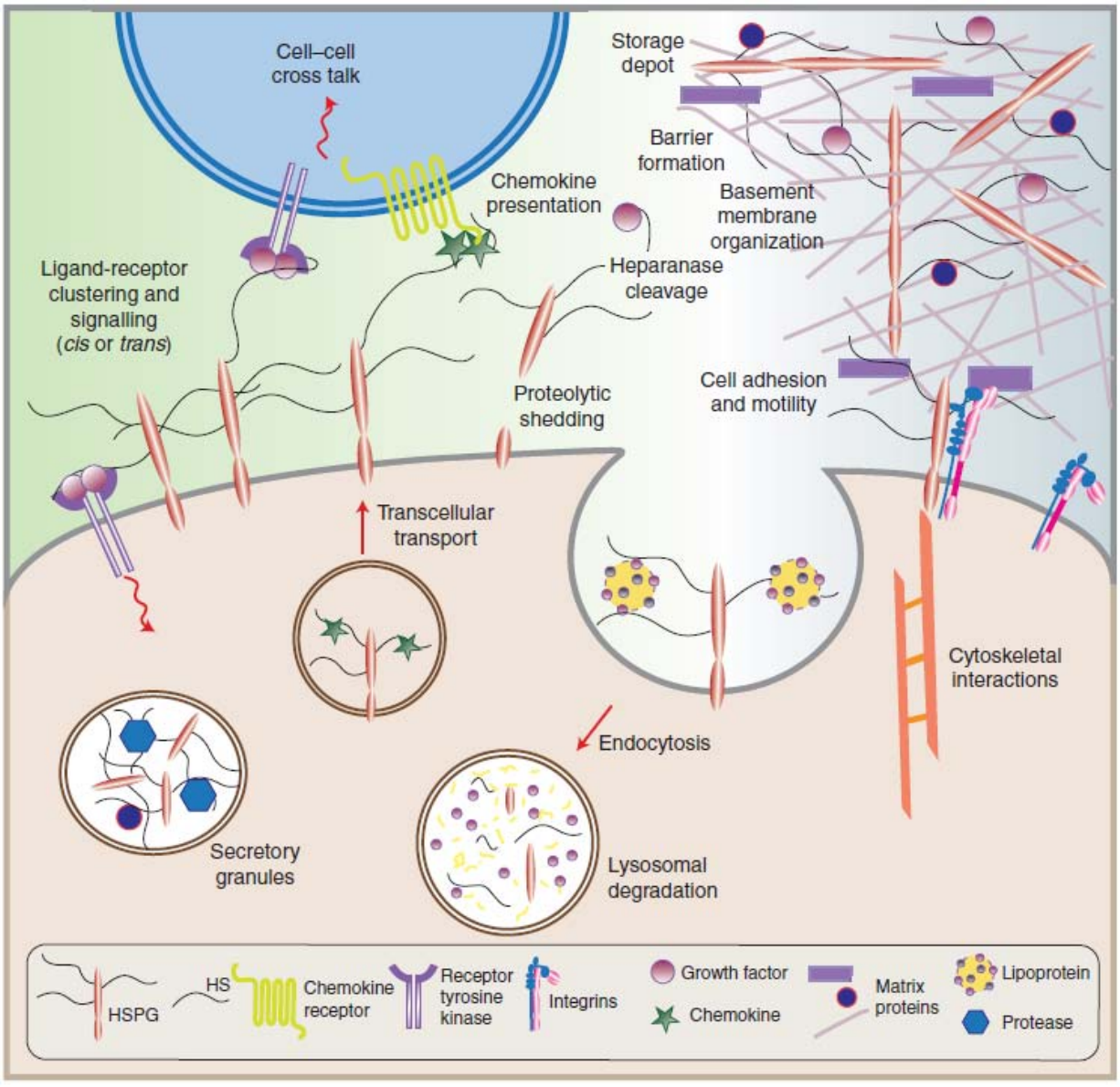

Figure 1.8. Heparan Sulfate Proteoglycans have Diverse Biological Activities (Sarrazin et al., 2011)

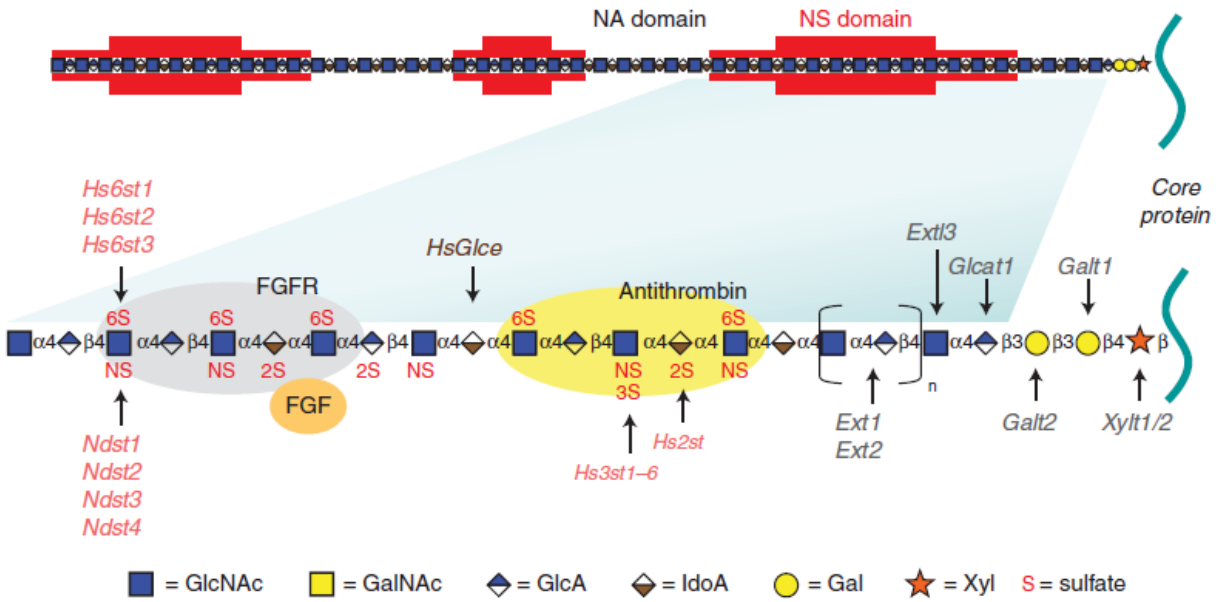

Figure 1.9. Heparan Sulfate Biosynthesis and Fine Structure. Heparan sulfate glycosaminoglycans are attached to a serine residue of the core protein by a tetrasaccharide linker. Then, alternating units of N-acetylglucosamine (GlcNAc) and glucuronic acid (GlcA) are added to generate HS. Successive modification by N-deacetylase-N-sulfotransferases (NDSTs), epimerases, and O-sulfotransferases (HS2STs, HS6STs, HS3STs) results in mature HS GAG chains. Note that not all biosynthesis occurs in a linear sequence, and some enzymes depend on the previous while others are independent. The structure can be characterized by tracts of contiguous N-acetylated disaccharide units (NA domain), contiguous N-Sulfated sequences of variable length (NS domain) and alternating N-acetylated and N-sulfated units (NA/NS domain). Regions have been implicated in binding specific ligands, e.g. FGF-1/FGF2 and antithrombin. (Sarrazin et al., 2011)

HS GAGs are amongst the most negatively charged biopolymers in nature and variations in chain number, chain length and GAG sulfation level lead to extreme diversity in chemical and biological properties. Arrangement of negatively charged sulfate groups and orientation of carboxyl groups can specify ligand binding sites (e.g. antithrombin, FGF; Figure 1.9). Additionally, clusters of sulfated residues (NS domains) are separated by non-sulfated regions rich in glucuronic acid (NA domains; Figure 1.9) (Bishop et al., 2007; Esko and Lindahl, 2001; Esko et al., 2009; Sarrazin et al., 2011). Patterns of HS GAG sulfation are more specific to cell type rather than to specific core proteins (Kato et al., 1994).

FGF Signaling in Limb Regeneration

One of the most studied signaling pathways regulated by heparan sulfates is fibroblast growth factor (FGF) signaling. FGF signaling is dependent on heparan sulfates because HS GAGs function as co-receptors to stabilize FGF/FGFR binding and prevent degradation of FGF (Olwin and Rapraeger, 1992; Yayon et al., 1991). There is heparan sulfate structural specificity for different FGFs (Guimond et al., 1993; Raman et al., 2003; Rudd et al., 2010). Knockdown of HS6ST in the chick limb bud resulted in decreased 6-O sulfation in the limb bud which resulted in reduced FGF-8 and FGF-10 expression and truncated limbs (Kobayashi et al., 2010). Therefore, there may be heparan sulfates mediating FGF signaling during axolotl limb regeneration.

FGF signaling is important in pattern formation during limb development and regeneration. FGF-10 in limb bud mesenchyme and FGF-8 in the apical epithelium of the limb bud constitute a positive feedback loop required for limb outgrowth and patterning (Lewandoski et al., 2000; Mariani, 2010; Mariani et al., 2008; Martin, 1998; Ohuchi et al., 1997; Xu et al., 1998)

Similarly, FGFs are expressed again during axolotl limb regeneration (Christensen et al., 2001; Han et al., 2001) and frog regeneration (Christen and Slack, 1997; Yokoyama et al., 2000). FGF10 can stimulate regeneration of non-regenerative frog limb buds (Yokoyama et al., 2001).

Grafting FGF1, FGF2 or FGF4 soaked beads into the flank of chick embryos induced complete ectopic limbs (Cohn et al., 1995). FGF8 is associated with anterior-posterior patterning in *Xenopus,* and is expressed during limb development and regeneration (Christen and Slack, 1997). FGF2 maintains ZPA (comparable to posterior

positional information) signaling of cultured posterior mouse limb bud cells (Anderson et al., 1993). FGF2 can convert anterior mouse limb bud cells to ZPA signaling cells in the chick limb bud (Anderson et al., 1994). FGF2 also has been shown to induce regeneration in the chick wing bud (Taylor et al., 1994).

Despite similarities between development and regeneration, an intriguing difference is the dependence of regeneration on nerve signaling. Limbs can develop normally in the absence of nerves; however, regeneration ceases if a limb is denervated before or during the early stages of regeneration (Wallace, 1981). FGF2 protein has been detected in the AEC (Apical Epithelial Cap, comparable to apical ectodermal ridge (AER) of the limb bud) and the nerves of the axolotl limb blastema (Mullen et al., 1996). Implantation of FGF2 rescues denervated medium/late bud blastemas and allows regeneration to progress to completion (Mullen et al., 1996). FGF7/KGF is expressed in axolotl nerves and induces expression of *Sp9*, a limb development marker and nerve-dependent blastema marker (Satoh et al., 2008b). FGFR1 is expressed in blastema mesenchyme (Poulin et al., 1993). KGFR (FGFR2-IIIb) and FGFR2 are expressed during regeneration in the wound epithelium and mesenchyme, respectively, with opposing dorsal ventral gradients (Poulin and Chiu, 1995). FGF1 (aFGF), FGF4, FGF8, and FGF10 have been shown to be expressed during axolotl limb regeneration (Boilly et al., 1991; Christensen et al., 2001). FGF8 is expressed in the axolotl limb blastema where it is concentrated in the anterior region of the distal mesenchyme (Han et al., 2001). Taken together, evidence demonstrates that FGF is crucial to limb regeneration and patterning. I hypothesize that regulation of FGF signaling by heparan sulfates during regeneration mediates limb pattern formation.

Regenerative Capacity of Mammals

Adult urodeles, like the axolotl, have an amazing ability to regenerate injured body structures. The ability of anurans, like *Xenopus*, to regenerate is reduced compared to the axolotl but markedly better than mammals (Tamura et al., 2010). Mammals appear to have very limited regenerative ability. In humans, a wound that crosses the basement membrane of the epidermis results in scar formation instead of functional skin tissue. Tissue repair leads to rapid and firm wound closure, but functional integrity is limited and complicated by inflammation and fibrosis (Menger et al., 2010).

However, mammals do have some regenerative capacity. Certain organs undergo a constant process of renewal (blood, hair, antlers). Some tissues undergo compensatory regeneration in response to damage or injury (liver, kidneys). The epidermis and muscle have adult cells that can be induced to repair damage (e.g. muscle satellite cells). Particular strains of mice seem to have enhanced ear healing ability (Clark et al., 1998). When cutaneous wounds are large enough, regeneration of hair can occur in adult mice, rabbits and even humans (Billingham and Russell, 1956; Breedis, 1954; Ito et al., 2007; Kligman and Strauss, 1956) . The African spiny mouse can shed the majority of its skin as a defense mechanism and regenerate it back (Seifert et al., 2012b). Human fetuses can undergo scarless cutaneous wound healing (Menger et al., 2010) . Mammals can undergo epimorphosis to regenerate digit-tips (Han et al., 2008; Muneoka et al., 2008a). Studies suggest that humans can undergo limb regeneration *in utero*, but this ability is lost as the embryo develops (Gardiner and Holmes, 2012).

In spite of the apparent differences in regenerative capacity, there are similarities between mammalian and amphibian regeneration. Cellular contribution is similar between axolotl limb regeneration and mouse digit-tip regeneration (Kragl et al., 2009; Monaghan and Maden, 2013; Rinkevich et al., 2011). Nerves play an important role in both mammalian and amphibian wound healing (Barker et al., 2006; Westerman et al., 1993). Impaired neurological function can lead to chronic cutaneous wounds, delayed wound contraction, reduced vascularization, hypertrophic scarring, and a prolonged inflammatory phase (Barker et al., 2006; Buckley et al., 2012). The MRL mouse has been shown to heal ear punches through a blastema-like structure similar to amphibian epimorphic regeneration (Buckley et al., 2012; Clark et al., 1998; Rajnoch et al., 2003) . Taken together, this evidence suggests that mammals may have regenerative ability that is lost or inhibited after early development.

An area of contention in regeneration is whether limb regeneration is salamander specific. Prod1, nAG, nsCCN have been proposed as salamander-specific proteins that are the key to regeneration (Brockes and Gates, 2014; Garza-Garcia et al., 2009; Kumar et al., 2007a, 2007b; Looso et al., 2012; da Silva et al., 2002).However, my hypothesis is that since mammals can develop limbs during embryogenesis and appear to have some regenerative ability in utero that is lost over time, then mammals may have the ability to regenerate.

The goal of my work is to learn how the axolotl successfully regenerates and determine how this information might be used to increase the regenerative ability of humans.

Summary of Dissertation Aims

The goal of my dissertation project was to elucidate the molecular mechanism of positional information in axolotl limb regeneration and determine if it is conserved in mammals. To do this, my specific aims were:

1. Do heparan sulfates of the ECM regulate anterior/posterior positional information during axolotl limb regeneration?
2. Do heparan sulfates mediate positional information by regulating FGF signaling during axolotl limb regeneration?
3. Is the role of heparan sulfates in mediating positional information conserved in mouse ECM?
4. What are the other extracellular factors that regulate axolotl limb regeneration?

CHAPTER 2:

Heparan Sulfates Mediate Anterior/Posterior Positional Information by Position-Specific Growth Factor Regulation during Axolotl Limb Regeneration

Abstract

Salamanders are unique among adult tetrapods in their ability to regenerate complex body structures after traumatic injury. Much is yet to be learned before regeneration can be enhanced in humans, including understanding how to recreate the appropriate pattern of the structures that were lost. In axolotl regeneration, the cells maintain a memory of their original position and use this positional information to recreate the missing pattern. The purpose of this study was to elucidate the molecular mechanism of positional information. In this study, I used an *in vivo* gain-of-function assay for positional information to determine whether components of the extracellular matrix (ECM) have positional information that is sufficient to induce formation of *de novo* limb pattern in an ectopic regeneration blastema. I discovered that cell-free anterior and posterior ECM have position-specific signaling properties that either inhibit regeneration or induce *de novo* limb pattern, and that this difference is mediated by growth factor-interacting heparan sulfates in the ECM. The position-specific functionality of the ECM is associated with position-specific differential expression of heparan sulfate sulfotransferases during regeneration. My findings indicate that heparan sulfates are both necessary and sufficient to mediate positional information in axolotl limb regeneration by regulating both blastema formation and pattern formation. This study demonstrates a novel specific mechanism for positional information in axolotl limb regeneration.

Introduction

Salamanders are unique among adult vertebrates in their ability to regenerate complex body structures after traumatic injury. There are many steps remaining before regeneration can be made successful in humans including learning how to obtain all the cell types required, organize the cells into tissues, and reestablish the three-dimensional pattern and structure that was lost. The last step is a major hurdle that may be impossible without studying a model system that can regenerate pattern and structure (Endo et al., 2004).

Much is being learned from stem cell biology about how to obtain, expand and differentiate multipotent cells that can give rise to various tissues. The next challenge will then be to ensure that these cells form tissues that have the appropriate spatial patterns relative to each other so as to restore organ function (McCusker and Gardiner, 2014). For example, the muscles, tendons, ligaments and bones of the arm have to be functionally integrated (make connections and span joints) in order for the limb to move. These tissues have to become innervated and vascularized to function properly. Thus achieving successful regeneration in humans will require understanding how to provide the necessary cues to these stems cells in the adult environment to recreate pattern and regenerate function.

In axolotl regeneration, the cells maintain a memory of their original position and use this positional information to recreate the missing pattern. The purpose of this study was to elucidate the molecular mechanism of positional information.

The way in which cells use positional information to regenerate the limb pattern was formally conceptualized by the Polar Coordinate Model (Bryant et al., 1981; French

et al., 1976) such that cells have a positional code with respect to the three limb axes: proximal/distal, anterior/posterior and dorsal/ventral. When cells with different positional codes (i.e. come from different positions relative to the limb axes) interact with each other, they are induced to proliferate and their progeny acquire new positional information that is required to replace the missing parts of the pattern. This process of "intercalation" is reiterated until all of the missing pattern is restored and regeneration is completed (Bryant et al., 1981; French et al., 1976; Nakamura et al., 2007). Experimentally, the stimulation (or lack of stimulation) of supernumerary structures by intercalation allows for identification of the presence and distribution of positional information encoded by cells from different locations of the limb (Gardiner and Bryant, 1989).

It has been established that positional information is localized to the loose connective tissue of the limb (Bryant et al., 1981, 2002; French et al., 1976; Nacu et al., 2013; Rinn et al., 2006; Rollman-Dinsmore and Bryant, 1984), which is composed of both cells and a biochemically complex extracellular matrix (ECM). Since the connective tissue cells are responsible for synthesis of the ECM, I hypothesized that positional information is stably encoded in the ECM by these cells.

The ability of the ECM to mediate cell-cell signaling has been demonstrated for a number of signaling pathways, and is best understood for FGF signaling which is dependent on heparan sulfates in the ECM (Olwin and Rapraeger, 1992; Rapraeger et al., 1991; Yayon et al., 1991).

Heparan sulfate glycosaminoglycans are a major component of the ECM that can regulate growth factors signaling by: 1) sequestering growth factors in the ECM, 2)

protecting growth factors against proteolysis, and 3) acting as a necessary co-receptor for signaling (Bass et al., 2009; Esko et al., 2009; Sarrazin et al., 2011). Heparan sulfates have been shown to regulate growth factors important for regeneration including: SHH, WNT, BMP, TGFβ and FGF(Häcker et al., 2005). Additionally, there may be distinct HS requirements to mediate specific FGF signaling (Guimond et al., 1993).

I therefore also hypothesized that the ability of cells to encode position-specific information in the ECM is dependent on position-specific modifications of heparan sulfates.

Here I report the results of experiments designed to discover the minimal components of skin grafts that are capable of stimulating ectopic limb structures. Since the grafted skin with posterior positional information contains both cells and ECM, I decellularized anterior and posterior donor skin prior to grafting into wounds with deviated nerves in order to determine whether the ECM encodes positional information (Figure 2.1C,F).

I discovered that anterior and posterior ECM have position-specific signaling properties that either inhibit regeneration or induce *de novo* limb structure, and that this difference is mediated by growth factor-interacting heparan sulfates in the ECM. In addition, I found evidence that the position-specific functionality of the ECM arises as a consequence of position-specific differential expression of heparan sulfate sulfotransferases during regeneration. Finally, I discovered that an artificial matrix of heparan sulfate is sufficient to induce *de novo* limb patterning. Based on these results, I

propose a novel specific mechanism for positional information in axolotl limb regeneration.

Results

The Accessory Limb Model as an *in vivo* Gain-of-function Assay for Limb Regeneration

To determine whether or not the ECM encodes positional information, I took advantage of the Accessory Limb Model (ALM), an *in vivo* gain-of-function assay for signaling that regulates blastema formation and positional information (Endo et al., 2004; Satoh et al., 2007). In this assay, an ectopic blastema is induced on the side of the arm by making a small full-thickness skin wound and surgically deviating the brachial nerve to the wound site (Figure 2.1A,B,D,E). Within a few days (5-10) post-surgery an ectopic blastema develops and grows (Figure 2.1H); however, without further signaling, it does not form ectopic limb structures and eventually reintegrates into the limb. The ectopic blastema can be induced to form an ectopic limb if positional information is provided from the side of the limb that is opposite to the position of the surgically created wound. This is done by grafting a piece of skin (epidermis plus dermis) from the opposite side of the limb (e.g. posterior skin grafted to an anterior wound with a deviated nerve, 75% efficiency) (Endo et al., 2004).

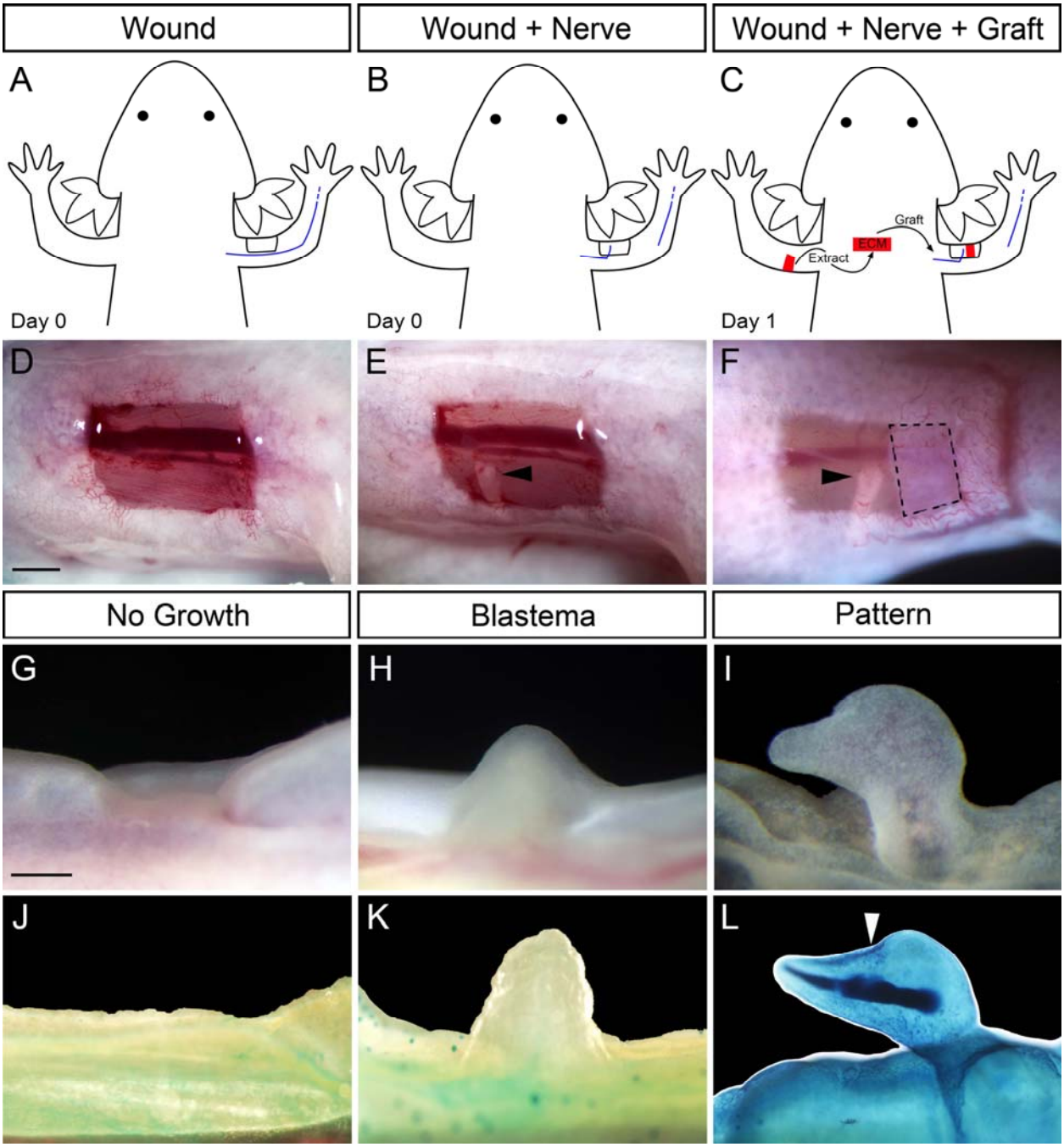

Figure 2.1. The Accessory Limb Model as an in vivo Gain-of-Function Assay for Limb Regeneration. (A, D) A full-thickness skin wound was made on the anterior region of the upper arm. (B, E) The brachial nerve was severed at the elbow and deviated to the wound site which resulted in the formation of an ectopic blastema (H). (C, F) Grafts of ECM were placed in the wound site to assay for pattern formation. Observed outcomes of the assay are wound healing with “No Growth” of a blastema (G, J), “Blastema” but no pattern (H, K) or blastema with “Pattern” (I, L). (J, K, L) Appearance of samples after preparation to visualize skeletal patterns in whole-mount preparations. Dashed lines (F) outline the ECM graft. Black arrowheads (E, F) indicate the severed end of the deviated nerve. White arrowhead (L) indicates the position of the joint of the induced digit-like structure. Scale bar = 1 mm

Previous studies have demonstrated that formation of an ectopic limb on the anterior side of an axolotl limb requires a graft of connective tissue derived from the posterior side of the limb (Endo et al., 2004). These studies have involved the grafting of full thickness skin that included cells as well as the ECM, and thus both posterior (graft-derived) and anterior (host-derived) cells participated in regeneration of the *de novo* limb. Without a posterior skin graft, an ectopic blastema can be induced to form which is derived only from anterior cells, but it does not progress to form an ectopic limb (Endo et al., 2004; Satoh et al., 2007). These findings have led to the conclusion that although anterior cells can be induced to form regeneration-competent blastema cells, they need to interact with cells that have posterior positional information in order to regenerate an ectopic limb (Endo et al., 2004; Satoh et al., 2007). Since a posterior skin graft that supplies the necessary posterior information contains both cells and ECM, I grafted decellularized posterior skin into an anterior wound to test whether or not posterior positional information is present in the ECM and whether it is sufficient to induce anterior cells to form limb pattern.

Treatment of axolotl limb skin with urea kills the cells and subsequent washing removes most water-soluble cellular components (Gilbert et al., 2006). Macromolecules associated with the ECM or the lipid membranes remain associated with the ECM graft (e.g. glycosaminoglycans and any bound factors) (Gilbert et al., 2006). I found that this urea-treated ECM preparation had considerable biological activity, and that when relatively crude ECM was treated further to remove biologically active molecules (e.g. by enzyme treatment or washing with detergent and high concentrations of NaCl), this

activity was lost (Table 2.1). Therefore, for the remainder of my studies, all ECM grafts were extracted with 2M urea treatment.

Table 2.1. Extensively Treated ECM does not Maintain Biological Activity when Grafted into Anterior Wounds with Deviated Nerves.

Graft Type	Total	Blastema	Pattern
Enzyme+Detergent+Salt Treated Anterior ECM	4	4 (100%)	0
Enzyme+Detergent+Salt Treated Posterior ECM	13	13 (100%)	0

Full-thickness skin wounds on the side of an axolotl arm exhibited a range of regenerative responses depending on how the wounds were treated (Endo et al., 2004; Satoh et al., 2007). If the wound was allowed to heal without further manipulation (Figure 2.1A, D), the wound healed without forming an ectopic blastema (Figure 2.1G, J). As described below, I sometimes observed a similar phenotype in response to grafted ECM ("No Growth"). If the brachial nerve was severed distally and surgically deviated to the site of the wound (Figure 2.1B, E), an ectopic blastema that is equivalent to an amputation-induced blastema formed ("Blastema"; Figure 2.1H, K). These blastemas increased in size over a period of two to three weeks, but then began to regress without forming ectopic limb structures (Endo et al., 2004). If a graft of full-thickness skin from the side of the arm opposite to the wound was grafted into the site of the wound/deviated nerve, a well-patterned ectopic limb formed (Endo et al., 2004; Satoh et al., 2007). In the present study, a similar procedure was used to graft decellularized ECM from the side of the arm opposite to the wound (Figure 2.1C, F) to assay for the induction of ectopic limb skeletal elements ("Pattern"; Figure 2.1I, L). Pattern formation is defined by the progression of the ectopically induced blastemas past blastema formation to the stage of rediferrentiation and development of limb structures rather than disappearing through regression as is the case with no graft. I

focused on anterior wounds because, due to the anatomy of the limb, nerves or grafts placed in posterior wounds can become dislodged when the animal begins swimming and rubs the posterior side of their limbs against their flank. To maintain consistency with the breadth of stylopod experiments and the basis of the development of the Accessory Limb Model, wounds were always done on the upper limb.

Cell-free Extracellular Matrix (ECM) Derived from Different Positions around the Limb Circumference can both Inhibit and Enhance Ectopic Limb Regeneration

Anterior wounds with a deviated nerve responded differently to grafts of anterior ECM or posterior ECM (Table 2.2; Figure 2.2A). As reported previously (Endo et al., 2004), nerve-deviated anterior wounds without a graft formed ectopic blastemas at a high frequency, but did not form any pattern (Table 2.2; Figure 2.1H, K; Figure 2.2A). In response to a graft of posterior ECM, some nerve-induced ectopic blastemas (30%) formed ectopic cartilaginous structures that were morphologically similar to a distal phalangeal element (Table 2.2; Figure 2.1I, L; Figure 2.2). These structures were elongated, tapered at the tip and appeared to form a joint (Figure 2.1L, arrowhead). Surprisingly, grafts of anterior ECM inhibited blastema formation in all cases (Table 2; Figure 2.2). I also grafted anterior ECM to wounds on the posterior side of the arm. In all cases (n=5), ectopic blastemas without pattern formed, which is the same response observed when ectopic blastemas are induced without an ECM graft (Table 2.2, Figure 2.1H, K; Figure 2.2A). I thus observed a differential response of anterior limb cells to anterior ECM compared to posterior ECM as well as a differential ability of anterior ECM to inhibit regeneration from anterior wounds but not from posterior wounds. I interpret this difference in both signaling and response to indicate that the ECM encodes

position-specific information that is involved in the regulation of regeneration. Henceforth, these two position-specific effects will be referred to as posterior ECM induction of pattern formation or 'posterior patterning' and anterior ECM inhibition of blastema formation or 'anterior inhibition.'

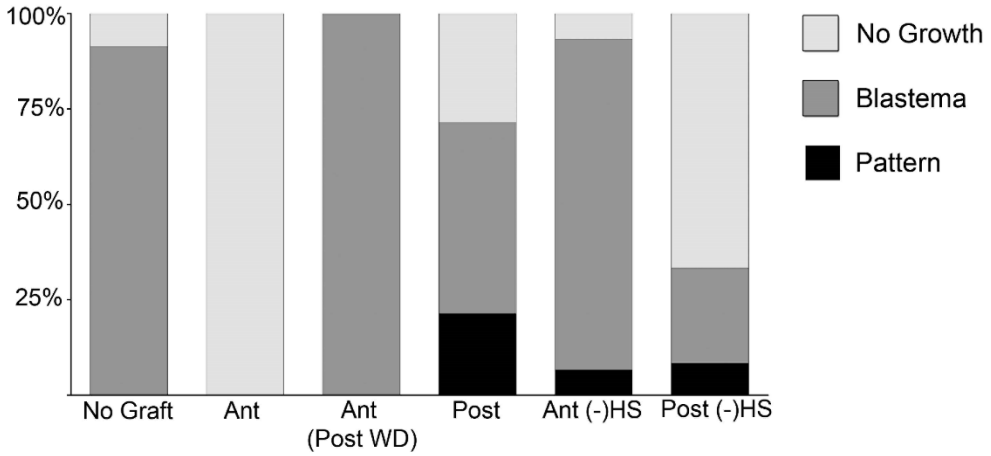

Figure 2.2. Heparan Sulfates (HS) Mediate Position-specific Regulation of Blastema Formation and Pattern Formation during Regeneration. Differential regenerative responses to grafts of anterior/posterior ECM with or without heparitinase (HepIII) treatment. Ant = Anterior, Post = Posterior, (-) HS = HepIII treated to remove HS from the ECM.

Table 2.2. Position-specific Effects of Anterior/Posterior ECM grafts into Anterior Wounds with Deviated Nerves on Blastema Formation and Pattern Formation are dependent on Heparan Sulfates

Graft Type	Total	Blastema*	Pattern**
No Graft	23	21 (91%)	0
Anterior ECM	8	0	0
Anterior ECM grafted in Posterior Wound	5	5 (100%)	0
Posterior ECM	14	10 (71%)	3 (30%)
Heparitinase-Treated Anterior ECM	15	14 (93%)	1 (7%)
Heparitinase-Treated Posterior ECM	12	4 (33%)	1 (25%)

*percentage of total number of grafts that developed an ectopic blastema
**percentage of ectopic blastemas that developed skeletal elements with pattern

Position-specific Information in the ECM is Dependent on the Presence of Heparan Sulfates

Growth factor signaling, including FGF, BMP, Wnt, and TGF-β is important in the initiation and progression of axolotl limb regeneration (Christen and Slack, 1997;

Christensen et al., 2001; Ghosh et al., 2008; Guimond et al., 2010; Han et al., 2001; Kawakami et al., 2006; Lévesque et al., 2007; Mullen et al., 1996; Satoh et al., 2008b, 2010b), and heparan sulfates (HS) in the ECM are known co-factors required for growth factor signaling (Baeg et al., 2001, 2004; Kamimura et al., 2011; Lin, 2004; Matsumoto et al., 2010; Olwin and Rapraeger, 1992; Rapraeger et al., 1991; Sarrazin et al., 2011; Yayon et al., 1991). I therefore tested the hypothesis that heparan sulfates function to encode the position-specific information in anterior versus posterior ECM. I selectively cleaved heparan sulfates from the ECM by treatment with heparitinase (HepIII, specific to heparan sulfates) prior to grafting anterior or posterior ECM into an anterior nerve-deviated wound as described above. Treatment of anterior ECM resulted in the loss of anterior inhibition of blastema formation (Table 2.2, Figure 2.2). Of the 14 blastemas that formed, one also formed pattern; however, given the low frequency of this response, it is unclear whether removal of heparan sulfates from anterior ECM was sufficient to induce pattern formation. The frequency of ectopic blastema formation decreased about 50% when posterior ECM was treated with HepIII (Table 2.2; Figure 2.2; 33 % compared to 71%) and only one of the ectopic blastemas formed pattern suggesting a loss of the posterior patterning. The differential response to HepIII treatment of anterior ECM and posterior ECM is consistent with the hypothesis that the position-specific signaling properties of the ECM are dependent on heparan sulfates.

Heparan sulfate (HS) is Sufficient to Induce Pattern Formation in an Ectopic Blastema

To determine if heparan sulfates (HS) are sufficient to pattern an ectopic limb, I created and grafted an artificial matrix (artificial ECM). The artificial ECM was composed

of varying amounts of HS combined with type I collagen (Schaller and Muneoka, 2001). The artificial ECM was grafted into nerve-deviated anterior wounds (Figure 2.3A).

Grafts of artificial ECM containing only type I collagen resulted in the formation of ectopic blastemas without pattern, a result that is comparable to the result when no ECM was grafted (Tables 2.2, 3; Figure 2.4).Remarkably, addition of HS to the collagen matrix resulted in pattern formation. Medium-HS (~1.0 mg of HS in a 1:12 ratio to collagen) artificial ECM grafts induced complex limb skeletal patterns in nearly half of the ectopic blastemas (Table 2.2; Figure 2.3; Figure 2.4). The induced patterns contained multiple skeletal elements with joints (Figure 2.3F, arrowheads), as well as elements that bifurcated (Figure 2.3H, arrowhead). All of the ectopic patterns included distal elements that tapered with the same morphology as terminal phalanges.

The frequency of ectopic blastema formation and pattern formation was altered in response to changes in the concentration of heparan sulfates in the artificial ECM. When artificial ECM containing low amounts of heparan sulfates (~0.5 mg of HS in a 1:24 ratio to collagen) was grafted, the frequency of blastema formation decreased by 50% (Table 2.3; Figure 2.4; 43% compared to 90% for High-HS artificial ECM), and only one of the ectopic blastemas formed pattern. In contrast, increasing the amount of heparan sulfate in (~2.0 mg of HS in a 1:6 ratio to collagen) the artificial ECM had no effect on the frequency of blastema formation; however, High-HS artificial ECM grafts did not induce pattern formation in these blastemas (Table 2.3; Figure 2.4). The observed changes in bioactivity of artificial ECM containing heparan sulfate when grafted into nerve-deviated wounds is consistent with the hypothesis that heparan sulfate has the potential to regulate the regeneration response (both blastema formation

and pattern formation). These results demonstrate that heparan sulfate is sufficient to induce pattern formation in an ectopic blastema in a dose-dependent manner.

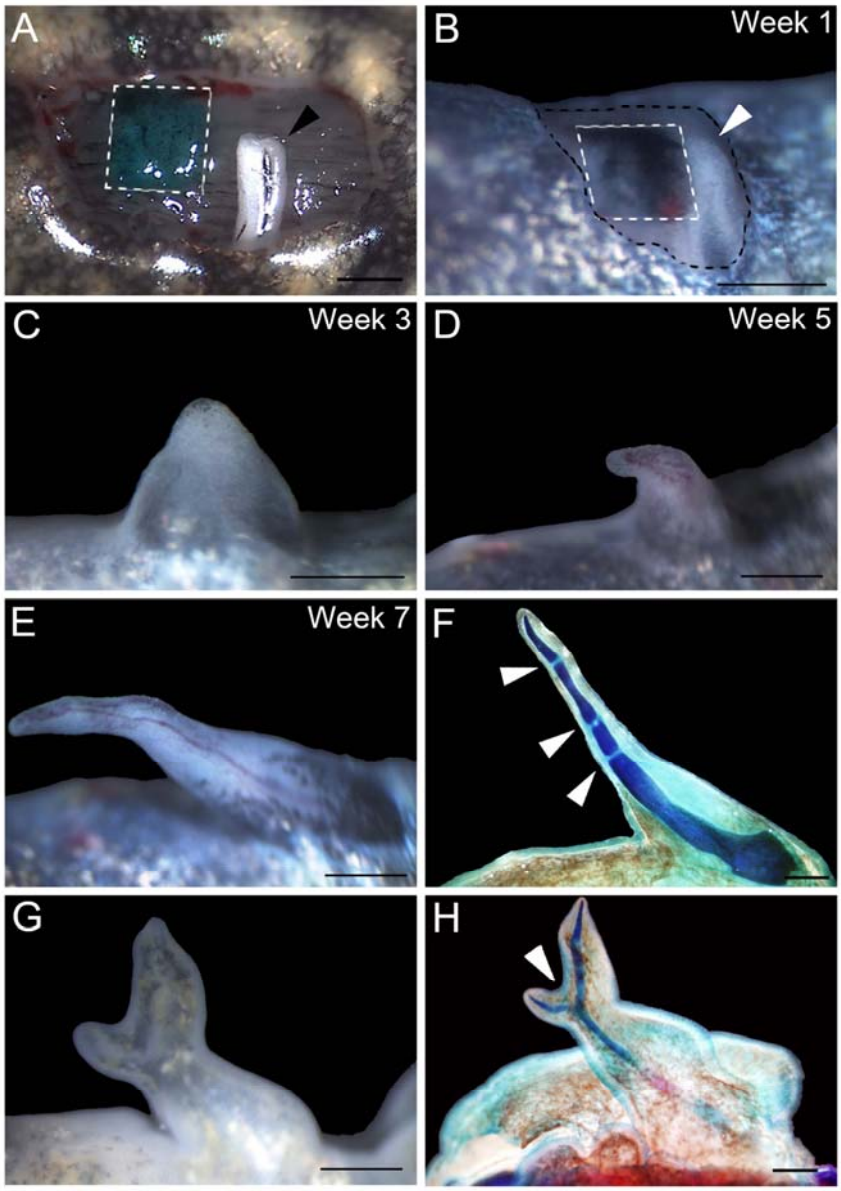

Figure 2.3. Heparan Sulfate is Sufficient to Induce Ectopic Limb Pattern during Regeneration. (A) Example of the Accessory Limb Model surgery illustrating a wound that has received an artificial ECM graft (green, outlined with dashed white lines) and a deviated nerve (white with black arrowhead). (B) One week after nerve-deviation (white with white arrowhead) and artificial ECM graft (black India ink, outlined with dashed white lines). Growth of induced blastema three weeks (C), five weeks (D) and seven weeks (E) after surgery. (F) Whole-mount staining of the skeletal pattern formed in (E). Arrowheads indicate joint-like segmentations. (G, H) Example of a bifurcated limb pattern (indicated by white arrowhead) induced by an artificial ECM graft. Blue = cartilage, Red = ossified bone, Scale bars = 1 mm

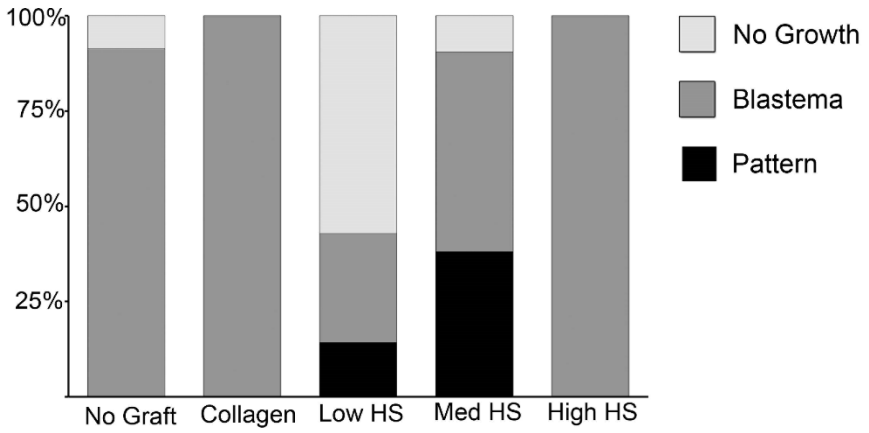

Figure 2.4. Dose-dependent Induction of Pattern Formation by Grafts of Artificial ECM Containing Heparan Sulfate (HS). Low HS = 0.5 mg, Med HS = 1.0 mg, or High HS = 2.0 mg of HS (Sigma, porcine intestinal mucosa) mixed with 12 mg of type I collagen (Sigma, calf skin)

Table 2.3. Heparan Sulfate is Sufficient to Induce Pattern Formation in Ectopic Blastemas.

Graft Type	Total	Blastema*	Pattern**
Collagen I only	6	6 (100%)	0
Low-HS Artificial ECM	7	3 (43%)	1 (33%)
Medium-HS Artificial ECM	21	19 (90%)	8 (42%)
High-HS Artificial ECM	5	5 (100%)	0

*percentage of total number of grafts that developed an ectopic blastema
**percentage of ectopic blastemas that developed skeletal elements with pattern

The ECM can Function both as a Source and Sink of Growth Factors for Regulating Regeneration

Heparan sulfates (HS) have binding sites for growth factors which enable cell-surface heparan sulfate proteoglycans to act as co-receptors that are required for signaling (e.g. FGF signaling) (Sarrazin et al., 2011). Heparan sulfates can function as a sink for growth factors, sequestering bound growth factors and inhibiting their ability to activate signaling. Heparan sulfates in the ECM grafts also can function as a source of growth factors, delivering bound growth factors to the anterior cells in the wound. It is unclear how heparan sulfates of the ECM grafts function to affect blastema formation and pattern formation during limb regeneration. To determine this, I washed the ECM grafts with 1M or 2M NaCl, which disrupts the charge-charge interactions binding

growth factors to the ECM, to remove any bound factors and grafted the washed ECM into an anterior wound site with a deviated nerve to observe if anterior ECM inhibition of blastema formation and posterior ECM induction of pattern formation is lost, maintained or increased.

The most dramatic result was that NaCl ECM wash completely relieved anterior ECM inhibition of blastema formation. However, NaCl ECM wash of anterior ECM did not affect pattern formation (Table 2.4; Figure 2.5). Based on this result, I hypothesize that the anterior ECM inhibition of blastema formation was a consequence of the ECM acting as a source of bound growth factor that inhibited blastema formation, since NaCl washes removed this inhibition.

In contrast, NaCl treatment of posterior ECM did not have an effect on posterior patterning. NaCl treatment of posterior ECM did appear to increase blastema formation (Table 2.4, Figure 2.5). Based on this result, I hypothesize that the posterior ECM induction of pattern formation is a consequence of the ECM acting as a growth factor sink, since removing bound growth factors with NaCl washes did not affect patterning.

These results further support the hypothesis that anterior ECM and posterior ECM have position-specific properties that respond differently to NaCl. I propose a model in which asymmetry of the limb can be created by the anterior ECM acting as a source and the posterior ECM acting as a sink regulating growth factor signaling to reestablish the anterior/posterior limb axis during limb regeneration.

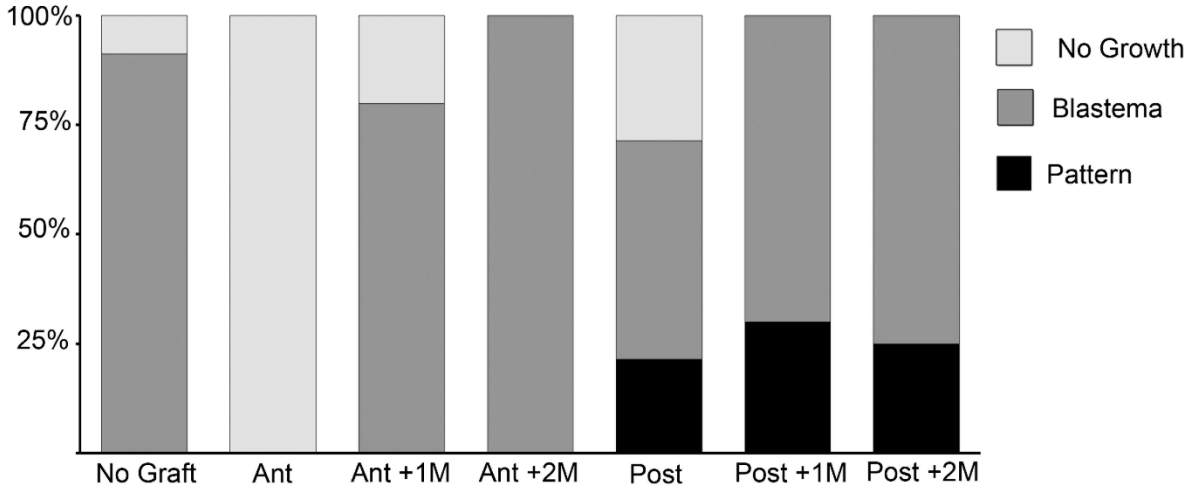

Figure 2.5. Position-Specific Effects of Treating ECM Grafts with NaCl on Blastema formation and Pattern Formation. Anterior (Ant) and posterior (Post) ECM grafts were washed with either 1M or 2M NaCl prior to grafting.

Table 2.4. Washing of ECM Grafts with NaCl Relieves Anterior Inhibition but does not Affect Pattern Formation

Graft Type	Total	Blastema*	Pattern**
Anterior ECM	8	0 (0%)	0
Anterior ECM + 1M NaCl	10	8 (80%)	0
Anterior ECM + 2M NaCl	8	8 (100%)	0
Posterior ECM	14	10 (71%)	3 (30%)
Posterior ECM + 1M NaCl	10	10 (100%)	3 (30%)
Posterior ECM + 2M NaCl	8	8 (100%)	2 (25%)

*percentage of total number of grafts that developed an ectopic blastema
**percentage of ectopic blastemas that developed skeletal elements with pattern

Position-specific Mediation of FGF Signaling Regulates Blastema Formation and Pattern Formation

Although the heparan sulfates are known to regulate numerous growth factor signaling pathways including FGF, BMP, Wnt and TGF-β (Sarrazin et al., 2011), for our initial studies, I decided to focus on the best studied phenomenon of heparan sulfate-dependent regulation of FGF (fibroblast growth factor) signaling.

Heparan sulfate plays a critical role in the regulation of FGF signaling (Olwin and Rapraeger, 1992; Rapraeger et al., 1991; Yayon et al., 1991). Additionally there may be distinct HS requirements to mediate specific FGF signaling (Guimond et al., 1993). Of

particular relevance to our study are reports that FGF2 and FGF8 are expressed and function during limb regeneration (Boilly et al., 1991; Christen and Slack, 1997; Christensen et al., 2001; Han et al., 2001; Mullen et al., 1996). It has been proposed that FGF2 functions during blastema formation and that exogenous FGF2 can compensate for nerve-dependency of regeneration in salamanders and chicks (Mullen et al., 1996; Taylor et al., 1994). In addition, FGF8 is required for limb development and patterning (Christensen et al., 2001; Mariani et al., 2008; Sun et al., 2002). Lastly, recent studies have shown that FGF2 and FGF8 (along with GDF5) can substitute for nerve signaling during axolotl limb regeneration (Makanae et al., 2013). I therefore hypothesized that differential regulation of FGF2 and FGF8 signaling by anterior and/or posterior HS is functionally involved in the experimental results observed in response to ECM grafting. To test this hypothesis, I soaked ECM preparations (with or without prior treatment with HepIII) in either FGF2 or FGF8 prior to grafting into anterior wounds with deviated nerves.

Pretreatment of anterior ECM grafts with either FGF2 or FGF8 relieved anterior ECM inhibition of blastema formation (Table 2.5; Figure 2.6A). As discussed above, NaCl treatment of anterior ECM also relieved anterior inhibition, presumably by removing inhibitory factors. It therefore is possible that both FGF2 and FGF8 competed with inhibitory factors in the ECM, and were able to rescue blastema formation. It is unclear if this is the result of competitive binding (bind to same HS binding sites) or competitive signaling (FGF inhibitor). In addition to the ability to rescue blastema formation, FGF2 treatment also induced pattern formation in 30% of the grafts (Table 2.5; Figure 2.6A; Figure 2.7A). The ability of FGF2 to induce pattern formation was even

more evident in anterior ECM pretreated with HepIII to remove HS (62% compared to 30% without HepIII treatment, Figure 2.6A, Figure 2.7B-C). HepIII pretreatment of FGF2-pretreated anterior ECM grafts seemed to lead to the regeneration of skeletal elements with a more proximal morphology (instead of only the distal phalangeal elements), along with the formation of a connection with the host stylopod (suggesting that the ectopic element corresponded to the zeugopod) (Figure 2.7B-C). There has been previous evidence of FGF2 inducing the regeneration of more proximal limb pattern (Satoh et al., 2010a). Treatment of anterior ECM with FGF8 did not induce any pattern formation whether or not the grafts had been treated with HepIII. These results suggest that anterior ECM mediated a differential regeneration response whether pretreated with FGF2 or FGF8.

Table 2.5. Effects of FGF2 and FGF8 on Blastema and Pattern Formation in Response to Anterior ECM Grafts.

Graft Type	Total	Blastema*	Pattern**
Anterior ECM	8	0 (0%)	0
Anterior ECM + FGF2	12	10 (83%)	3 (30%)
Anterior ECM + FGF8	6	5 (83%)	0
Heparitinase Anterior ECM	15	14 (93%)	1 (7%)
Heparitinase Anterior ECM + FGF2	8	8 (100%)	5 (62%)
Heparitinase Anterior ECM + FGF8	11	11 (100%)	0

*percentage of total number of grafts that developed an ectopic blastema
**percentage of ectopic blastemas that developed skeletal elements with pattern

Although untreated posterior ECM grafts in general did not inhibit blastema formation, the frequency of ectopic blastema formation increased in response to treatment with either FGF2 or FGF8 (from 70% to 100%; Table 2.6; Figure 2.6B). This was the same result observed with NaCl treatment (Table 2.4; Figure 2.5), suggesting that FGF2 and FGF8 compete with inhibitory factors in both anterior and posterior ECM, and are able to rescue/increase the frequency of blastema formation. As with anterior

ECM grafts, FGF2 treatment but not FGF8 treatment increased the frequency of pattern formation (60% compared to 30% for untreated posterior ECM grafts, Table 2.6, Figure 2.6B, Figure 2.7D-H). The induced pattern in response to FGF2 treatment (Figure 2.7D-H) again seemed to be more proximal compared to untreated posterior ECM grafts (Figure 2.1L). The FGF2-treated posterior ECM grafts appear to result in stylopod elements (humerus and femur) rather than autopod (phalanges). There were not as many supernumerary skeletal elements that tapered distally (Figure 2.7D-F), and there was evidence of distinct epiphyseal and diaphyseal regions that are characteristic of long bones (e.g. humerus, femur).

Strikingly, treatment with FGF8 completely inhibited the ability of posterior ECM to induce pattern formation. In contrast to anterior ECM, the ability of FGF2-treated posterior ECM to induce pattern was dependent on HS such that HepIII pretreatment inhibited pattern formation (Table 2.5; Figure 2.4C). Taken together these results further demonstrate the differential regenerative response between anterior and posterior ECM in terms of the regulation of FGF signaling.

Table 2.6. Effects of FGF2 and FGF8 on blastema and pattern formation in response to posterior ECM grafts.

Graft Type	Total	Blastema*	Pattern**
Posterior ECM	14	10 (71%)	3 (30%)
Posterior ECM + FGF2	10	10 (100%)	6 (60%)
Posterior ECM + FGF8	6	6 (100%)	0
Heparitinase Posterior ECM	12	4 (33%)	1 (25%)
Heparitinase Posterior ECM + FGF2	7	7 (100%)	0
Heparitinase Posterior ECM + FGF8	11	11 (100%)	0

*percentage of total number of grafts that developed an ectopic blastema
**percentage of ectopic blastemas that developed skeletal elements with pattern

There are at least three intriguing and consistent conclusions that emerge from these FGF pretreatment experiments. First, treatment with either FGF2 or FGF8

increased the frequency of blastema formation, suggesting that there is an endogenous inhibitor of blastema formation that competes with FGFs. Second, FGF2 increased the frequency of pattern formation; whereas, FGF8 inhibited pattern formation. Finally, posterior but not anterior ECM-mediated pattern induction was dependent on HS, in as much as depletion of HS inhibited pattern formation induced by FGF2-treated posterior ECM, but doubled pattern formation by anterior ECM. Together, these results are consistent with the hypothesis that FGF signaling plays critical roles in blastema formation and pattern formation, and that there are mechanisms for regulating FGF signaling in a position-specific manner during regeneration.

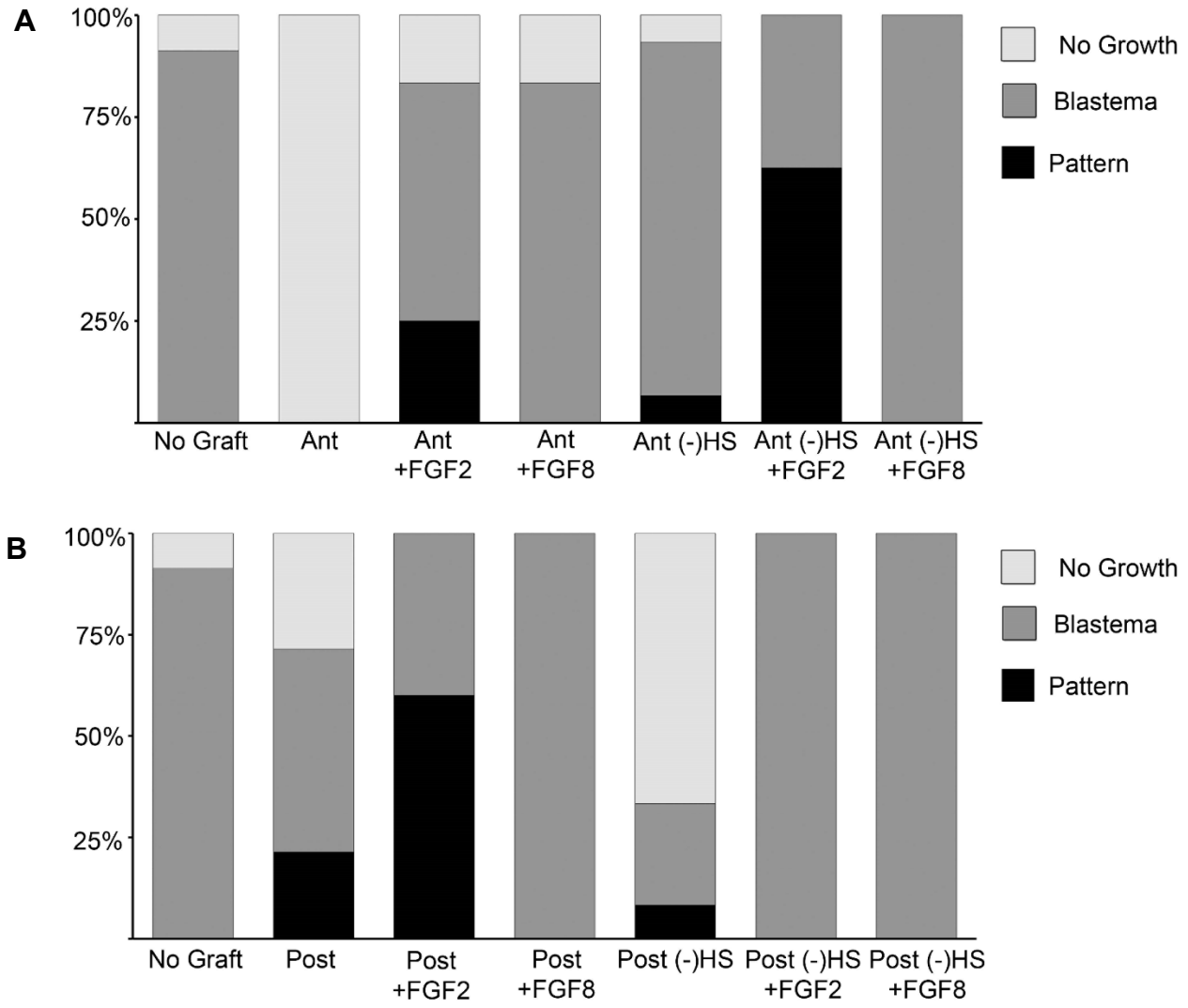

Figure 2.6. Position-specific Effects of Treating ECM Grafts with FGF2 or FGF8 on Blastema and Pattern Formation. (A) Anterior ECM grafts (Ant) were soaked in either FGF2 or FGF8 prior to grafting. (-) HS = HepIII treated to remove HS from the ECM. (B) Posterior ECM grafts (Post) were soaked in either FGF2 or FGF8 prior to grafting. (-) HS = HepIII treated to remove HS from the ECM.

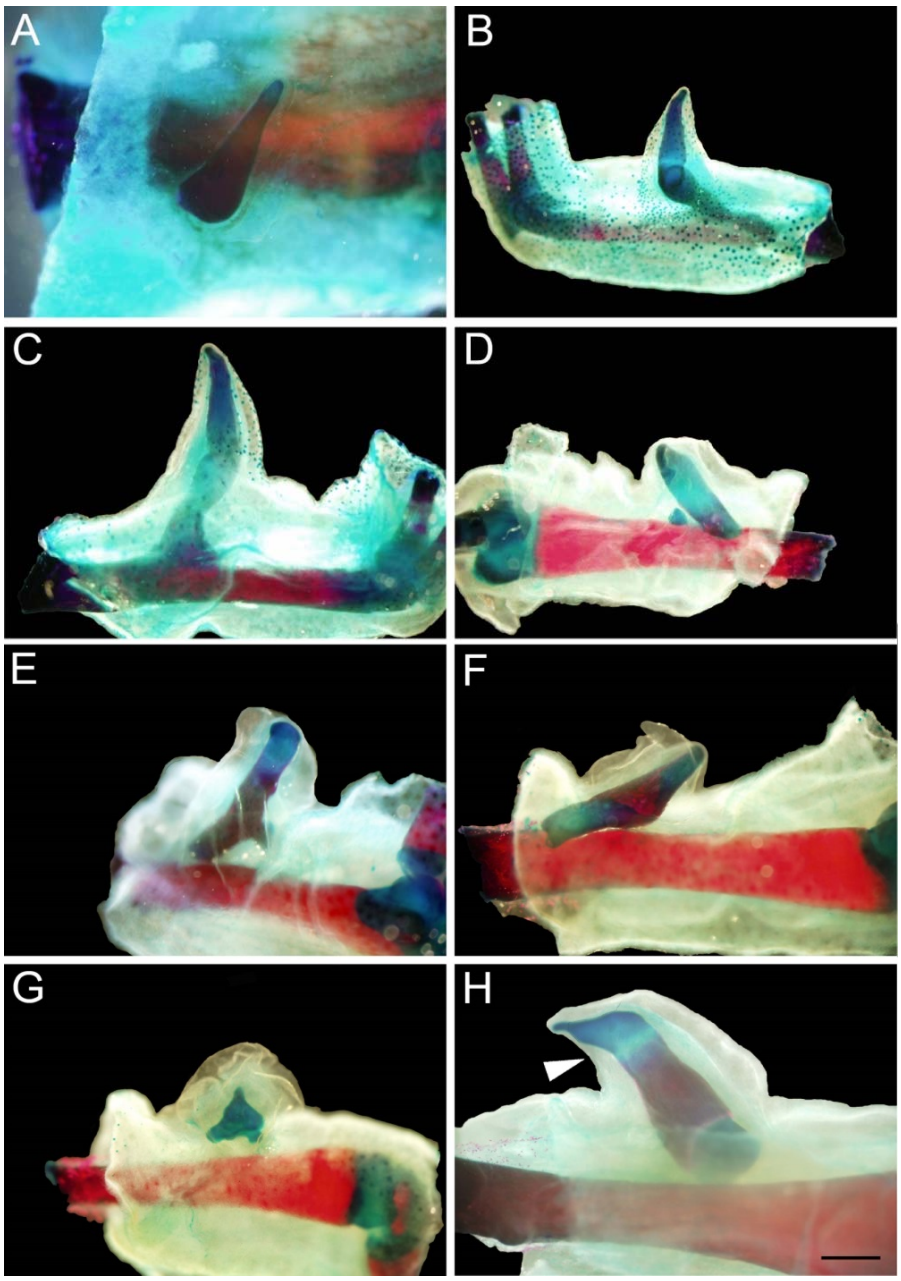

Figure 2.7. FGF2 Increased Induction of Pattern Formation by ECM Grafts. (A) Result of FGF2-treated anterior axolotl ECM. (B,C) Results of FGF2 and HepIII-treated anterior axolotl ECM. (D, E,F,G,H) Results of FGF2-treated posterior axolotl ECM. Whole-mount skeletal preparations to visualize skeletal elements by Alcian Blue and Alizarin Red Staining, Blue = Cartilage, Red = Ossified Bone.

Heparan Sulfate Sulfotransferases are Differentially Expressed in Anterior and Posterior Blastema Cells during Regeneration

Based on the results above, it appeared that HS-mediated growth factor signaling was different between the anterior and posterior ECM, and was associated with the positional interactions that control blastema formation and pattern formation during regeneration. Presumably these differences arose during limb development, and they were reestablished during limb regeneration. I thus hypothesized that there must be either quantitative differences in the levels of different HS, and/or qualitative differences in the types of sulfation patterns. To determine how position-specific differences in heparan sulfate properties are established I looked at expression of the enzymes (heparan sulfate sulfotransferases) responsible for creating qualitative and quantitative differences in heparan sulfates.

My search of the *Ambystoma* EST database (http://www.ambystoma.org) identified ten axolotl heparan sulfate sulfotransferases expressed in axolotl tissues (Table 2.7). I used semi-quantitative RT-PCR to determine which of these were expressed in either uninjured or regenerating limb tissues. Of the six genes that were expressed during limb regeneration, three (heparan sulfate 3-O sulfotransferase 1 [HS3ST1], heparan sulfate 6-O sulfotransferase 1 [HS6ST1], and N-deacetylase/N-sulfotransferase 2 [NDST2]) were expressed differentially between anterior and posterior regions of regenerating limb blastemas (Table 2.7; Figure 2.8). Expression of two of these (HS6ST1 and NDST2) was detected in uninjured limb skin. For all three, expression appeared to increase coincident with blastema formation and growth, with maximal levels observed around the medium to late bud stages of regeneration (when

symmetry breaks) (Figure 2.8). At that stage, expression of NDST2 and HS6ST1 appeared to be higher in the anterior half of the blastema; whereas, expression of HS3ST1 appeared to be higher in the posterior half.

I confirmed that these three genes were differentially expressed along the anterior-posterior axis of medium-late bud blastemas by RNA *in situ* hybridization (Figure 2.8B-D). Expression of all three genes was detected in blastema mesenchyme cells in both anterior and posterior regions. Consistent with the RT-PCR results, there was a gradient of expression for each, with the domain of expression for HS3ST1 being more limited in the anterior as compared to the posterior, and the posterior domain being more limited for HS6ST1 and NDST2. By RT-qPCR of HS6ST1, I determined that HS6ST1 is expressed ~2x more in the anterior then the posterior during axolotl limb regeneration. These data are consistent with the hypothesis that the anterior/posterior difference in the ability of axolotl limb ECM to control blastema formation and pattern formation arises as a consequence of the spatial and temporal regulation of heparan sulfate sulfation enzymes.

Table 2.7. Expression of Heparan Sulfate Sulfotransferases Identified from the *Ambystoma* EST Database

Gene	Uninjured Skin	Blastema
NDST1	+	+ (A=P)
NDST2	**+**	**+ (A>P)**
NDST3	-	-
NDST4	-	-
HS6ST1	**+**	**+ (A>P)**
HS2ST1	+	+ (A=P)
HS3ST1	**-**	**+ (P>A)**
HS3ST2	+	-
HS3ST2B1	-	+ (A=P)
HS3ST4	-	-

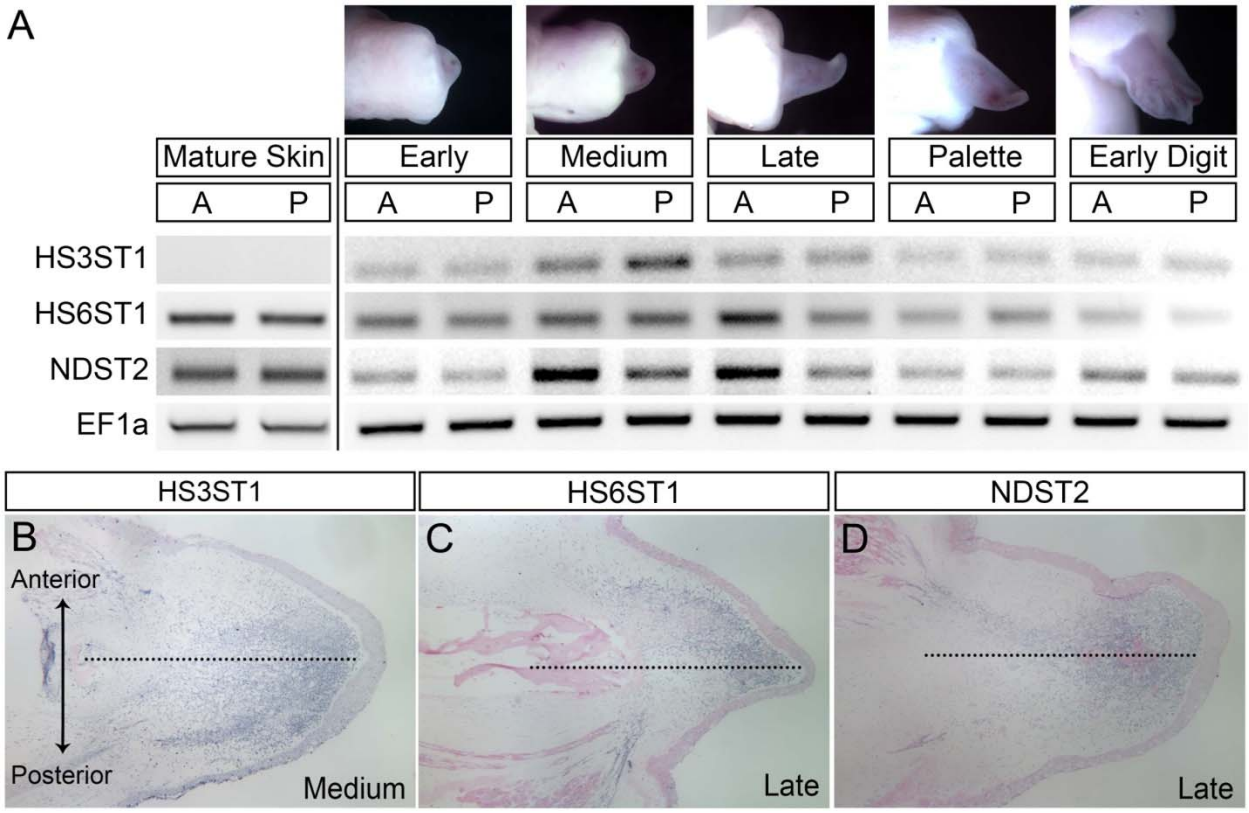

Figure 2.8. Anterior/Posterior Differential Expression of Heparan Sulfate Sulfotransferases during Limb Regeneration. (A) Reverse-transcription PCR expression analysis of the heparan sulfate sulfotransferases HS3ST1, HS6ST1 and NDST2 in the anterior and posterior of blastema at progressive stages of limb regeneration. EF1α was used as a normalizing expression control. A = Anterior, P = Posterior blastema portions from early bud, medium bud, late bud, palette and early digit stages of blastema growth. (B, C, D) RNA *in situ* hybridization for expression of HS3ST1 (B), HS6ST1 (C) and NDST2 (D). Dotted lines indicate midline between anterior (top) and posterior (bottom) sides of the limb that correspond to the plane of bisection for collection the blastema tissue samples.

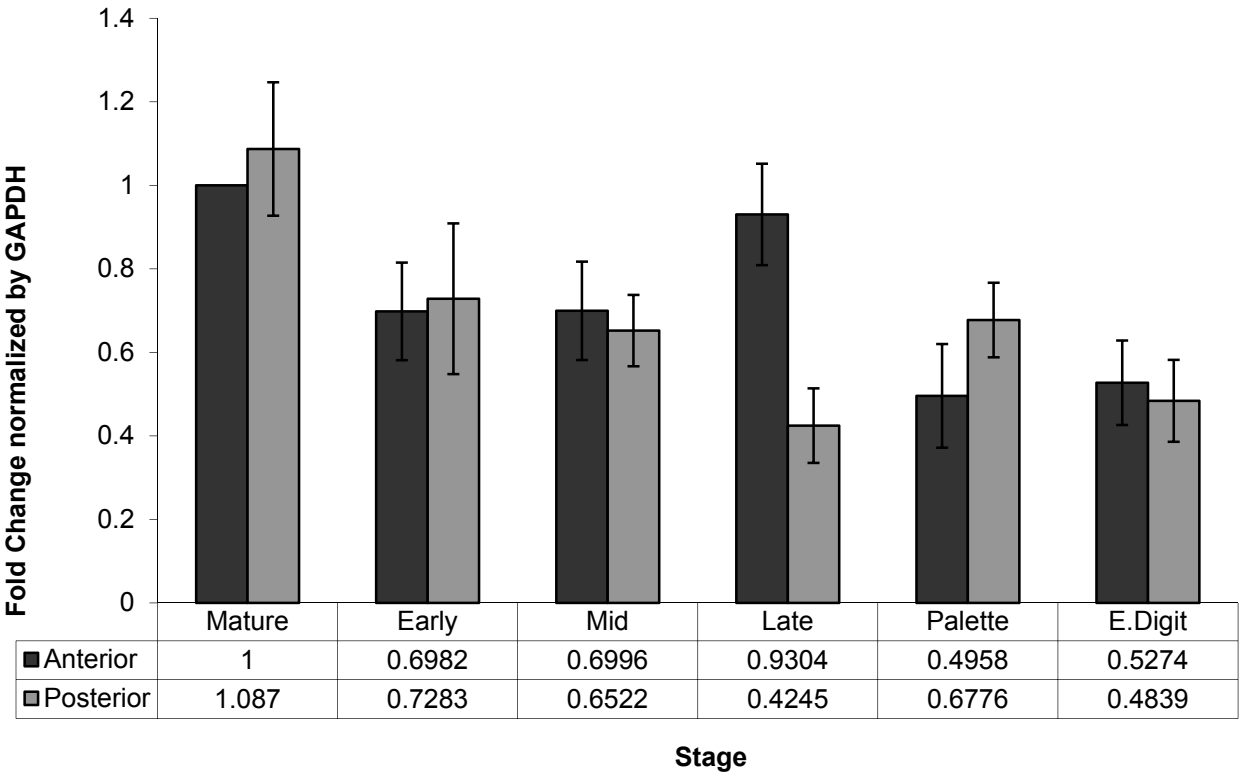

	Mature	Early	Mid	Late	Palette	E.Digit
Anterior	1	0.6982	0.6996	0.9304	0.4958	0.5274
Posterior	1.087	0.7283	0.6522	0.4245	0.6776	0.4839

Figure 2.9. Spatial-temporal expression of HS6ST1 during regeneration by RT-qPCR. Values normalized by GAPDH expression. Mature anterior expression was set at 1. Each RNA sample was extracted from 4-18 pooled blastemas. Error bars are from 3 independent biological samples.

Differential Levels of Glycosaminoglycan Sulfation across the Anterior/Posterior Limb Axis

Based on the anterior/posterior differential expression of heparan sulfate sulfotransferases, I hypothesized that there would be quantitative and qualitative differences in HS sulfation between the anterior and posterior. To measure relative levels of sulfated glycosaminoglycans (GAGs) in axolotl anterior or posterior skin, I used the dimethylmethylene blue dye-binding Blyscan Assay. Sulfated GAGs bind to the 1,9-dimethlymethylene blue dye and are precipitated. The amount of precipitated dye is measured by absorbance at 656 nm and quantified by comparison to a reference standard curve. Relative levels of N and O-sulfation are measured by nitrous acid cleavage of N-sulfated GAGs before dye-binding quantification. I found that there was 2.5x more sulfated glycosaminoglycans in the anterior skin, and there is a higher proportion of N-sulfated glycosaminoglycans in the anterior skin (Figure 2.10). Both observations were consistent with the heparan sulfate sulfotransferase expression data (higher levels of NDST2 expression in the anterior region of the blastema).

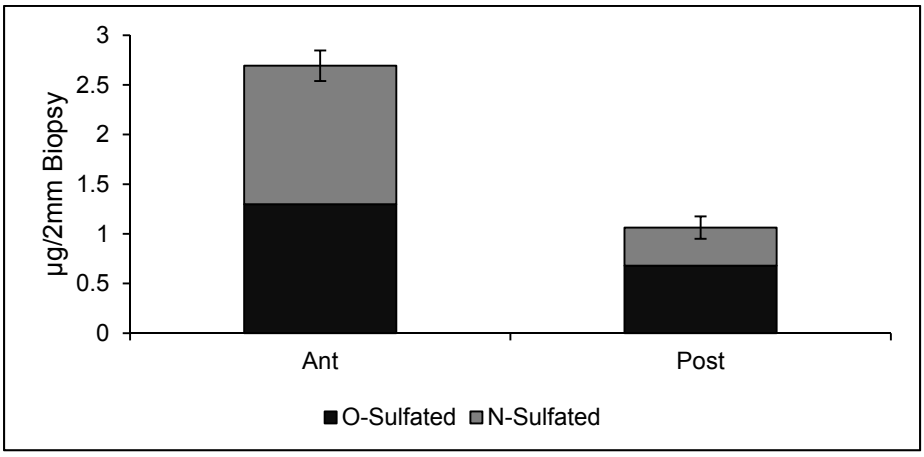

Figure 2.10. Higher Levels of GAG sulfation in Anterior Axolotl Skin by Blyscan Glycosaminoglycan Assay. Error bars are from 3 independent biological samples.

Discussion

The ability to regenerate a limb is dependent on both regeneration competent cells and the information that regulates the behavior of those cells in order to reform the structure and reestablish the function of the amputated limb (Muneoka et al., 2008b). The necessity of having positional information is evident from studies involving the formation of limbs *de novo* on the side of the arm of axolotls (Endo et al., 2004; Hirata et al., 2013; McCusker et al., 2014; Mitogawa et al., 2014; Satoh et al., 2007). Nerve-associated signaling is necessary to recruit regeneration competent cells to form an ectopic blastema, but is not sufficient to induce regeneration of a limb. Limb formation requires the presence of information both from the wound site as well as from the opposite side of the limb (e.g. by grafting of posterior skin to an anterior wound). Regeneration competent cells are recruited from the stump either by dedifferentiation (e.g. connective tissue cells) or by activation of adult stem cells (e.g. satellite cells that give rise to muscle) to form the blastema (Bryant et al., 2002; Sandoval-Guzmán et al., 2014). The molecular nature of the positional information required for regeneration is largely unknown, though it is localized to loose connective tissues (Bryant et al., 2002). My findings indicate that the molecular basis of positional information involves interactions between ECM with position-specific heparan sulfate modification patterns, growth factors (FGFs in particular), and regeneration competent cells. I have demonstrated that heparan sulfates are necessary and sufficient to induce *de novo* limb pattern formation by blastema cells during regeneration.

Based on my findings, I theorize that the molecular mechanism of positional information during axolotl limb regeneration is a “heparan sulfate code” in the ECM of

loose connective tissue in which position-specific growth factor signaling is mediated by specific heparan sulfate sulfation patterns created by differential expression of heparan sulfate sulfotransferases.

I propose a model in which sulfation patterns of the heparan sulfates in the ECM are modified in both time and space, resulting in both qualitative and quantitative differences in heparan sulfate glycosaminoglycan sulfation mediating position-specific growth factor regulation of blastema formation and pattern formation (Figure 2.11).

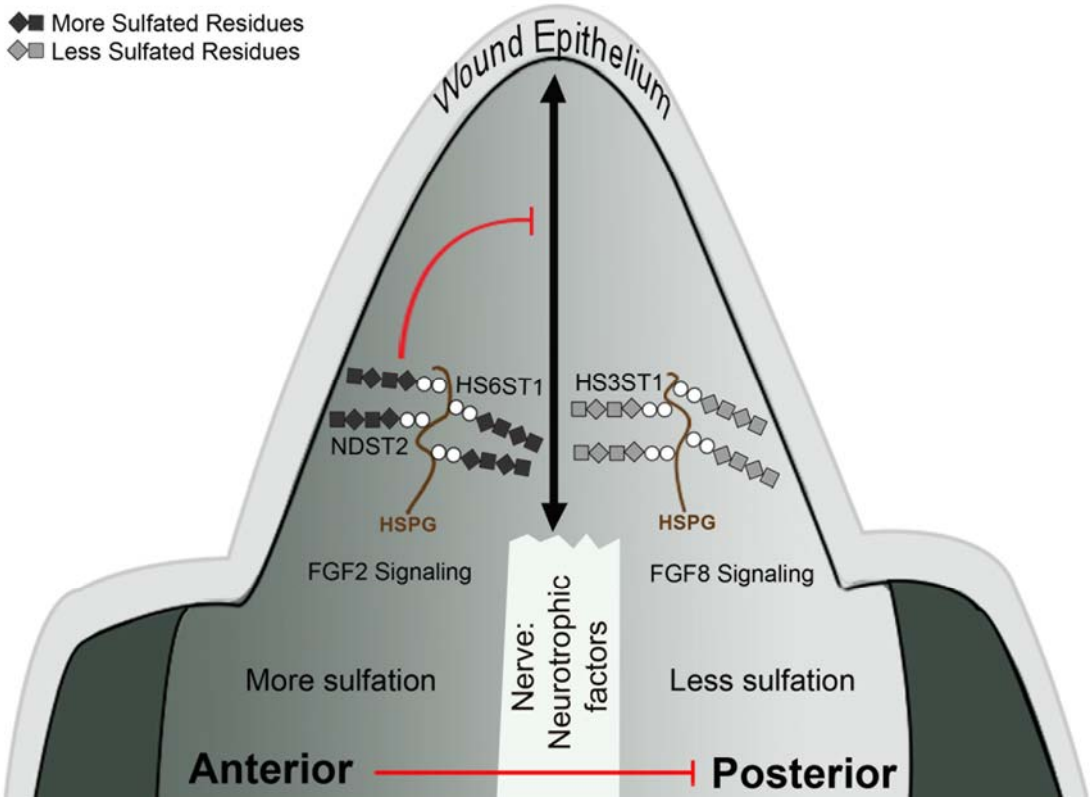

Figure 2.11. Model of Heparan Sulfate Position-Specific Regulation of Growth Factor Signaling to Mediate Positional Information during Axolotl Limb Regeneration. In the regenerating limb blastema, the nerve interacts with the wound epithelium to release neurotrophic factors that induce blastema formation and generate regeneration competent cells. Differential expression of heparan sulfate sulfotransferases establishes quantitative and qualitative differences in heparan sulfate composition resulting in differential FGF2 and FGF8 signaling thereby recreating the anterior/posterior limb axis and inducing pattern formation during limb regeneration.

Differential expression of HS3ST1, HS6ST1 and NDST2 results in qualitative and quantitative differences of heparan sulfate sulfation across the anterior/posterior axis. Differentially sulfated heparan sulfate glycosaminoglycans (GAG) in the anterior or posterior ECM acting as a source or a sink regulate FGF2 and FGF8 signaling preferentially to reestablish the anterior/posterior limb axis in the blastema. This model is consistent with the ECM grafting, gene expression and GAG sulfation data. Consistent with the Polar Coordinate Model (Bryant et al., 1981; French et al., 1976) and previous studies with the Accessory Limb Model (Endo et al., 2004; Satoh et al., 2007), when a disparity in positional information is created, either from migration of cells from opposite sides of the limb following amputation or by experimentally grafting posterior skin/ECM into an anterior wound, pattern formation is induced. Also consistent with the Polar Coordinate Model, when there is no disparity in positional information (anterior into anterior), no growth and intercalation is induced, and no pattern formation results. The formation of ectopic limb pattern in the present study is consistent with the hypothesis that cell-free posterior ECM encodes positional information that is different from that the information associated with anterior cells and ECM.

The amount of ectopic limb pattern induced in response to posterior ECM grafts in this study was less than in response to posterior skin grafts that contained both cells and ECM (Endo et al., 2004) (Figure 2.1L). Since the ECM was synthesized by the cells, the matrix-encoded positional information was dependent on the presence of cells with the same positional information. Therefore, it is possible that positional signaling by posterior ECM is sufficient to induce pattern formation but without viable cells to

continue to make more matrix, it was not sustained over a long enough period of time to allow for the complete limb pattern to form.

The ECM grafting data indicate the presence of a regeneration inhibitory activity that is associated with anterior ECM, but not with posterior ECM. Since this anterior inhibition could be removed by washing with high concentrations of NaCl, it presumably is a factor that binds to the ECM. This anti-regeneration activity also was removed by treatment with HepIII, and thus most likely is a factor that is bound by anterior-specific heparan sulfate modifications. In addition, regeneration (blastema formation) could be rescued by treating anterior ECM with FGF2, which presumably out-competed the inhibitory factor. It has been hypothesized that there is a regeneration-inhibiting factor present in the mature limb stump that can prevent regeneration of aneurogenic limbs (Tassava and Olsen-Winner, 2003). More detailed studies are required to determine what this inhibitory factor is. Since the inhibitory factor can be eluted from anterior ECM with NaCl, a fairly straight forward approach to identifying candidate inhibitory factors would be to preform mass spectrometry analysis of salt washes of anterior and posterior ECM. The candidate inhibitory factor would be preferential to anterior ECM and increase between 1M and 2M NaCl washes. Once candidates are identified, ability to inhibit blastema formation can be assayed by resorbing the factor back into ECM or by incorporation into a bead and grafting into a wound with a deviated nerve. Although it is outside the scope of this study, uncovering the mechanisms underlying how regeneration can be inhibited could be invaluable to regenerative medicine.

The discovery that anterior ECM can inhibit regeneration is important because there are very few ways to inhibit salamander limb regeneration reversibly. Severing the

nerves innervating the limb prevents regeneration, and if the nerves are allowed to regenerate the limb will regenerate when reinjured (Salley and Tassava, 1981; Singer, 1946, 1947), indicating that nerves are necessary for regeneration. In contrast, the response to anterior ECM grafts indicates that anti-regeneration signals are present, and that regeneration can be rescued when they are removed (e.g. by HepIII, NaCl, or FGF treatment). These data also point out that the lack of a regenerative response does not mean that an animal does not have the ability to regenerate. Therefore, the lack of a regenerative response (e.g. in humans) could be a consequence of inhibition rather than a lack of ability to regenerate. Since the regenerative failure in the axolotl is comparable to the response in humans, understanding how to de-repress the inhibitory activity will allow for testing of whether regenerative failure in humans is a consequence of anti-regenerative signaling activity. Understanding the signals and responses of cells, whether they are pro- or anti-regenerative will be critical to achieving the goal of regenerative engineering to reform complex structure and restore function in humans (Laurencin and Khan, 2013).

It should be noted that although the data presented here suggest that heparan sulfates are necessary and sufficient to mediate positional information, the HepIII treatment data also suggest that heparan sulfates do not solely mediate the position-specific ECM signaling. HepIII treatment of anterior and posterior ECM grafts did not produce equivalent results in terms of blastema formation and pattern formation. Therefore, the position-specific ECM properties though dependent on heparan sulfates, cannot be completely accounted for by heparan sulfates alone. I will discuss a few experiments implicating chondroitin sulfate in regulating regenerative responses during

limb regeneration in Chapter 4. In addition, other biologically active ECM molecules such as dermatan sulfate, keratan sulfate, collagen, fibronectin and tenascin also likely play a role in position-specific growth factor regulation and mediation of positional information.

It may be surprising that the artificial ECM of porcine heparan sulfate induced *de novo* limb pattern; however, it is equivalent to the earlier finding by Schaller and Muneoka that an artificial ECM containing heparan sulfate induced ectopic limb pattern when grafted into a chick limb bud (Schaller and Muneoka, 2001), which motivated us to do the comparable experiment using our assay for limb regeneration. The fact that this source of heparan sulfate (porcine intestinal mucosa, Sigma) is rich in 3-O sulfation (personal communication, R. Lawrence, Esko Lab UCSD) is consistent with the finding that posterior ECM grafts induced *de novo* pattern and also have higher levels of 3-O sulfotransferase expression. Our finding that purified ECM macromolecules (porcine heparan sulfate) can induce axolotl blastema cells to form limb structures *de novo*, as well as the report that mammalian growth factors (FGF and BMP) can induce blastema formation (Makanae et al., 2013), indicates that the signals regulating regeneration are conserved between salamanders and mammals. The ability of axolotl regeneration competent cells to respond to mammalian heparan sulfate suggests that the axolotl (Accessory Limb Model in particular) can be a powerful assay for mammalian positional information and dedifferentiation/differentiation signals crucial for the development of regenerative therapies.

Further evidence that quantitative changes in heparan sulfate can regulate the regenerative response comes from the responses of wounds to artificial ECM grafts

(Table 2.3; Figure 2.3; Figure 2.4). At an intermediate concentration of heparan sulfate, blastemas formed and nearly half of them formed complex patterns. At lower concentrations of heparan sulfate, blastema formation was inhibited; whereas, at higher concentrations pattern formation was inhibited. These results correlate well with the finding that posterior ECM (less sulfated HS) induced pattern formation and anterior ECM (more sulfated HS) did not.

The increase of pattern formation by FGF2 but inhibition of pattern formation by FGF8 treatment is further evidence for the qualitative specificity of the ECM modifications involved in regulating this phenomenon. Different sulfation modifications of heparan sulfate are known to regulate specifically the affinity for different members of the FGF family (Guimond et al., 1993). Since I did not observe anti-regeneration activity associated with posterior ECM, I presume that there are posterior-specific heparan sulfate modifications that do not bind the inhibitory factor, or that synthesis of the factor is restricted to the anterior portion of the limb. Further studies of position-specific sulfation patterns of heparan sulfate will be required to answer these questions.

Schaller and Muneoka also demonstrated FGF specificity in ECM regulation of anterior/posterior limb patterning (Schaller and Muneoka, 2001). They demonstrated that ECM derived from mouse posterior limb bud cells could induce a secondary ZPA and posterior supernumerary structures when grafted into the anterior of a chick limb bud. However, if the ECM was treated with FGF2 or FGF8, the ability to induce a secondary ZPA and supernumerary limb structures was lost. Alternatively if FGF4 or FGF10 was used, the secondary ZPA and supernumeraries were maintained. These experiments provided in part the conceptual basis for my own FGF experiments.

The ability of ECM grafts treated with FGF2 to induce ectopic limb patterns indicates that dedifferentiated anterior blastema cells can be reprogrammed to acquire a more posterior identity by regulating FGF signaling. Thus increasing FGF2 signaling induces (Table 2.5; Figure 2.6A; Figure 2.7A-C) or enhances (Table 2.6; Figure 2.6B; Figure 2.7D-H) pattern formation. This is consistent with previous studies by Anderson et al showing that FGF2 can help mouse limb bud cells in culture maintain their posterior identity or convert from anterior to posterior identity (Anderson et al., 1993, 1994)

It may be possible, that in addition to posteriorizing the ECM grafts, FGF2 is proximalizing the ECM grafts. Although this particular study focused on anterior/posterior patterning, the Polar Coordinate Model and the concept of positional information applies to all the limb axes, including the proximal/distal axis. Positional disparity across the proximal/distal axis also induces growth and intercalation (Bryant et al., 1981; French et al., 1976; McCusker and Gardiner, 2013). Satoh et al had demonstrated that beads of FGF2 can proximalize growth and intercalation (Satoh et al., 2010a). The regenerates in this study resulting from FGF2 treated ECM grafts seem to display a more proximal morphology (Figure 2.7). Therefore, the increase in pattern formation by FGF2 treatment may be the result of posterior and/or proximal positional information. It may be the case that the heparan sulfate independent pattern formation induced by HepIII and FGF2 anterior ECM grafts was a result of proximal/distal intercalation rather than anterior/posterior intercalation, and that the increase in pattern formation by posterior ECM with FGF2 treatment was a result of anterior/posterior

(posterior ECM induced) intercalation in addition to proximal/distal intercalation (FGF2 induced).

Both HS6ST1 and NDST2 were expressed at higher levels in the anterior portion of blastemas, and both add high levels of sulfate to glycosaminoglycan substrates (Thacker et al., 2013). In contrast, HS3ST1 was expressed at higher levels in the posterior portion of blastemas, but it has a low level of sulfation activity (Thacker et al., 2013). Similar expression patterns of HS2ST1, HS3ST1 and HS6ST1 in the regenerating limb of the axolotl were found by Stewert et al using RNA-seq (Stewart et al., 2013). A similar anterior/posterior differential expression pattern of HS6ST1 in the developing chick limb bud (Kobayashi et al., 2010; Nogami et al., 2004) was found to be playing a similar functional role (regulation of limb development by FGF8 signaling). These expression data predict that the overall level of ECM sulfation is higher on the anterior side of the blastema as compared to the posterior side. This prediction was confirmed by the Blyscan GAG sulfation analysis (Figure 2.10).

The findings presented in this study have at least three implications towards the long term goal of developing regenerative therapies for humans. First, decades after its first conceptualization, a molecular mechanism for positional information in the Polar Coordinate Model (Bryant et al., 1981; French et al., 1976) has been discovered. With the explosion of knowledge about stem cell biology and the development of iPS cell technologies, the major challenge of regenerative medicine moving forward will be to learn how to coordinate the differentiation of multipotent cells in order to recreate functional pattern while minimizing the risk of teratomas.

Second, live axolotl cells are not required to induce pattern formation during limb regeneration. Therefore, development of regenerative therapies will be saved the complications and risks of trying to use grafts of salamander cells in humans. Going forward, regeneration can focus on the more tractable challenge of how to manipulate and maintain signaling by the ECM.

Third, this study demonstrates that mammalian heparan sulfate is sufficient to induce pattern formation. Therefore, now that we know that mammalian heparan sulfate can be used to mediate positional information, we no longer have to use salamander ECM and can use mammalian sources of heparan sulfate instead. In so doing, it will be possible to screen for the effects of specific ECM modifications and thus reduce the risk of future adverse effects in humans.

Materials and Methods

Ethics statement

This study was carried out in accordance with the recommendations in the Guide for Care and Use of Laboratory Animals of the National Institutes of Health. The experimental work was conducted in accordance with procedures approved by the Institutional Animal Care and Use Committee of the University of California Irvine.

Animals

Experiments were performed on white and wild-type axolotls (*Ambystoma mexicanum*) measuring 12-15 cm snout to tail tip that were spawned at the University of California Irvine or at the Ambystoma Genetic Stock Center at the University of Kentucky. The animals were maintained in 40% Holtfreter's salt solution and were anesthetized prior to any procedure in a 0.1% solution of MS222 (Ethyl 3-

aminobenzoate methanesulfonate salt, Sigma), pH 7.4. After every surgical procedure, animals were placed on ice for two hours to allow the wound to heal and to stabilize the placement of the nerve and ECM grafts, after which the animals were returned to 40% Holtfreter's solution.

Induction of ectopic blastemas and limbs

The technique for inducing ectopic blastemas and limbs from wounds on the side of the limb has been described in detail previously (Endo et al., 2004; Satoh et al., 2007). Briefly, full-thickness skin wounds on the anterior side of the limb were created by surgically removing a square of skin (2-3 mm on a side) from the anterior side of the stylopod (region of the humerus/femur), making sure that the underlying muscle was not damaged (Figure 2.1A, D). An ectopic blastema was induced by surgically deviating the brachial nerve beneath the skin to bring the cut end of the nerve to the center of the skin wound (Figure 2.1B, E). As demonstrated previously, to induce an ectopic limb, it was necessary to graft a piece of full-thickness skin from the side of the limb that was opposite from the wound (Endo et al., 2004; Satoh et al., 2007). In this study I used two variations of this surgical procedure and grafted either decellularized skin (ECM graft, Figure 2.1C, F) or artificial ECM (Figure 2.3A) in place of the full-thickness skin. Wounds that were created on the posterior side of the arm responded to a deviated nerve and/or skin graft the same as anterior wounds (Endo et al., 2004). However, because of the anatomy of the limb, the deviated nerve and grafts in posterior wounds often became dislodged or damaged when the animal recovered from anesthesia and began swimming. I therefore focused on the response of anterior wounds to ECM-mediated signaling.

ECM preparation

Cell-free (decellularized) ECM grafts were prepared by rinsing 2 mm x 2 mm pieces of full-thickness skin in Ca^{+2}/Mg^{+2} free Hanks solution, followed by incubation in 2 M urea for 15 minutes. Samples were then rinsed in PBS and stored in PBS at 4°C until grafted (Schaller and Muneoka, 2001). Axolotl limb skin ECM was derived from white and wild-type axolotls 12-15 cm snout to tail tip.

Extensively treated ECM grafts were prepared by immersing 2 mm x 2 mm pieces of full-thickness skin in hypotonic Tris buffer (10mM Tris, pH 7.5, 10mM NaCl, 10mM EDTA) containing 0.35mg/l phenylmethyl-sulfonyl fluoride (PMSF) at 4°C for 24h with constant agitation. The tissue was then extracted by immersion in 1% Triton X-100 in tris-buffered saline (TBS) with PMSF for 24h at 4°C with agitation, rinsed in Hank's balanced salt solution, treated with 10 U/ml DNase I at 37°C for 1h, and rinsed in PBS and stored in PBS at 4°C until grafted. (Procedure adapted from protocol obtained through correspondence with Dr. Tetsuya Endo).

ECM treatments

Heparan sulfate moieties were removed enzymatically by incubating decellularized ECM preparations in 0.008 IU/ml heparitinase (Seikagaku) for 4 hours at 37°C, after which they were rinsed in PBS and stored in PBS at 4°C until grafted. Growth factors and other signaling molecules that were bound to the ECM grafts were removed by incubating decellularized ECM preparations in 1M or 2M NaCl for 4 hours at room temperature, after which they were rinsed in PBS and stored in PBS at 4°C until grafted (Schaller and Muneoka, 2001). Growth factors were incorporated into ECM grafts by incubating decellularized ECM preparations in 500 µg/ml FGF2 or FGF8 (R&D

Systems) for 2 hours at room temperature, after which they were rinsed in PBS and grafted into host wounds.

Artificial ECM preparation

Artificial ECM was made by combining 100 µl of 2.5 mg/ml (low HS), 5.0 mg/ml (medium HS), or 10 mg/ml (high HS) heparan sulfate (porcine intestinal mucosa; Sigma) with 1.2 ml of 5.0 mg/ml type-I collagen (calf skin; Sigma). This solution was incubated overnight at 4^{o}C to form a precipitate that was then pelleted by centrifugation (10,000 rcf for 15 minutes) and grafted (Schaller and Muneoka, 2001). Fast Green FCF and India ink were used to visualize the graft and determine that it was still present in the wound site post-grafting (Figure 2.3A, 2.3B).

ECM grafting

The host site was prepared by creating a full-thickness wound and surgically deviating the brachial nerve as described above. A wound epithelium formed and covered the wound within 6 to 12 hours (Endo et al., 2004). The next day (18 to 24 hours post-wounding) an incision was made through the uninjured skin adjacent to one side of the skin wound, and fine-tipped forceps were used to create a tunnel underneath the wound epithelium into which the graft was placed. ECM grafts were inserted through the tunnel with forceps and positioned adjacent to but not in contact with the deviated nerve (Figure 2.1C, 2.1F). As with ECM grafts, artificial ECM was grafted 18-24 hours after the initial surgery to create a wound and deviate a nerve. Because artificial ECM was viscous and could not be easily manipulated with forceps, the grafting procedure was modified by making an incision along three sides of the initial wound, the wound epithelium was then lifted up, and the artificial ECM graft was placed adjacent to but not

in contact with the deviated nerve. The wound epithelium was then repositioned and allowed to heal back in place.

Histological analysis

Skeletal elements in whole-mount preparations were imaged and analyzed by fixing samples in 4% PFA. They then were stained with 0.03% Alcian Blue 8GX (Sigma) and 0.01% Alizarin Red S (Sigma), and cleared with decreasing graduations of potassium hydroxide (KOH) and increasing graduations of glycerol.

Reverse-transcription PCR

RNA was collected using an RNeasy Mini Kit (Qiagen). cDNA was reverse transcribed with Transcriptor (Roche) for subsequent PCR with goTaq Green PCR Mix (Promega). After 25 cycles (30 seconds at 95^{o}C, 30 seconds at 58^{o}C, 30 seconds at 72^{o}C) PCR products were separated by electrophoresis and visualized with Ethidium Bromide. Quantitative RT-PCR was performed on a Roche LightCycler 480 with LightCycler 480 SYBR Green I Master. To design primers, EST sequences of heparan sulfate sulfotransferases were retrieved from the Ambystoma Database (http://www.ambystoma.org/) according to homology to known full sequences using tblastx. Primer3 was used to create primer sequences that generate 150-200 base pair amplicons. EF1α was used as the normalizing expression control adapted from (Satoh et al., 2007).

HS2ST1	Forward: 5'- TGCGCTTAGCCAAAGATTCCGCG
	Reverse: 5'- AGGAAAAGCATTGCCACCCCGA
HS3ST1	Forward: 5'- TGCCGGCGTAACACAAACTAGCG
	Reverse: 5'- GGGACCGCTGTTTGCACGAGT
HS3ST2	Forward: 5'- TGGTGGTGCGAAACCCGGTT
	Reverse: 5'- TTTCACCGGCTGGGTCCGTG
HS3ST3B1	Forward: 5'- CCGCCAATGTGTCGTCATCGTCG
	Reverse: 5'- TTGGGCGGCAGAGAGGCATTC

HS3ST4	Forward: 5’- TTGTGACCAAGGACGCCCCAAAG
	Reverse: 5’- TGTCTATCAAGCCGGTGCTGGCA
HS6ST1	Forward: 5’- ACGCCTGACCCACACTACGTCA
	Reverse: 5’- CCAGGCGCACATTTTGTACCAGGT
NDST1	Forward: 5’- CCTCAGCGTCTTTGTCTCCGCA
	Reverse: 5’- AGGGGTCCGTGCGGGATGAATC
NDST2	Forward: 5’- CACACGCATGAAGGTGTCCGATGT
	Reverse: 5’- TCTGCTCTGCCAGGACAGTGACA
NDST3	Forward: 5’- GAAGCTTGCCCTGTCTCTTGATCGG
	Reverse: 5’- AGAACTCATCCGACCGACCCCA
NDST4	Forward: 5’- AAAACTGGCACCACGGCACTGT
	Reverse: 5’- GCGCCAACTCGTTTTGGGGCTT
EF1α	Forward: 5’- AACATCGTGGTCATCGGCCAT
	Reverse: 5’- GGAGGTGCCAGTGATCATGTT

RNA *in situ* hybridization

RNA *in situ* hybridization was performed on paraffin-sectioned axolotl limb tissues as previously described (Lee and Gardiner, 2012). Digoxigenin (DIG)-labeled antisense RNA probes for axolotl HS3ST1, HS6ST1, and NDST2 were used to perform *in situ* hybridization. RT-PCR was performed to amplify the sequences for antisense RNA probes with gene specific PCR primers. The specific PCR primers for the individual genes were as follows:

HS3ST1	Forward: 5’- GATGGAAGAGAGAGATGCTTGC
	Reverse: 5’- CGTGCGGTGTTATCAAGAGATG
HS6ST1	Forward: 5’- GTCTCTACCACAAAGGTGGAAC
	Reverse: 5’- TCTAGAAGATGGCAAGGGTAGG
NDST2	Forward: 5’- CACTCAAAGCAAACTGAGGACC
	Reverse: 5’- GCAGGATGCATAGTGAGGAAAG

All template clones were subcloned into the pCRII vector (Invitrogen). The RNA probes were synthesized with the DIG RNA Labeling Kit (Roche) according to the manufacturer’s protocol using T7 or Sp6 RNA polymerases. For tissue sample collection, tissues were collected and fixed in MEMFA (0.1M MOPS, pH7.4, 2 mM EGTA, 1 mM MgSO4, 3.7% formaldehyde), skeletal tissues were decalcified in

Decalcifier I, dehydrated with an ascending series of ethanol (25%, 50%, 75% and 100%), cleared in xylene, and embedded in paraplast. Paraffin sections were cut at 6μm thickness. Sections were treated with 7.5 μg/ml of Proteinase K (Invitrogen) for 20 min at 37°C, refixed with 4% paraformaldehyde, and then hybridized with antisense RNA probes at 60°C overnight. After hybridization, sections were washed with buffer #1 (Formamide: water: 20X SSC = 2:1:1), then with buffer #2 (5:4:1), and blocked with 2% blocking reagent (Roche) in TBST for 30 min. The sections were then incubated with 1:2,000 diluted alkaline phosphatase (AP)-conjugated anti-DIG antibody (Roche) overnight at 4°C. The color staining reaction was performed using BM purple (Roche) as a substrate for AP.

Glycosaminoglycan sulfation analysis

The level of glycosaminoglycan (GAG) sulfation was quantified by the dimethlymethylene blue assay (Blyscan Assay Kit, Biocolor, UK). Anterior and posterior limb skin samples were collected from the stylopod region of uninjured limbs with 2mm biopsy punches.

CHAPTER 3:

Positional Information in Mammalian Extracellular Matrix

Abstract

There are two essential requirements for limb regeneration; all the appropriate cell types need to be recruited to reform the missing structures and the behavior of these cells need to be orchestrated in order to remake the appropriate pattern of the limb. It is likely that variation in regenerative abilities between different organisms is a consequence of variability in the efficacy of these two fundamentally requisite processes. The challenge to understanding how to induce and enhance a regenerative response in animals that do not regenerate well (e.g. humans) is to discover which of these processes fail and why they fail.

The purpose of this study was to ascertain whether mammals can orchestrate cells to regenerate pattern. In the previous chapter, I determined that axolotls regenerate pattern through ECM-mediated heparan sulfate-dependent positional information. Therefore, the next logical question was whether this mechanism was conserved in mammalian ECM. I again used an *in vivo* gain-of-function assay to determine if ECM derived from mouse limb skin had similar regeneration regulating properties to axolotl limb skin.

I discovered that ECM from mouse limbs is capable of inducing limb pattern in axolotl blastemas in a position-specific, heparan sulfate-dependent manner. In addition, I found that the position-specific properties of mouse limb skin ECM changed though mouse skin development (E11.5 - PN9). As in the axolotl, it appears that this spatial-temporal variation of positional signaling in mouse limb skin ECM is regulated by differential regulation of the expression of specific heparan sulfate sulfotransferase enzymes that modify the sulfation patterns of heparan sulfates in the ECM.

The ability to regulate axolotl regeneration with mammalian ECM has allowed us to identify target mechanisms to induce regeneration in animals that cannot regenerate, such as humans. This study establishes a crucial functional link between salamander regeneration and mammals.

Introduction

The ability of animals to regenerate varies widely. Some (e.g. planarian and hydra) can regenerate an entirely new organism from relatively small pieces of their bodies; whereas, vertebrate regeneration is limited to organs (e.g. limbs in salamanders) or tissues (e.g. muscle and bone in mammals). In animals in which regenerative abilities are relatively limited in adults, this ability is typically greater at earlier stages and lost at later stages (Gardiner, 2005; Gardiner and Holmes, 2012). Thus, regenerative ability varies between species as well as between different stages of development within a species.

Based on studies from model organisms that can regenerate well, it is evident that there are two essential requirements for robust regeneration. In addition to the obvious necessity of generating/recruiting all the required cell types, it is necessary to orchestrate the behavior of these cells in order to remake the appropriate pattern of the limb (McCusker and Gardiner, 2014; Tamura et al., 2010). Therefore, variation in regenerative abilities presumably is a consequence of variability in the efficacy of these two fundamentally requisite processes, recruiting regeneration-competent cells and regulating pattern formation. The challenge to understanding how to induce and enhance a regenerative response in animals that do not regenerate well (e.g. humans) is to discover which of these processes fail and why they fail.

Regeneration is an intrinsically stepwise process that is initiated in response to injury (Endo et al., 2004). Since any given step must occur successfully in order for the system to progress to the next step, failure of one step results in the failure of all downstream steps to occur. Consequently, it is not possible to identify the downstream

steps in order to test whether or not they have the potential to occur (regenerative potential). Thus, one strategy for discovering how to induce regeneration in a non-regenerating animal is to identify the stepwise developmental process that are required by studying an animal that can regenerate (e.g. the axolotl) and then determining whether or not those processes can occur in mammals. It is possible to identify and assay for signals regulating each of the steps of regeneration in the axolotl by using the Accessory Limb Model (ALM). As described in Chapter 1 and Chapter 2, the ALM is an *in vivo* gain-of-function assay for signaling that regulates blastema formation and positional information during limb regeneration (Endo et al., 2004; Satoh et al., 2007).

Using the ALM, I was able to assay for positional information in cell-free ECM preparations (Chapter 2). The ability to assay ECM rather than cells allowed us to expand our study to include mammals in a way that was not possible before. In addition to the immune and graft rejection complications, mammalian and amphibians cells cannot survive at the same temperature (37^{o}C versus 22^{o}C). However, I found that mouse ECM grafts are tolerated and incorporated into axolotl regenerative blastemas.

By grafting mouse limb skin ECM into the axolotl ALM, I found that mouse limb skin ECM grafts can either inhibit blastema formation, can induce limb skeletal pattern, or can have no effect on regeneration depending on the source of the graft (anterior/posterior) or on the stage of development of the mouse skin (E11.5 - PN9) used as the graft source. For both axolotl and mouse ECM grafts, the ability of the ECM to provide position-specific signaling was dependent on the presence of heparan sulfate. Similar to the axolotl, spatial-temporal variation of positional signaling in mouse limb skin ECM was regulated by differential expression of specific heparan sulfate

sulfotransferases that modify the sulfation patterns of heparan sulfates in the ECM. This establishes a crucial functional link between salamander regeneration and mammals.

Results

Mouse ECM Induces Heparan Sulfate-dependent Pattern Formation in Axolotl Blastemas

Axolotls have an amazing ability to regenerate after traumatic injury; however, this ability is not observed in mammals. One strategy for enhancing the regenerative capacity of humans is to identify the requirements for successful regeneration in axolotls (Endo et al., 2004; Muneoka et al., 2008b), which would allow for the identification of the necessary steps that do not occur following injury in mammals. Given that axolotl limb ECM has the ability to regulate blastema formation and pattern formation, I tested whether mammalian ECM has comparable signaling abilities. To do this, I repeated the experiment of grafting urea-extracted/heparitinase-treated anterior and posterior ECM using neonatal (PN3-4) mouse limb skin rather than axolotl limb skin (Figure 3.1). Mouse limb skin ECM induced a range of regenerative responses when grafted into nerve-deviated wounds on the side of the axolotl arm (Figure 3.1). Similar to axolotl ECM, mouse ECM either inhibited blastema formation (Figure 3.1C), induced ectopic limb skeletal pattern (Figure 3.1E, Figure 3.2), or had no effect on regeneration.

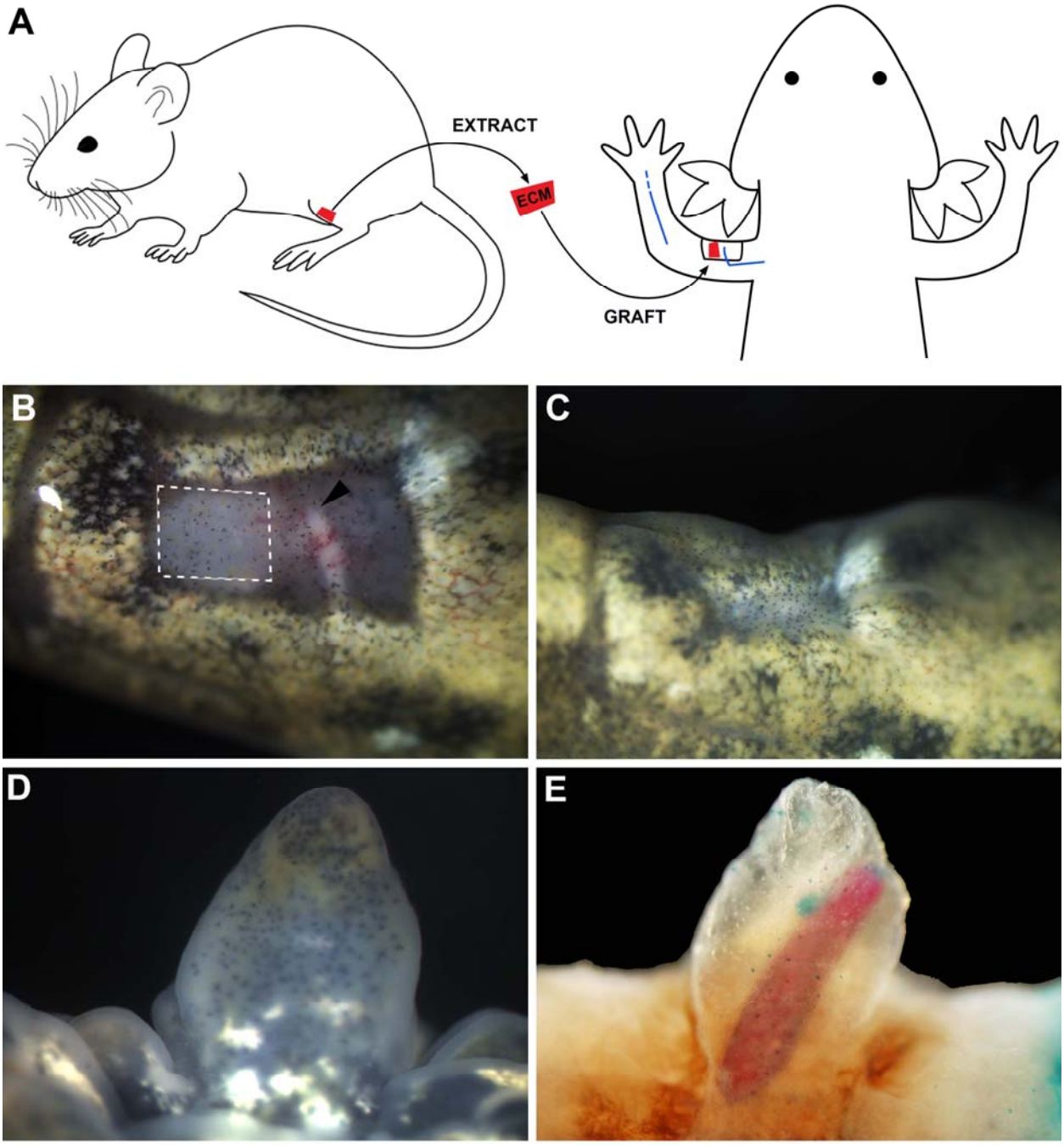

Figure 3.1. Utilization of the Axolotl Accessory Limb Model as an in vivo Gain-of-Function Assay for Positional Information in Mouse Limb Skin. (A) Schematic Diagram of Surgical Procedures. Mouse hindlimb (femur) skin samples (red) were collected from mice for ECM extraction and extracted ECM was grafted into an axolotl lateral skin wound with a deviated brachial nerve (blue) (B) Example of axolotl lateral skin wound with a deviated nerve (black arrowhead indicates end of nerve) and mouse skin ECM graft (outlined in white) 6 days post grafting (C) Example of result from grafting mouse anterior hindlimb skin ECM collected from postnatal day 1 mouse into axolotl lateral skin wound with a deviated nerve 14 days post grafting. (D) Example of blastema formation from grafting mouse posterior limb ECM into a wound with a deviated nerve 61 days post grafting (E) Whole-mount skeletal preparation of (D) A skeletal-like element formed by axolotl blastema cells in response to an ECM graft from the posterior of a mouse limb. red = ossified bone, blue = cartilage

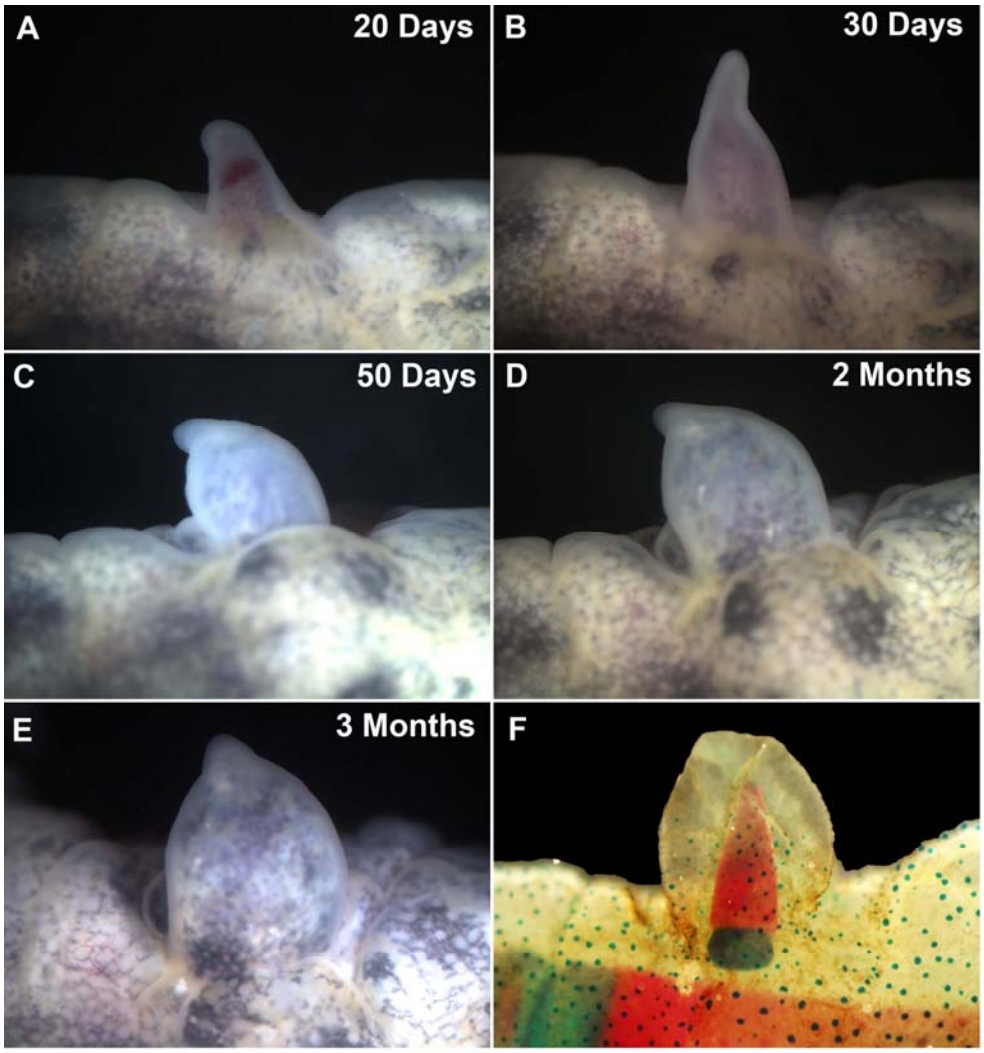

Figure 3.2. Ectopic Axolotl Skeletal Element Induced by Mouse Limb ECM. An example of the formation, growth and differentiation of an ectopic axolotl blastema that had received an ECM graft collected from a postnatal day 3-4 mouse at the indicated time points post grafting. 20 days (A), 30 days (B), 50 days (C), 2 months (D), 3 months (E,F). The final ectopic skeletal pattern was visualized after the ectopic blastema in (E) was collected, fixed and stained with alcian blue (cartilage) and alizarin red (ossified bone). Blue spots in (F) are dermal glands in the skin that stain with alcian blue.

Ectopic blastemas that formed limb pattern developed over the same time course as observed previously for ectopic limbs induced by a deviated nerve and posterior limb skin graft (Endo et al., 2004) (Figure 3.2). Nerve-deviated blastemas without a skin graft form and grow for about three weeks, and then are reintegrated into the host limb (Endo et al., 2004). In contrast, ectopic blastemas that form skeletal elements continue to grow and eventually ectopic skeletal elements differentiate (Figure 3.2F)

Unlike axolotl anterior ECM, mouse anterior ECM did not inhibit blastema formation (Figure 3.3 compare to Figure 2.2). Mouse anterior ECM grafts gave equivalent results to no graft (Figure 3.3).

Comparable to what was observed with axolotl posterior ECM grafts, mouse posterior ECM grafts induced limb pattern formation by axolotl blastema cells (Figure 3.1D-E, Figure 3.2), and this signaling ability was dependent on the presence of heparan sulfate since it was lost when the grafts were treated with heparitinase (HepIII) (Figure 3.3, Table 3.1). Previous studies demonstrated that skeletal elements are formed in nerve-deviated ectopic blastema only if positional information is provided (e.g. by grafting posterior skin (Endo et al., 2004)). Therefore, mouse skin ECM also contains the necessary positional information to induce limb skeletal formation in axolotl blastemas.

The skeletal elements induced by mouse limb ECM grafts were elongated, tapered at the tip and often formed cartilage at the proximal boundary (Figure 3.1E, Figure 3.2F); and thus appeared to be distal phalangeal elements. In all instances, these skeletal elements stained with alizarin red, indicating that they were calcified, and thus axolotl cells in the ectopic blastema were induced to differentiate as bone. In contrast, grafts of axolotl skin/ECM induced axolotl blastema cells to form cartilaginous (alcian blue positive) skeletal elements (Figures 2.1L, 3.1E, 3.2F). Thus posterior mouse ECM was able to induce limb-like pattern formation by axolotl cells, but these cells differentiated into calcified tissue that would be the fate of mouse mesenchymal cells, rather than into cartilage that would be their normal axolotl fate. Therefore, mouse

limb skin contains heparan-sulfate dependent anterior/posterior positional information that is similar to axolotl but with mammalian specific differentiation signals.

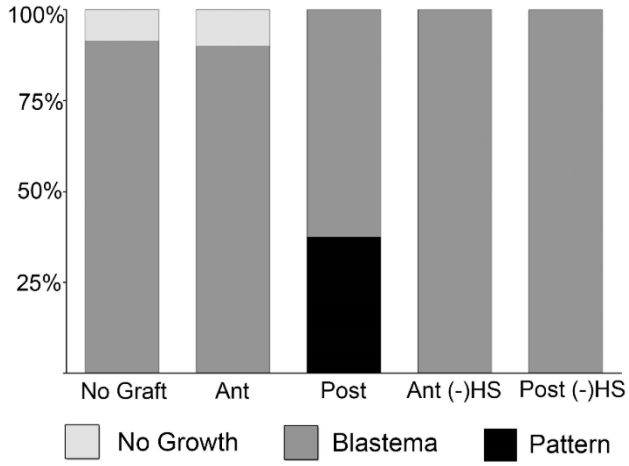

Figure 3.3. Posterior Mouse ECM Induces Heparan Sulfate-dependent Pattern Formation by Axolotl Blastema Cells. Differential regenerative responses to grafts of mouse-derived anterior or posterior ECM with or without heparitinase treatment. Ant = Anterior, Post = Posterior, (-) HS = heparitinase treatment to remove heparan sulfates from the ECM.

Table 3.1. The Position-specific Ability of Anterior/Posterior Mouse Limb Skin ECM Grafts to Induce Pattern Formation in Ectopic Axolotl Blastemas is Dependent on Heparan Sulfates

Graft Type	Total	Blastema*	Pattern**
No Graft	23	21 (91%)	0
Mouse Anterior ECM	10	9 (90%)	0
Mouse Posterior ECM	8	8 (100%)	3 (37%)
Mouse HepIII Anterior ECM	8	8 (100%)	0
Mouse HepIII Posterior ECM	10	10 (100%)	0

*percentage of total number of grafts that developed an ectopic blastema
**percentage of ectopic blastemas that developed skeletal elements with pattern

The Ability of Mouse Limb ECM to Affect Ectopic Axolotl Limb Regeneration is both Position-specific and Developmental Stage Dependent

Mouse limb ECM grafts collected between embryonic day 11.5 and postnatal day 9 (E11.5 - PN9) mice induced a range of regenerative responses when grafted into nerve-deviated axolotl wounds (Figure 3.4). Nerve-deviated wounds almost always form an ectopic blastema (Endo et al., 2004; Satoh et al., 2007). When ECM collected from

postnatal day 1 (PN1) mouse hindlimbs was grafted in a nerve-deviated axolotl wound, ectopic blastemas often did not form (Figure 3.4; 70% N=24). Since a nerve had been deviated surgically, the expectation was that all wounds should have formed an ectopic blastema (Endo et al., 2004; Satoh et al., 2007; Chapter 2). However, PN1 mouse limb ECM grafts inhibited axolotl blastema formation at a high frequency. This inhibitory activity appeared higher in ECM derived from the posterior side of the mouse limb (78% compared to 50% for anterior-derived grafts, Figure 3.4).

In contrast to PN1 ECM grafts, ECM grafts collected from limb buds of E11.5 mice had no effect on blastema formation, and all limbs formed an ectopic blastema as expected (Figure 3.4). ECM grafts from E11.5 and PN1 could be observed for at least 7 days post grafting (Figure 3.1B), but were no longer evident after 14 days (Figure 3.1C). Presumably there is an ontogenetic change in mouse ECM around the time of birth that makes it more resistant to remodeling and removal by the axolotl wound environment. Similarly, the axolotl wound microenvironment can regulate the integrity and persistence of the ECM, which is likely related to the observation that axolotl skin wounds heal without scar formation (Denis et al., 2013; Endo et al., 2004; Gilbert, 2013; Murawala et al., 2012).

Mouse skin ECM grafts from later stages (PN3 - PN9) induced axolotl blastema cells to form skeletal elements with digit-like patterns (Figure 3.1E, Figure 3.2F, Figure 3.4). The ability to induce limb pattern varied between anterior and posterior mouse ECM grafts such that PN3-4 posterior ECM induced pattern (38%, N=8) but PN3-4 anterior ECM did not (0%, N=10). The frequency of skeletal pattern induction increased for PN5-7 posterior ECM grafts (60%, N=5), but was lost by PN9 (Figure 3.4). A low

level of skeletal pattern induction was observed for anterior ECM grafts from PN5-7 (17%, N=12) as well as from PN9 (17%, N=6). Thus the ability of mouse limb skin ECM to affect ectopic axolotl limb regeneration was both position-specific and developmental stage dependent.

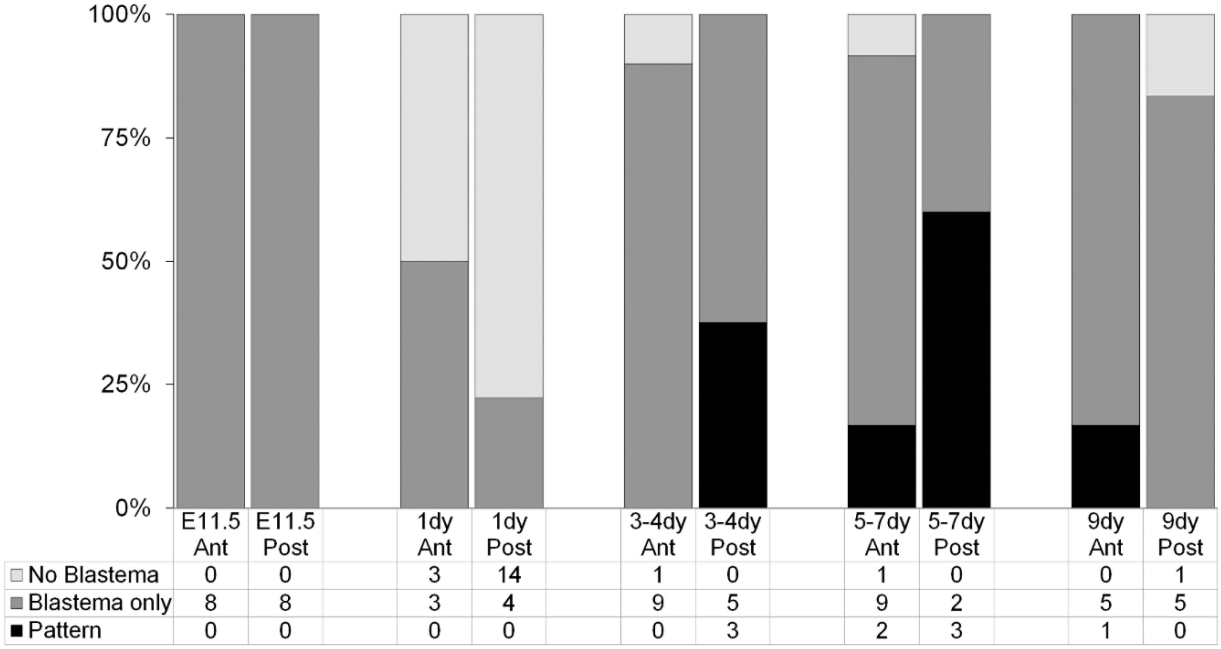

	E11.5 Ant	E11.5 Post	1dy Ant	1dy Post	3-4dy Ant	3-4dy Post	5-7dy Ant	5-7dy Post	9dy Ant	9dy Post
No Blastema	0	0	3	14	1	0	1	0	0	1
Blastema only	8	8	3	4	9	5	9	2	5	5
Pattern	0	0	0	0	0	3	2	3	1	0

Figure 3.4. Age-dependent Position-Specific Abilities of Mouse-derived ECM grafts to affect the Behavior of Axolotl Blastema Cells. E11.5 = mouse embryonic day 11.5, 1dy = mouse postnatal day 1, 3-4dy = mouse postnatal day 3-4, 5-7dy = mouse postnatal day 5-7, 9dy = mouse postnatal day 9, Ant = Anterior, Post = Posterior, No Blastema = no growth observed (example Figure 3.1C), Blastema only = Growth of blastema observed (example Figure 2.1H) but no pattern (no skeletal elements induced), Pattern = Blastema growth followed by pattern development confirmed by alcian blue and alizarin red skeletal preparation (example Figures 3.1E, 3.2F).

The Expression of Heparan Sulfate Sulfotransferases is Differentially Regulated in both Time and Space

Based on the finding that the ability of mouse limb skin ECM to induce pattern formation in axolotl blastemas is dependent on heparan sulfates (Figure 3.3), I hypothesized that there is differential regulation of heparan sulfate across the anterior

and posterior axis established by differential expression of heparan sulfate sulfotransferases during mouse skin development.

I analyzed the expression of seven mouse heparan sulfate sulfotransferases (HSSTs) that are expressed in mouse hindlimb skin in PN3-4 and PN9 stage mice by semi-quantitative RT-PCR (Figure 3.5). Similar to axolotl HSST expression during regeneration (Figure 2.8), NDST2 and HS6ST1 were more highly expressed in the anterior mouse limb skin at PN3-4. Although expression of HS3ST1 was not higher in the posterior skin like in the axolotl, expression of both HS3ST2 and HS3ST3a appeared to be higher in posterior skin. In addition, NDST1 and HS2ST1 were also more highly expressed in PN3-4 anterior mouse limb skin (Figure 3.5). Strikingly, these position-specific expression profiles were not observed in skin from PN9 day mice.

By postnatal day 9, expression of NDST1, HS3ST1, HS3ST2, and HS3ST3a were no longer expressed at detectable levels, and NDST2 appeared to change to a more posterior expression in mouse limbs. Taken together the mouse HSST expression patterns correlated well with the position-specific age-dependent ability of mouse limb skin ECM to induce limb pattern formation.

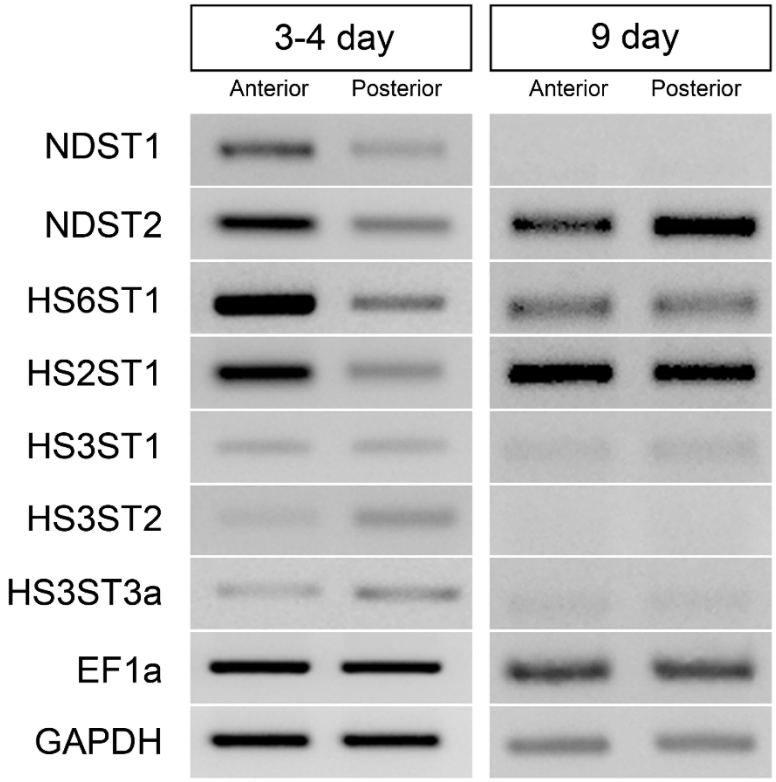

Figure 3.5. Age-dependent Anterior/Posterior Differential Expression of Heparan Sulfate Sulfotransferases in Mouse Skin. Reverse-transcription PCR expression analysis of heparan sulfate sulfotransferases in the anterior and posterior skin of mouse hindlimb (femur) during postnatal day 3-4 (PN3-4) and postnantal day 9 (PN9). Similar to the axolotl, N, 6-O and 2-O sulfotransfereases are more highly expressed in the anterior of the limb in 3-4 day old mice (compare to Figure 2.8). Differential expression diminished by postnatal day 9. EF1α and GAPDH were used as loading controls.

Discussion

The use of the ALM to assay for pro- and anti-regenerative activity by the ECM has allowed us to address the critical question of whether what happens in an axolotl has relevance to what happens in mammals.

In this study, I was able to assay for regeneration-associated signaling properties in mammalian skin. I was able to do this because of the *in vivo* gain-of-function assay (the ALM) for factors that regulate regeneration, and because of the finding that axolotl ECM is sufficient to mediate positional information. Given the differences in physiology of axolotls and mammals (e.g. temperature), it is not possible to test the ability of mammalian cells to participate in axolotl regeneration. However, it is possible to assay

for positional information in the cell-free ECM. I therefore have been able to demonstrate that mouse limb skin ECM has position-specific signaling properties that are comparable to axolotl ECM and that these properties likely are mediated by spatial and temporal regulation of sulfation patterns in the ECM; thus, establishing a critical functional link between the response to injury in axolotls and mice.

My data demonstrating the presence of position-specific signaling properties of mouse limb skin are consistent with earlier studies from developing mouse limb buds in which cultured posterior mouse limb bud cells synthesized ECM that induced ectopic limb pattern when grafted into the anterior region of chick limb buds (Schaller and Muneoka, 2001). Our finding that mouse ECM and purified ECM macromolecules (porcine heparan sulfate) can induce axolotl blastema cells to form limb structures *de novo* (Chapter 2, Figure 2.3), as well as the report that mammalian growth factors (FGF and BMP) can induce blastema formation (Makanae et al., 2013), indicate that the signals regulating regeneration are conserved between salamanders and mammals. The ability of axolotl regeneration competent cells to respond to mouse ECM by generating mammalian-specific ossified tissue suggests that the axolotl (ALM in particular) can be a powerful assay for mammalian positional information and differentiation signals crucial for the development of regenerative therapies.

I found that the signaling properties of mouse limb ECM change over a short period of time after birth of the mouse embryo. The dynamic nature of the pro-regenerative properties of mouse ECM is consistent with the generalization that regenerative abilities are associated with earlier developmental states and then decline with age (Gardiner and Holmes, 2012; Menger et al., 2010; Muneoka et al., 2008b). The

phenomenon of this ontogenetic decline in regenerative abilities has been extensively studied during frog metamorphosis and a number of hypothesis have been proposed (Levin, 2012; Muneoka et al., 1986; Sessions and Bryant, 1988; Slack et al., 2004). Although technically difficult to study in mammals, it appears that regenerative abilities are greater at earlier stage mammalian embryos, and lost at later stages (Gardiner and Holmes, 2012; Muneoka et al., 2008b). I hypothesize that the changes in the properties of mouse limb ECM maybe to related to the changes that cause the decline of regenerative ability in mammals. However, this hypothesis requires further experimentation.

For both the mouse and the axolotl, the underlying mechanism for ECM mediated signaling is associated with position-specific differential expression of heparan sulfate sulfotransferases. A similar model of regulation of growth and pattern formation by spatial and temporal modifications of heparan sulfates has been hypothesized for developing chick limb buds (Kobayashi et al., 2010; Nogami et al., 2004). For the mouse, HSST expression correlates with graft results. At the developmental stages when there were anterior/posterior grafting differences (PN3-4), HSSTs were differentially expressed. When there were less anterior/posterior graft differences (PN9), there was less differential HSST expression. Collectively, these findings suggest that there is a conserved function for heparan sulfate modifications in both mouse and axolotl ECM. The change in mouse expression over time compliments previous studies that have found that most differences between human fetal and adult skin were at the level of dermal ECM molecule expression and that dermal ECM components are important in fetal scarless wound healing (Coolen et al., 2010).

A better understanding of the mechanisms of ECM mediated regenerative signaling will be relevant for regenerative engineering approaches to treating injuries (Laurencin and Khan, 2013). Not only can ECM grafts provide information that is necessary for forming new structures, they also can direct the differentiation of target cells. Thus axolotl ECM induced chondrogenesis and mouse ECM induced osteogenesis in the same population of axolotl host cells in the wound. This finding indicates that engineered changes in biomaterials for implantation can differentially and specifically regulate behavior of the host cells The ability of synthesized materials to regulate the regenerative response can be assayed using the ALM, which could allow for the design and engineering of grafts that would mimic the necessary ECM modifications and thus bypass the need to regulate the expression of genes responsible for those modifications (e.g. sulfotransferases) in time and space.

Finally, the observation that ECM from E11.5 and PN1 mouse limb ECM was remodeled and resorbed by the axolotl wound microenvironment provides an opportunity to explore wound healing and scar formation. In the present study, I observed dramatic changes in the ECM of mouse skin that occurred over a brief period of time (Figure 3.4). Initially (E11.5) the ECM had no effect on regeneration and was quickly remodeled and resorbed. Shortly thereafter (PN1), the ECM inhibited regeneration. A few days later (PN3-4 and PN5-7), the ECM changed again, gaining the ability to persist in the wound and to induce axolotl blastema cells to make patterned skeletal elements. However by PN9, this position-specific ability declined. It should be noted that although the grafted mouse ECM changed, the axolotl host cells were essentially the same (at least before grafting). Thus, further studies of the interaction of

mouse ECM with axolotl connective tissue cells in an axolotl wound environment could lead to novel insights into the regulation of fibroblast biology and fibrosis.

A fundamental question in regenerative biology is why amphibians (salamanders) regenerate so well, but mammals (humans, mice) do not. Towards answering that question, I have discovered that mammals do have the positional information necessary to mediate pattern regeneration; although, it is lost as the animal ages. This finding is encouraging in terms of inducing regeneration in humans because we initially had this ability as embryos. I hypothesize that the ability of mammals to regenerate is not lost during evolution, but rather is lost through aging. Therefore, increasing regenerative ability in humans involves identifying the required regeneration factors lost during aging and engineering methods to reintroduce them safely and effectively.

Materials and Methods

(not already described in previous chapters)

Surgical Procedures

The technique for inducing ectopic blastemas and limbs from wounds on the side of the limb has been described in detail previously (Endo et al., 2004; Satoh et al., 2007, Chapter 2). In this study, I used a variation of this procedure where decellularized mouse skin (ECM graft, Figure 3.1) was used in place of the axolotl full-thickness skin.

Mouse anterior or posterior hindlimb stylopod skin or limb bud ECM was derived from FVB/NJ mice (E11.5-PN9). Pilot experiments with ECM derived from C57BL/6J or NOD SCID mice PN3-4 mice gave similar results, suggesting there is not mouse strain specificity. Cell-free (decellularized) ECM grafts were prepared by rinsing 2 mm x 2 mm pieces of full-thickness skin or limb bud halves in Ca^{+2}/Mg^{+2} free Hanks solution,

followed by incubation in 2 M urea for 15 minutes at room temperature. Samples were then rinsed in PBS and stored in PBS at 4°C until grafted (Schaller and Muneoka, 2001). Heparan sulfate moieties were removed enzymatically by incubating decellularized ECM preparations in 0.008 IU/ml heparitinase (Seikagaku) for 4 hours at 37°C, after which they were rinsed in PBS and stored in PBS at 4°C until grafted.

The host axolotl wound site was prepared by creating a full-thickness lateral skin wound and surgically deviating the brachial nerve as described previously(Endo et al., 2004). A wound epithelium formed and covered the wound within 6 to 12 hours (Endo et al., 2004). The next day (18 to 24 hours post-wounding), an incision is made along three sides of the initial wound, the wound epithelium was then lifted up, and the mouse ECM graft was placed adjacent to but not in contact with the deviated nerve. The wound epithelium was then repositioned and allowed to heal back in place.

Reverse-Transcription PCR

RNA was collected using an RNeasy Mini Kit (Qiagen). cDNA was reverse transcribed with Transcriptor (Roche) for subsequent PCR with goTaq Green PCR Mix (Promega). After 25 cycles (30 seconds at 95^{o}C, 30 seconds at 58^{o}C, 30 seconds at 72^{o}C) PCR products were separated by electrophoresis and visualized with Ethidium Bromide. Primer3 was used to create primer sequences that generate 150-200 base pair amplicons. EF1α and GAPDH were used as the normalizing expression controls.

NDST1	Forward: 5’- GCTTCCCAAAGCTTCTTATC
	Reverse: 5’- AAGAACTCCATGTACCAGTC
NDST2	Forward: 5’- CTGCTGATTGGTTTCAGTCTTGT
	Reverse: 5’- CCACTGCTACTACAGTCTCCC
HS6ST1	Forward: 5’- CGGACCCACATTACGAGAAAA
	Reverse: 5’- GATTGGGCCGATAGCAGGTG
HS2ST1	Forward: 5’- TATGATGCCGCCCAAGTTG
	Reverse: 5’- CTGTTCAATTTCTCGGACTTCGT

HS3ST1	Forward: 5’- CCCAGCTTGTGCATTCCCA
	Reverse: 5’- TGTGGAACCATTGGATGCTGT
HS3ST2	Forward: 5’- GTGGACGTGTCTTGGAACG
	Reverse: 5’- CACTGACGAAGTGGATCTGGG
HS3ST3a	Forward: 5’- ACCGGGATTTGATGCCCAG
	Reverse: 5’- GTCTGCGTGTAGTCCGAGAT
EF1α	Forward: 5’- CAACATCGTCGTAATCGGACA
	Reverse: 5’- GTCTAAGACCCAGGCGTACTT
GAPDH	Forward: 5’- TGTGTCCGTCGTGGATCTGA
	Reverse: 5’- TTGCTGTTGAAGTCGCAGGAG

CHAPTER 4:

Extracellular Factors in Axolotl Limb Regeneration

Introduction

The previous two chapters of this dissertation have focused on positional information and specifically on induction of pattern formation by heparan sulfate glycosaminoglycans in the ECM. However axolotl limb regeneration is a complex process integrating many factors regulating multiple steps. In this next chapter, I will discuss other factors important in axolotl limb regeneration including: nerve signaling, HSPG core protein expression, and chondroitin sulfate.

First, I have focused thus far on the third step of regeneration, positional information to induce pattern formation. However, a major area of research in regeneration is discovering how to induce regeneration-competent multipotent progenitor cells *in vivo* by neurotrophic signaling from the nerve to induce blastema formation. I have integrated the findings of blastema induction studies with my positional information data in Chapters 2 and 3 to synthetically induce axolotl limb regeneration with all defined, commercially available mammalian-derived factors.

Second, everything discussed thus far has focused on the role of heparan sulfate glycosaminoglycans in mediating positional information. However, heparan sulfates are synthesized covalently attached to core proteins known as heparan sulfate proteoglycans (HSPGs). In order to better understand the role that the core proteins play in regeneration, I have analyzed the expression of membrane HSPGs and found that syndecan 1, syndecan 2, glypican 1, and glypican 6 are expressed during axolotl limb regeneration.

Lastly, although I have focused on heparan sulfate glycosaminoglycans in the ECM, there are numerous other bioactive ECM components capable of regulating

regenerative responses. I have investigated the properties of a glycosaminoglycan that is similar to heparan sulfate, chondroitin sulfate and found that it can affect axolotl limb regeneration.

Results and Discussion

A Limb from Scratch: Synthetic Induction of Axolotl Limb Regeneration by Defined Mammalian Factors

A major goal in the field of regeneration is to learn how the salamander regenerates and then use this information to develop therapies to induce a regenerative response in humans. The Accessory Limb Model (ALM) was designed to advance this goal by functioning as an *in vivo* gain-of-function assay for the requirements of axolotl limb regeneration (Endo et al., 2004; Satoh et al., 2007).

The ALM demonstrated that there are three discrete steps required for axolotl limb regeneration: 1) formation of a wound epithelium generated by wound healing following injury, 2) neurotrophic signaling between the cut end of a nerve and the wound epithelium to induce dedifferentiation and formation of a mass of multipotent progenitor cells (blastema formation), and 3) positional information that instructs the blastema cells where to differentiate in order to reform the lost pattern.

The ALM allows for the functional testing of candidate signaling factors that are required for each step in regeneration: wound healing, blastema formation, and pattern formation. Although a limb can be induced *de novo* by surgically deviating a nerve and grafting skin in an axolotl, these techniques are not realistic for human therapies. Therefore, discovering the underlying mechanisms by which the nerve and skin grafts

function and how they can be replaced with human viable strategies would be the most important step to moving the field of regeneration towards medical application.

Data presented in Chapter 2 (Figures 2.3-2.4) demonstrated that the pattern-inducing activity can be mimicked by grafts of artificial ECM composed of purified mammalian factors (porcine heparan sulfate and bovine collagen) as a substitute for a skin graft. Similarly, the signaling from a deviated nerve can be mimicked by implanting gelatin beads that have been soaked in purified human growth factors (FGF and BMP) into an axolotl wound, which results in blastema formation (Makanae et al., 2013). Since the two steps required for stimulating an axolotl wound to form an ectopic limb (blastema formation and pattern formation) can be induced individually by defined mammalian factors, I reasoned that a combination of these factors should be sufficient to induce axolotl limb regeneration with a deviated nerve or skin graft.

A *de novo* ectopic limb (limb from scratch) was induced in response to grafts of five commercially available, mammalian-derived factors (Figure 4.1). As reported previously (Makanae et al., 2013), an ectopic blastema was induced either by surgically deviating the brachial nerve (Endo et al., 2004), or by grafting an acidic gelatin bead (Figure 4.1B, white, black arrowhead) soaked in recombinant human FGF2, FGF8, and BMP2 (300 ng/μl, R&D Systems). At the same time, artificial ECM (porcine heparan sulfate isolated from intestinal mucosa, Sigma) and bovine type I collagen (isolated from calf skin, Sigma) was grafted into the wound bed (Figure 4.1A-B, blue, outlined in white). An ectopic blastema was induced in all limbs that received either a deviated nerve or an FGF/BMP bead graft, but none of these blastemas formed limb pattern unless artificial ECM was also grafted (Table 4.1). As reported in chapter 2, grafting

artificial ECM in conjunction with a deviated nerve resulted in induction of ectopic limb pattern at a high frequency (42%, 8/21 grafts). Induction of ectopic limb pattern was not observed when an FGF/BMP bead and artificial ECM were grafted three days after wound (Table 4.1). Ectopic limb structures were induced twice when the bead and ECM were grafted two days after wounding, including one structure that was bifurcated and formed multiple joints with two distally tapering terminal phalangeal elements (Figure 4.1).

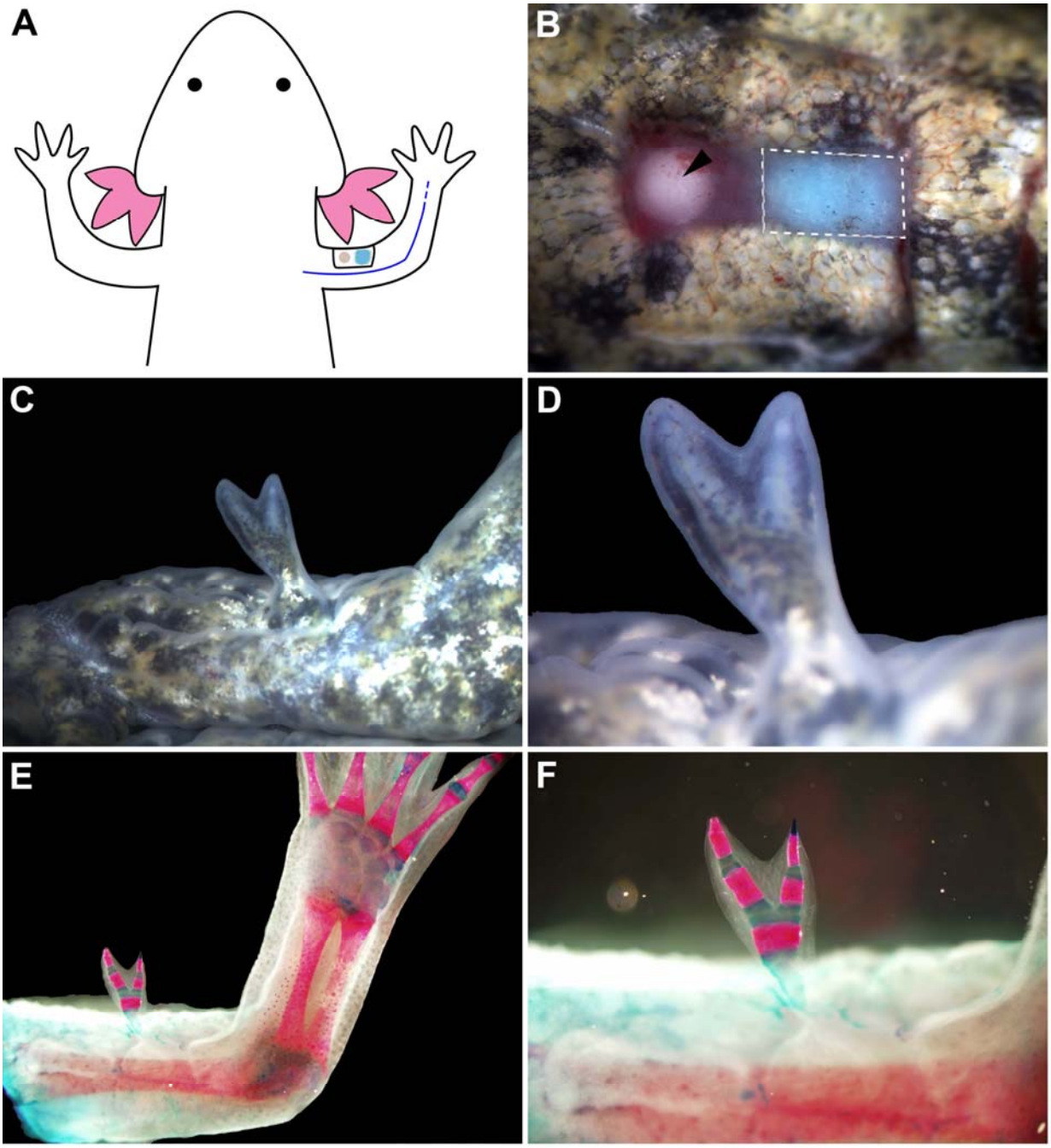

Figure 4.1. A Limb from Scratch: Synthetic Induction of Axolotl Limb Regeneration by Defined Mammalian Factors. (A) Schematic diagram of the technique to synthetically induce ectopic axolotl limb regeneration. A growth factor-soaked bead was grafted into the wound in order to substitute for surgically deviating a nerve. Artificial matrix was grafted to substitute for a posterior skin graft. (B) Image of the growth factor soaked bead (white black arrowhead) and artificial matrix (blue, white outline) grafting into a wound. (C,D) Images of a synthetically-induced ectopic limb on a live animal 2 months after grafting (D is higher magnification of C). (E,F) Skeletal preparation of limb form (C,D) with alcian blue stained cartilage and alizarin red stained bone (F is higher magnification of E).

Table 4.1. Induction of an Ectopic Limb with Synthetic Factors

Graft Type	Total	Blastema*	Pattern**
Nerve + Collagen I (1dpw)	6	6 (100%)	0
Heparan Sulfate + Collagen I (1dpw)	5	0 (100%)	0
Nerve + Heparan Sulfate + Collagen I (1dpw)	21	19 (90%)	8 (42%)
Bead (3dpw)	5	5 (100%)	0
Bead + Heparan Sulfate + Collagen I (3dpw)	12	10 (83%)	0
Bead + Heparan Sulfate + Collagen I (2dpw)	12	12 (100%)	2 (17%)

*percentage of total number of grafts that developed an ectopic blastema
**percentage of ectopic blastemas that developed skeletal elements with pattern

By demonstrating that the nerve and skin graft of the Accessory Limb Model could be replaced with synthetic mammalian-derived factors, I have shown a salamander specific factor is not required for regeneration.

Regenerative techniques are already being developed based the on the ability of heparan sulfates to direct the differentiation of human mesenchymal stem cells (Okolicsanyi et al., 2014). Dermal substitutes to treat full-thickness skin defects in pigs have increased efficacy with the addition of glycosaminoglycans (Kim et al., 2013). Human collagen-based multilayer scaffolds are engineered with glycosaminoglycans for tissue regeneration (Soo Kim et al., 2013). In addition, growth factors are also engineered for super-affinity to the ECM to enhance tissue healing (Martino et al., 2014). Therefore, what we have learned from the ‘limb from scratch’ can complement and improve regenerative engineering techniques already being developed.

My data indicates that there is a “window” of time relative to wounding during which it is possible to induced ectopic limb formation. With the ALM, wound, nerve deviation and skin grafting all occurred within an hour of each other, and ectopic limbs formed at a high frequency (~75%; Endo et al., 2004). In my studies involving grafting artificial ECM into a wound with a deviated nerve, the ECM was grafted within 24 hours post wounding and nerve deviation, and ectopic limbs formed at a lower frequency

(42%, Chapter 2, Table #). In the original report that growth factor soaked beads could induce ectopic blastemas (Makanae et al., 2013), the beads were grafted three days post wound. I confirmed that beads grafted at this time point induced blastemas at a high frequency (100%, Table 4.1); however none of the wounds that received an artificial ECM at three days formed ectopic strucutres (N=12). I only observed ectopic limb formation when the growth factor bead and artificial ECM were grafted two days post wounding. Artificial ECM is always made the night before grafting. Further experiments involving grafting at earlier time points are required to better define what appears to be a critical early window of time during with a pattern formation response can be induced.

A comparable temporal window of response to growth factor signaling has been reported for regeneration of the mouse digit (Yu et al., 2010, 2012). Exogenous BMP delivered by grafting a microcarrier bead can induce a regenerative response at four days post amputation. Whereas, at earlier or later time points it induced ectopic bone formation but not digit regeneration. Discovery of the appropriate time of delivery of pro-regenerative signaling factors to wounded tissues will be required to optimize regenerative therapies in humans. In addition, discovering the mechanisms that regulate the opening and closing of the regeneration window will further enhance the efficacy of such therapies. The axolotl “limb from scratch” model provides opportunities for the discovery of these mechanisms.

Expression of Cell-surface Heparan Sulfate Proteoglycans

Based on the data presented in Chapters 2 and 3, heparan sulfates have important functions during regeneration. Heparan sulfate glycosaminoglycan chains

exist covalently attached to core proteins, known as heparan sulfate proteoglycans (HSPGs) (Sarrazin et al., 2011). There are two classes of HSPGs, extracellular HSPGs and cell-surface HSPGs. Cell-surface HSPGs play a critical role as co-receptors in FGF signaling (Yayon et al., 1991). There are two principal classes of cell-surface heparan sulfate proteoglycans: transmembrane syndecans and glycosylphosphatidylinositol (GPI)-linked glypicans. Glypicans have only heparan sulfate GAG chains while syndecans have both heparan sulfate and chondroitin sulfate GAG chains. To determine the HSPGs functioning during regeneration, I characterized the expression of syndecans and glypicans during axolotl limb regeneration.

My search of the Ambystoma EST database (http://www.ambystoma.org) identified 3 syndecans (1,2,3) and 3 glypicans (1,4,6) expressed in axolotl tissues. To investigate the syndecan and glypican expression during amputation-induced blastema formation, regenerating blastema tissues from amputated forelimbs were analyzed by RT-PCR (Figure 4.2).

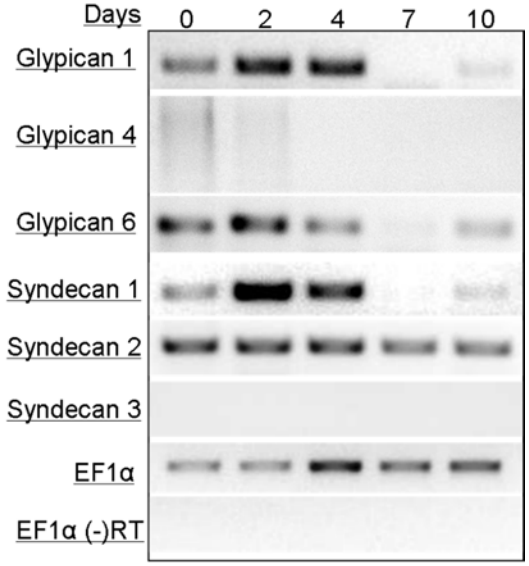

Figure 4.2. Syndecan and glypican expression in Regenerating Axolotl Forelimb during the first 10 Days of regeneration. EF1α as normalizing control.

Glypican-1, glypican-6, syndecan-1 show similar patterns of upregulated expression after injury, with a decrease at day 7. Syndecan-2 expression appeared uniform during this period of blastema formation and growth. Expression of glypican-4 and syndecan-3 appeared either weak or non-detectable. However, without a positive control, it is not clear if this is a lack of expression or failure of primer design and/or RT-PCR. Syndecan-3 is considered a muscle-specific HSPG so the lack of expression during regeneration can be expected (Figure 4.2). For the remainder of my studies, I focused on glypican-1, glypican-6, syndecan-1, syndecan-2.

After identifying which HSPGs were expressed in the amputation-induced regeneration blastema, I characterized HSPG expression in the nerve-induced ectopic blastema from the ALM used in Chapter 2 and 3 (Endo 2004, Satoh 2007). There were three questions that I addressed: 1) what HSPGs are expressed during nerve-induced ectopic blastema formation, 2) are there specific nerve-induced HSPGs related to blastema formation (wound + nerve) as compared to wound healing (wound), 3) how does HSPG expression compare between the site of injury (wound) and the adjacent uninjured tissue (border). To do this, I created a wound on one side of the animal, and a wound with a deviated nerve on the other side. During sample collection, I took the wound epithelium that formed over the injury as “wound” as well as a 1 mm border of uninjured skin around the wound as “border” (Figure 4.3).

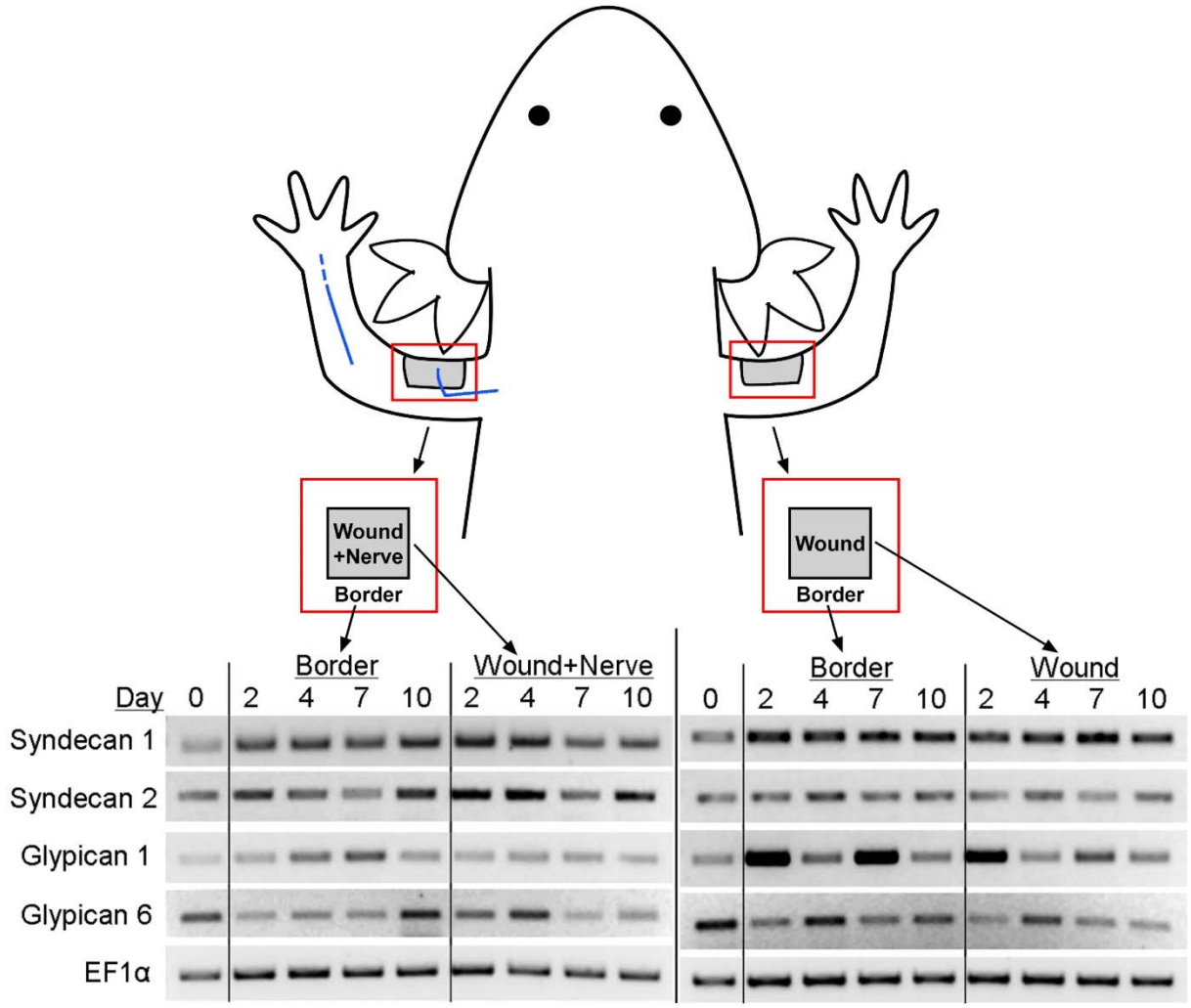

Figure 4.3. Expression of Syndecans and Glypicans during Axolotl Wound Healing and Nerve-Induced Ectopic Blastema Formation by RT-PCR. EF1α as loading control.

The expression patterns are complicated to interpret; nevertheless, there are four noteworthy observations. First, as with amputation-induced regeneration, syndecan-1, syndecan-2, glypican-1, and glypican-6 were all expressed during nerve-induced regeneration. Second, syndecan-1 expression remained constant in the border and the wound in the absence of nerve-induced blastema formation but decreased over time in the wound with a deviated nerve. This result has identified the downregulation of syndecan-1 expression as a marker for the difference between cutaneous wound healing and induction of a regenerative response (migration, proliferation,

dedifferentiation to form blastema). It is relevant to note that syndecan-1 is actually upregulated during mammalian wound healing (Elenius et al., 1991) and that syndecan 1 expression has been shown to be important in mammalian wound healing (Alexopoulou et al., 2007; Ojeh et al., 2008; Stepp, 2002). Third, glypican-1 is strongly unregulated in the absence of nerve signaling. Similar to Syndecan 1, it appears that downregulation of glypican-1 is associated with nerve-induced blastema formation. Lastly, glypican-1 expression is upregulated in border of wounds with or without nerves, demonstrating that cells within 1mm of the injury site respond to injury-associated signals.

Both syndecan-1 and glypican-1 are known to mediate FGF2 signaling, and compensate for each other (Ding et al., 2005). FGF2 induces syndecan-1 shedding (Ding et al., 2005). Mutations in glypican-6 impair endochondral ossification in humans (Campos-Xavier et al., 2009). FGF2 induces glypican-6 expression (Salehi, 2009). Syndecan 2 in *Xenopus* is important for early decisions in left-right asymmetry (Kramer and Yost, 2002) as well as in zebrafish (Chen et al., 2004).

In conclusion, I found that the HSPGs syndecan-1, syndecan-2, glypican-1 and glypican-6 are expressed during both amputation-induced and nerve-induced limb regeneration in the axolotl. There appears to be a difference in the patterns of syndecan-1 expression during mammalian and axolotl wound healing. In mammals, syndecan ectodomains are shed from the cell surface in response to injury, resulting in the upregulation of syndecan expression. One hypothesis based on the axolotl syndecan-1 expression is that since syndecan expression is not upregulated during blastema formation, HSPGs are not shed during wound healing in axolotls in contrast to

what occurs in mammals. If that is the case, and the heparan sulfate-dependent positional information required for regeneration is carried by the HSPGs, then the lack of regenerative ability in mammals could be due to the shedding of positional information in response to injury. Therefore, therapies to improve regeneration in humans could be to prevent shedding in the first place or add back the heparan sulfate. In fact, a number of studies have successfully demonstrated improved mammalian wound healing with topical heparan sulfate treatment (Rai et al., 2011; Tong et al., 2009, 2012).

Chondroitin Sulfate Glycosaminoglycans

Chondroitin sulfate (CS), another type of sulfated glycosaminoglycan is the most abundant GAG in the extracellular matrix. Chondroitin sulfate is similar to heparan sulfate, but consists of alternating sugars of acetylgalactosamine and glucuronic acid, and in general is not as sulfated as heparan sulfate. Chondroitin sulfate proteoglycans (CSPGs) may have functional overlap with HSPGs (Le Jan et al., 2012), opposing roles (Cregg et al., 2014) dictated by HS/CS ratio (Dow et al., 1994), or compensate for each other (Chen and Lander, 2001). In some cases, what chondroitin sulfate may lack in binding affinity compared to heparan sulfate is made up for in terms of its relatively higher abundance.

Most relevant to the issue of regeneration is that chondroitin sulfate is dynamically regulated in mammalian skin in relationship to the response to wounding. In humans, CS is more abundant in tissues capable of scarless wound healing, including human fetal skin (Coolen et al., 2010) and oral mucosa (Glim et al., 2014). The higher level of CS has been implicated in less inflammation and less contraction leading to

improved wound healing and decreased scar formation (Mak et al., 2009). Because of the role of chondroitin sulfate in wound healing and chondrogenesis, it has been integrated into regenerative therapies (Kim et al., 2013; Soo Kim et al., 2013). Because of its expression in mammals and its overlapping role with heparan sulfate, I decided to study whether CS also had the ability to regulate regenerative responses in the axolotl ALM.

Similar to the experiments described in Chapter 2, I enzymatically removed CS moieties from anterior and posterior axolotl limb skin ECM and made artificial matrix of chondroitin sulfate with type I collagen. I then grafted these into an axolotl wounds with a deviated nerve, and assayed for effects on blastema formation and pattern formation during axolotl limb regeneration (Figure 4.4).

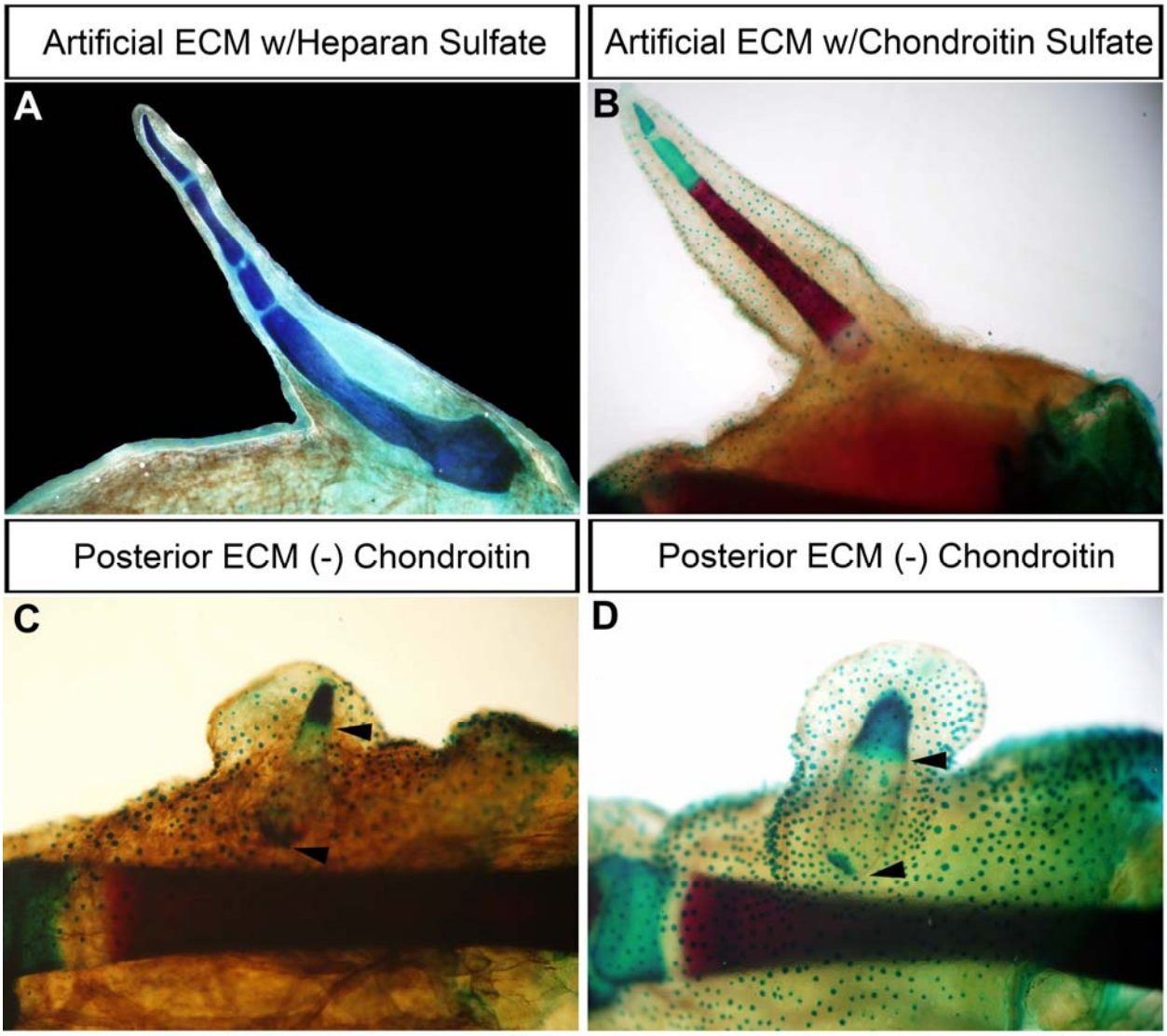

Figure 4.4. Chondroitin Sulfate can Induce Ectopic Limb Formation and Affects Ossification of Skeletal Elements in Axolotl Limb Regeneration. (A) Example of ectopic limb induced by grafting artificial matrix of heparan sulfate and collagen into an axolotl wound with a deviated nerve. (B) Example of ectopic limb induced by grafting artificial matrix of chondroitin sulfate and collagen. (C, D) Examples of ectopic skeletal elements induced by grafting posterior axolotl limb skin ECM treated with chondroitinase ABC. (A-D) Whole mount skeletal preparations to visualize induced ectopic structures by alcian blue (cartilage) and alizarin red staining (ossified bone). Blue dots are dermal glands that have retained dye.

The most visually striking result from the study of CS was the correlation between the presence of CS and ossified structures (Figure 4.4, red = ossified, blue = cartilage). When CS was used in place of heparan sulfate in artificial ECM, the resulting ectopic skeletal elements were ossified rather than cartilaginous (Figure 4.4 compare A

to B). Similarly, when chondroitin sulfate was removed from axolotl-derived ECM grafts, there was a ‘clear’ part of the induced ectopic skeletal element (Figure 4.4C-D, clear segments marked with black arrowheads). Presumably these skeletal elements are neither cartilaginous nor ossified. A possible explanation could be that like mammals, CS is required for osteogenesis, and without it, skeletal elements are neither cartilage nor ossified bone. This observation is particularly intriguing in the context of what is known about mammalian chondroitin sulfate expression and what is known from the mouse skin grafting experiments described in Chapter 3. In Chapter 3, grafts from mouse skin induced skeletal elements that were more ossified, and there are high levels of chondroitin sulfate in mammalian skin. Thus one mechanism by which mammalian skin ECM, and ECM in general, can specifically direct differentiation of host axolotl cells appears to involve the presence and/or absence of chondroitin sulfate and heparan sulfate. This hypothesis could be tested by varying levels of sulfation of heparan sulfate and chondroitin sulfate to determine if it is a HS/CS effect or an effect of overall sulfation level.

Artificial ECM composed of chondroitin sulfate induced ectopic limb structures when grafted into an axolotl wound with a deviated nerve at a lower frequency as compared to artificial ECM composed of heparan sulfate (Table 4.2, 17% vs 42%, 1.0 mg of CS or HS). Presumably, this finding reflects the fact that HSPGs and CSPGs can have overlapping functions (both induce limb pattern formation), but heparan sulfate is more highly sulfated, and thus more efficient at inducing ectopic limb structures.

There are two results of interest from the chondroitinase treatment of anterior and posterior axolotl ECM grafts. First, posterior ECM without CSPG was still capable of

position-specific induction of ectopic limb structures (Table 4.2). As reported previously (Chapter 2, Figure 2.2), removal of HS from the ECM reduced position-specific ectopic limb induction. Therefore, in axolotl ECM, although chondroitin sulfate can suffice (Figure 4.4B), heparan sulfate is responsible for the ability of posterior axolotl ECM to induce ectopic limb pattern, as this is not lost upon chondroitinase treatment. The inhibition of blastema formation by anterior ECM is, however, lost upon chondroitinase treatment (Table 4.2).

Table 4.2. Chondroitin Sulfate can Induce Ectopic Limb Formation

Graft Type	Total	Blastema*	Pattern**
Collagen I only	6	6 (100%)	0
Heparan Sulfate + Collagen I	21	19 (90%)	8 (42%)
Chondroitin Sulfate + Collagen I	8	6 (75%)	1 (17%)
Axolotl Anterior ECM (-) CS	10	10 (100%)	0
Axolotl Posterior ECM (-) CS	9	9 (100%)	2 (22%)

*percentage of total number of grafts that developed an ectopic blastema
**percentage of ectopic blastemas that developed skeletal elements with pattern

Taken together, I conclude that position-specific signaling by the ECM is a consequence of the integration of multiple components, including both chondroitin sulfate and heparan sulfate. Further studies are needed to characterize the specific activities of chondroitin sulfate and other ECM components.

Materials and Methods

(not already described in previous chapters)

Gelatin bead preparation and grafting

Acidic gelatin beads without CMC (carboxylmethyl cellulose) were prepared as previously described (Makanae et al., 2013; Satoh et al., 2011; Tabata et al., 1999). Briefly, gelatin was dissolved in boiling water to give a 10% solution, which was then

mixed dropwise with olive oil to form an oil-gelatin emulsion. This emulsion was washed with acetone and distilled water. The gelatin beads were then fixed overnight with 2 mM glutaraldehyde, residual glutaraldehyde was then blocked with 10 mM glycine for 2 hours. Finally, the beads are washed with distilled water repeatedly and lyophilized and stored at -20^{o}C until use. Lyophilized beads were allowed to swell overnight in solutions of FGF2, FGF8 and BMP2 (300 ng/µl, R&D Systems) in PBS. Before grafting, a skin 2x2 mm wound is made on the anterior side of the upper limb (stylopod). 1, 2 or 3 days after wounding (various states of wound healing), the growth factor soaked bead with or without artificial matrix was placed underneath the wound epithelium. An incision was made on three sides of the initial wound. The wound epithelium was then lifted up, the grafts were placed into the wound bed, and the wound epithelium was then repositioned and allowed to heal back in place.

Chondroitin sulfate artificial ECM

Similar to medium HS Artificial ECM in Chapter 2, Artificial ECM with chondroitin sulfate was made by combining 100 µl of 5.0 mg/ml chondroitin sulfate (A&B, bovine trachea, Sigma) with 1.2 ml of 5.0 mg/ml type-I collagen (calf skin; Sigma). This solution was incubated overnight at 4^{o}C to form a precipitate that was then pelleted by centrifugation (10,000 rcf for 15 minutes) and grafted (Schaller and Muneoka, 2001). Fast Green FCF and India ink were used to visualize the graft and determine that it was still present in the wound site post-grafting. Since ECM molecules were not directly labelled, exact timing of graft maintenance is uncertain.

Chondroitinase ABC treatment of axolotl ECM

Similar to the experimental procedures reported in Chapter 2, chondroitin sulfate moieties were removed enzymatically by incubating decellularized ECM preparations in 0.008 IU/ml Chondroitinase ABC (Seikagaku) for 4 hours at 37°C, after which they were rinsed in PBS and stored in PBS at 4°C until grafted.

Tissue collection

For Syndecan and Glypican expression analysis during amputation-induced limb regeneration, forelimbs were amputated at the level of the mid-upper arm. Regenerating tissues were collected by reamputation at the original amputation plane 2, 4, 7, and 10 days post injury. Uninjured skin was used as the 0 day sample. To compare wound healing and blastema formation, a square wound 1.5x1.5 mm was created on the mid-upper arm. Wounds were allowed to heal without further treatment (wound healing), or were induced to form an ectopic blastema by severing the brachial nerve and rerouting it under the skin to the center of wound (blastema formation). Wound tissues and surrounding border skin (1 mm wide) was collected for comparative analysis. Tissues were homogenized with a BioVortexer and 21-gauge needle.

Reverse-transcription PCR

Similar to the experimental procedures reported in Chapter 2, RNA was collected using Rneasy Mini Kit (Qiagen). cDNA was reverse transcribed with Transcriptor (Roche) for subsequent PCR with goTaq Green PCR Mix (Promega). To design primers, EST sequences of Syndecans and Glypicans were found on the Ambystoma Database (http://www.ambystoma.org/) according to homology to known full sequences using tblastx. Primer3 was used to create primer sequences that generate 150-200

base pair amplicons. EF1α was used as the normalizing expression control adapted from (Satoh et al., 2007).

Syndecan 1	Forward: 5'- TCCTCATTGATCGGGTCTTC
	Reverse: 5'- GGAAAGCCACTGAACCACAT
Syndecan 2	Forward: 5'- CGCCGAGACGACAACCCTAAAA
	Reverse: 5'- CGATGACCGCAGCCAAAACTTC
Syndecan 3	Forward: 5'- CAGCACCACGACCATGTTAC
	Reverse: 5'- TTATTGAGCTCTGGGCGAGT
Glypican 1	Forward: 5'- AGGAAAAGAGACAGCGACGA
	Reverse: 5'- CATCCCATTCCAACATTTGTC
Glypican 4	Forward: 5'- GGCCATGGAGGAGAAGTACA
	Reverse: 5'- GGCCATAGGTCCGTACAAGA
Glypican 6	Forward: 5'- GTGCAGCAACTACTGCCTCA
	Reverse: 5'- ATGGGATCCATGACCGACT
EF1α	Forward: 5'- AACATCGTGGTCATCGGCCAT
	Reverse: 5'- GGAGGTGCCAGTGATCATGTT

CHAPTER 5: Conclusions and Outlook

Figure 5.1 of this chapter is a reprint of the material as it appears in Molecular Biology of the Cell, 2002, authored by Bruce Alberts, Alexander Johnson, Julian Lewis, Martin Raff, Keith Roberts, and Peter Walter, © Garland Science

Summary

Axolotl limb regeneration is a stepwise sequence that involves three requisite processes: (1) scarless wound healing to generate a regenerative wound epithelium, (2) blastema formation by migration, proliferation and dedifferentiation to create a mass of multipotent regeneration-competent progenitor cells, and (3) induction of pattern formation by interaction of cells with opposing positional information. The challenge to understanding how to induce and enhance regenerative ability in humans is to discover which of these processes fail and why they fail.

The goal of my study was to determine the molecular mechanism of positional information in axolotl limb regeneration and whether it is conserved in mammals. By use of an *in vivo* gain-of-function assay for the requisite processes of axolotl limb regeneration (the Accessory Limb Model), I have found that positional information is mediated in part by position-specific heparan sulfate sulfation patterns in the extracellular matrix of axolotl limb skin, and that it is conserved in mice. Using this information, combined with recent discoveries regarding blastema formation, I was able to synthetically induce axolotl limb regeneration with commercially available mammalian-derived factors. This cell-free method demonstrates that the factors required for limb regeneration are not salamander specific.

Future directions include studies to characterize axolotl and mammalian positional information and map out the position-specific extracellular matrix properties, to determine how and why mammals lose regenerative ability, and to integrate this with mammalian stem cell biology to develop and translate positional information into engineering regenerative therapies in humans.

In addition to the fields of regeneration, development, and glycobiology, the novel mechanism of positional information that I have discovered has implications to the fields of cancer biology, which presumably involves cells that lack positional information or the ability to properly respond to it, and aging, which is associated with a loss of regenerative ability.

Novel Mechanism for Positional Information and Pattern Formation in Regeneration

In 1969, Lewis Wolpert outlined the concepts of “positional information” and “pattern formation” (Wolpert, 1969). Since then, the best evidence for these phenomena has been intercalation during regeneration (Agata et al., 2003; Bryant et al., 1981; French et al., 1976) . Freely diffusible morphogens and growth factors alone cannot account for positional specification and pattern formation; therefore, additional or alternative mechanisms involving interactions between cells are required (Kerszberg and Wolpert, 2007; Wolpert, 2011).

Glycans in the Extracellular Matrix as Candidates for Mediating Positional Information

One area of biology that is rapidly expanding is the field of glycobiology. For decades, the complex and indecipherable sugars attached to every extracellular and secreted protein and coating the surface of all cell membranes has been too difficult to study compared to the less diverse polymers (e.g. nucleic acids and proteins). However, with the development of new tools and the realization that complex biological processes cannot be explained simply with genes and proteins, glycobiology is one of the fastest growing research areas in the natural sciences. Biological cells are coated in a dense

layer of glycans (glycocalyx, Figure 5.1) that dominate the biological characteristics of the cell membrane and control the cell's interface with everything else outside.

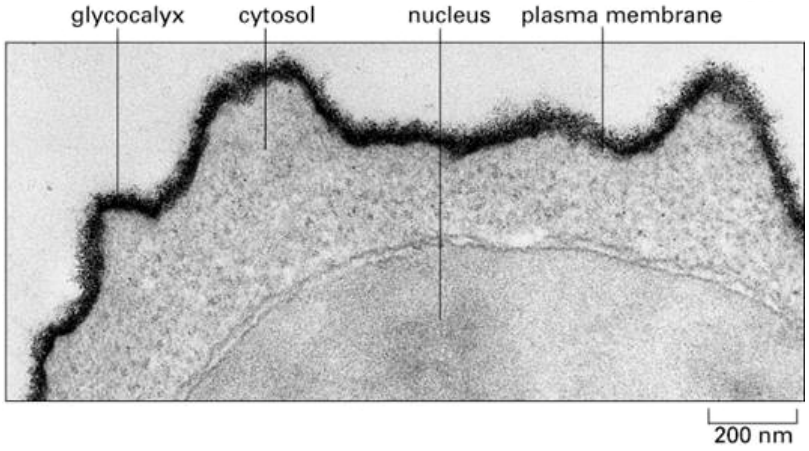

Figure 5.1. Biological Cells are Encompassed in a Dense Layer of Glycans (glycocalyx) >50 nm thick (Alberts et al., 2002)

Cells in organisms are embedded in an ECM full of glycans that determine the physical, chemical and biological properties of the cells and tissue. Virtually all cell-cell interaction is either cell-matrix-cell or cell-matrix communication. Therefore, if positional information is a result of cell-cell interactions, glycans in the extracellular matrix must be involved. In immunology, glycans serve as the basis of cell-host-invader recognition. Bacterial and viral infection and specificity are dependent on glycans (Nizet and Esko, 2009). Even blood groups in humans are determined by glycans. Unlike proteins, glycans do not have to be transcribed and translated and therefore are more dynamically regulated and can be altered at the cell surface. With hundreds of building blocks with thousands of modifications, and some glycosaminoglycan chains hundreds of residues in length, the possible glycan diversity is orders of magnitudes higher in complexity than genes or proteins. Therefore, sugars that can encode diversely specific cell-regulatory information, that are dynamically regulated on the outside of cells, that

function in organismal self-identity, and are in abundance at the cell interface where communication must occur, are the mostly likely suspects when looking for molecules that mediate positional information.

Positional Information is a Blueprint of Position-specific Growth Factor Regulation Embedded in the Extracellular Matrix

Based on all the work presented in this dissertation, I propose a model in which pattern formation is dictated by position-specific extracellular regulation of morphogens and growth factors that then transduce signaling into specific cells. I hypothesize that positional information is a large-scale blueprint of signaling instructions encoded in the ECM (see Figure 2.11). These blueprints dictate the body axes (anterior/posterior, dorsal/ventral, and proximal/distal) and gross morphology of organs and tissues. The blueprint directs position-specific growth factor signaling (e.g. FGF2 anterior, FGF8 posterior, BMP proximal, Wnt distal). These growth factors then instruct the cells to migrate, proliferate or differentiate in a manner orchestrated by the ECM to eventually integrate all the cells into a functional pattern (Figure 5.2).

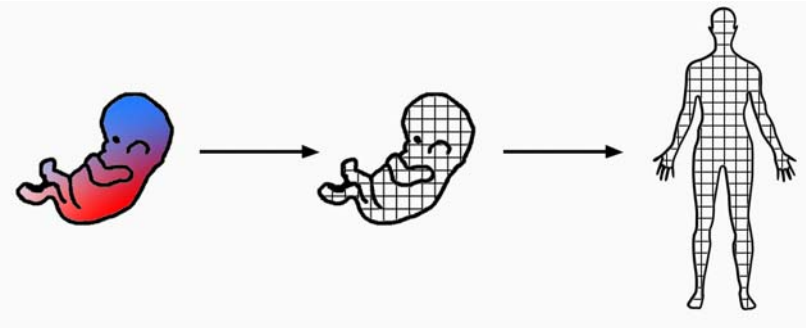

Figure 5.2. Model of Establishment of Positional Information

In addition to the studies discussed in this dissertation, there is other evidence that is consistent with this hypothesis. The necessity for morphogens and growth factors to interact with extracellular matrix components in order to function continues to gain

more evidence (Häcker et al., 2005; Sarrazin et al., 2011). Growth factors and artificial matrix components are being engineered based on their interaction to each other (Martino et al., 2014; Murali et al., 2013). The concept of heparan sulfates stabilizing and shaping morphogen gradients has been demonstrated in a number of systems (Akiyama et al., 2008; Häcker et al., 2005; Paine-Saunders et al., 2002; Ramsbottom et al., 2014; Takeo et al., 2005; Wang et al.; Yan and Lin, 2009). Specific chondroitin sulfate and heparan sulfate sulfation motifs are associated with sites of growth, differentiation and repair, molecular recognition sites (Melrose et al., 2012). Differential interactions of FGFs with heparan sulfate control gradient formation and branching morphogenesis (Makarenkova et al., 2009). Because of the specificity of heparan sulfate growth factor regulation and ability to identify specific heparan sulfate binding residue sequences, a “heparan sulfate code” has been proposed (Habuchi et al., 2004). This heparan sulfate code can be so tightly and rapidly controlled during development that FGF2 signaling during mouse embryonic day 9 can be changed to FGF1 signaling by embryonic day 11 (Nurcombe et al., 1993)

Future Directions

Mapping out ECM composition across the entire body

One of the first steps to developing regenerative therapies with positional information is to map out the ECM composition across the entire body. In the way that the Polar Coordinate Model assigned arbitrary numbers and letters to denote positional values, ECM composition based coordinates can be assigned to each position (e.g. high 3-O low N heparan sulfate sulfation = posterior forelimb mid stylopod). The heparan sulfate composition can be cross-referenced with already described growth

factor binding sites (e.g. FGF2, 2-O and N) and known areas of signaling (Shh in the ZPA). Transcriptional analysis of skin fibroblasts across the human body has shown site-specific expression patterns (Rinn et al., 2008). Similar methods could be used to analyze and map the heparan sulfate/growth factor code.

Other ECM components and growth factors

In this study, I focused on heparan sulfates in the anterior and posterior of the limb, but I also have shown that chondroitin sulfates can contribute to positional information (although they may not be necessary). A more thorough characterization of chondroitin sulfate, in addition to other GAGs (dermatan sulfate, keratan sulfate) should be conducted. A number of other ECM components have also been implicated in regeneration and/or cell signaling regulation including tenascin, fibronectin, and collagen.

Also, only FGF signaling was studied in this dissertation because its role has been well established in limb regeneration and the specificity of its interactions with heparan sulfate have been well characterized. However, numerous other growth factors are involved in limb regeneration and are regulated by heparan sulfates and other ECM components including: BMP, Wnt, TGF-β, VEGF, HGF, PDGF. Elucidation of the heparan sulfate/growth factor code will necessarily involve these other growth factors.

Mechanism for regulation of heparan sulfates

I found spatial-temporal regulation of heparan sulfate sulfotransferases as well as dynamic expression of heparan sulfate proteoglycans. However, there must be a higher level of regulation occurring. Presumably, pattern is initially formed during embryogenesis, with maternal and zygotic genes establishing the body axis. Hox genes

control HSPG expression (Crickmore and Mann, 2007). In animals that regenerate, this positional information is stored in the connective tissue in the form of a heparan sulfate code and specific factors preferentially bound to the code. Upon traumatic injury, the positional information is used to regenerate the missing part from what is remaining (Figure 1.1A). Therefore, cells that were initially proximal become distal and their positional information must be reprogrammed (McCusker and Gardiner, 2013). An epigenetic model for programming positional information in blastema cells has been proposed (Tamura et al., 2010). The HS3ST gene has been shown to have methylation-associated repression (Bui et al., 2010).

An additional model could be positive feedback with growth factors. Initially, the embryo is patterned by morphogens and growth factors. These growth factors then induce expression and synthesis of their corresponding heparan sulfate code. The code is maintained in the matrix through adulthood. Upon injury, the coded positional information is used to regulate those same growth factors to regenerate the limb as well as recreate the position-specific modifications. Either way, the mechanism of heparan sulfate regulation is an area that needs further study.

Why do Mammals have a Limited Ability to Regenerate?

Perhaps the biggest question in regeneration is “Why don’t mammals regenerate?” Presumably, at least one of the requisite steps of regeneration fails in mammals. This study focused on the third step of positional information induced pattern formation. In Chapter 1, I found that mouse skin ECM had similar heparan-sulfate position-specific signaling properties similar to axolotl skin ECM. However, these properties seem to change as the mouse ages. One hypothesis is that mammals initially

have the ability to regenerate but lose it as they develop (Gardiner, 2005; Gardiner and Holmes, 2012; Menger et al., 2010; Muneoka et al., 2008b) similar to what is seen in *Xenopus* (Muneoka et al., 1986). But what changes as a mammal ages?

The development of the immune system and the nervous system also could be a contributing factor (Menger et al., 2010; Tassava and Olsen-Winner, 2003). The development of the immune system is a particularly intriguing consideration for a number of reasons. First, amphibians have a less developed immune system compared to mammals. Similarly, mammalian embryos *in utero* (which have the highest regenerative ability) also have a less developed immune system (Menger et al., 2010). Finally, there are reports indicating a functional interaction between inflammation and regeneration: with more inflammation there is less regeneration, with less inflammation there is more regeneration (Martin and Leibovich, 2005; Menger et al., 2010; Mescher and Neff, 2006; Stramer et al., 2007; Wilgus, 2008).

One part of the inflammatory response during mammalian wound healing is the generation of wound fluid. During wound healing, enzymes (such as heparanases and MMPs) are released leading to the shedding of syndecans and breakdown of the extracellular matrix (Alexopoulou et al., 2007; Penc et al., 1998). Syndecan expression and shedding are required for rapid mammalian wound closure (Elenius et al., 1991; Ojeh et al., 2008). If positional information is stored in the HS GAG chains of the ECM, it is possible that it is lost during the developed mammalian response to injury which ensures rapid wound closure but prevents regeneration.

There have been intriguing insights from zebrafish regeneration on how regeneration may be lost. Sexually dimorphic zebrafish fin regeneration arises in males

after sexual maturity (Nachtrab et al., 2011). Dkk signaling required for homestasis of breeding ornaments interfers with Wnt signaling required for regeneration (Kang et al., 2013). In this case, loss of regenerative ability was effectively traded for increased fitness for mating. Decreased regenerative ability in higher organisms may have been lost as a consequence of developing other advantageous adaptations such as hair and sweat glands.

Implications for Cancer

In addition of applications to regeneration, developmental biology, and glycobiology, my work on positional information has implications for the fields of cancer. In many ways, regenerative blastema cells and cancer cells are similar. They both involve induced proliferation in response to injury, and reversion to a less differentiated state enabling the cells to migrate. There is a burst of oncogene expression in the early blastema during limb regeneration (Stewart et al., 2013). However, unlike cancer cells, blastema cells know when to stop migrating and proliferating, and when to redifferentiate. It is remarkable that during regeneration, the blastema makes only as many cells as needed to replace exactly what was lost; no more and no less.

Amphibians are remarkably resistant to cancer, such that injection of carcinogenic compounds induces patterned and differentiated ectopic limbs rather than unpatterned and undifferentiated tumors (Breedis, 1952). Even if proliferation of blastema cells is induced ectopically, these cells eventually will respond to the instructive positional information around them, and regress to return the limb to its proper pattern (Figure 1.5A-C). A lingering question from the ALM is “how does the blastema know to regress?” It is possible that cancer cells are in some ways cells that

either lack positional information or the ability to respond to it. If so, positional information could be used to direct proper behavior of adherent cells and induce tumors to either differentiate or regress. The idea of using developmental pathways to treat cancers by directing the cells to terminally differentiate has been gaining in popularity (Campos et al., 2010; Kawamata et al., 2006; Leszczyniecka et al., 2001; Sell, 2006).

There are already extensive studies on the role of heparan sulfates in cancer (Varki et al., 2009). Specific genes involved in synthesis and editing of heparan sulfate GAGs show altered expression patterns in breast cancer (Fernández-Vega et al., 2013). Altered content and distribution of HSPGs have been implicated in tumor pathogenesis, specific to degree of HS chain processing or degradation. Methylation-associated repression of HS3ST contributes to invasiveness of chondrosarcoma cells (Bui et al., 2010). Therefore, heparan sulfate and heparanases are being targeted in developing cancer therapies (Varki et al., 2009). If positional information can be completely characterized and mapped, perhaps this can be used to engineer therapies that dictate the behavior of cancer cells. If factors responsible for ectopic blastema regression can be found, it could prove to be a more useful and safe method then used currently in cancer treatment.

Implications for Aging

Finally, there are implications of regeneration and positional information for aging. In some aspects, aging can be thought of as a loss of regenerative ability over time. One of the hallmarks of aging is the accumulation of glycosylation. Age-related changes in rat myocardium altered GAG ability to potentiate growth factor signaling (Huynh et al., 2012). Dermal ECM components change as humans develop (Coolen et

al., 2010) corresponding with a decline in regenerative ability (Mak et al., 2009; Wong et al., 2009). It is evident that humans lose regenerative ability over time. Is it possible that this is in part due to the disruption of positional information over time? Glycosylation is dependent on diet, nutrition and metabolism. Without sugar precursors, glycans cannot be synthesized. Conversely, if there is an abundance of sugars, there can be increased levels of glycosylation. Either way over time, glycosylation can accumulate. If we can define aged tissue from young tissue by glycan composition, we may be able to prevent or reverse aging by manipulating the ECM (Figure 5.3).

Even though biology has become specialized into more and more discrete fields, there can be unifying principles that can encompass many areas of research. Regulation of growth and pattern by positional information mediated by position-specific extracellular factors has the potential to be one such unifying principle.

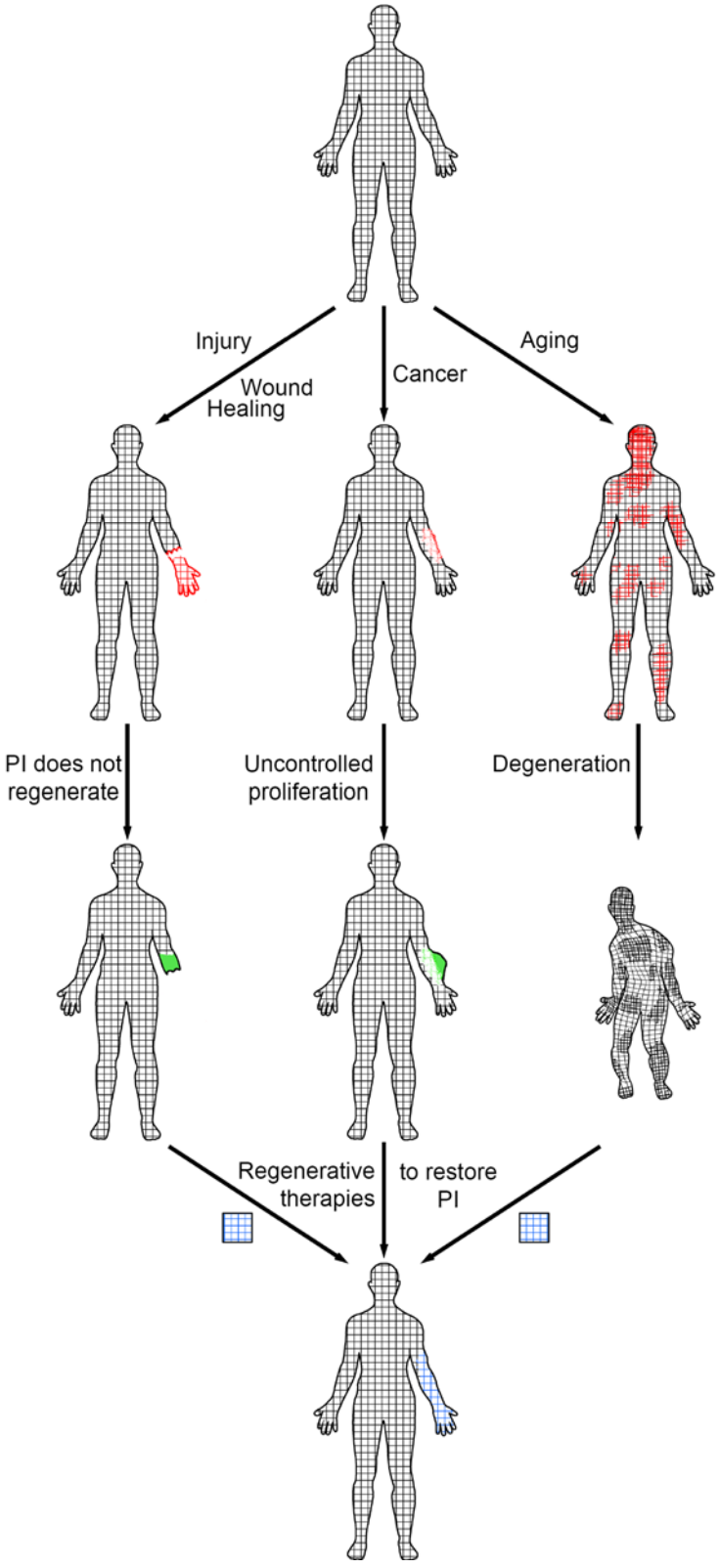

Figure 5.3. Model for Application of Positional Information to Development of Regenerative Therapies for Wound Healing, Cancer, and Aging. PI = Positional Information

REFERENCES

Agata, K., Tanaka, T., Kobayashi, C., Kato, K., and Saitoh, Y. (2003). Intercalary regeneration in planarians. Dev. Dyn. *226*, 308–316.

Agata, K., Saito, Y., and Nakajima, E. (2007). Unifying principles of regeneration I: Epimorphosis versus morphallaxis. Dev. Growth Differ. *49*, 73–78.

Akiyama, T., Kamimura, K., Firkus, C., Takeo, S., Shimmi, O., and Nakato, H. (2008). Dally regulates Dpp morphogen gradient formation by stabilizing Dpp on the cell surface. Dev. Biol. *313*, 408–419.

Alberts, B., Johnson, A., and Lewis, J. (2002). Membrane Proteins. In Molecular Biology of the Cell, (New York: Garland Science),.

Alexopoulou, A.N., Multhaupt, H. a B., and Couchman, J.R. (2007). Syndecans in wound healing, inflammation and vascular biology. Int. J. Biochem. Cell Biol. *39*, 505–528.

Anderson, R., Landry, M., and Muneoka, K. (1993). Maintenance of ZPA signaling in cultured mouse limb bud cells. Development *117*, 1421–1433.

Anderson, R., Landry, M., Reginelli, A., Taylor, G., Achkar, C., Gudas, L., and Muneoka, K. (1994). Conversion of Anterior Limb Bud Cells to ZPA Signaling Cells in Vitro and in Vivo. Dev. Biol. *164*, 241–257.

Baeg, G.H., Lin, X., Khare, N., Baumgartner, S., and Perrimon, N. (2001). Heparan sulfate proteoglycans are critical for the organization of the extracellular distribution of Wingless. Development *128*, 87–94.

Baeg, G.-H., Selva, E.M., Goodman, R.M., Dasgupta, R., and Perrimon, N. (2004). The Wingless morphogen gradient is established by the cooperative action of Frizzled and Heparan Sulfate Proteoglycan receptors. Dev. Biol. *276*, 89–100.

Bando, T., Mito, T., Maeda, Y., Nakamura, T., Ito, F., Watanabe, T., Ohuchi, H., and Noji, S. (2009). Regulation of leg size and shape by the Dachsous/Fat signalling pathway during regeneration. Development *136*, 2235–2245.

Barker, A.R., Rosson, G.D., and Dellon, A.L. (2006). Wound healing in denervated tissue. Ann. Plast. Surg. *57*, 339–342.

Bass, M.D., Morgan, M.R., and Humphries, M.J. (2009). Syndecans shed their reputation as inert molecules. Sci. Signal. *2*, pe18.

Beck, C.W., Izpisúa Belmonte, J.C., and Christen, B. (2009). Beyond early development: Xenopus as an emerging model for the study of regenerative mechanisms. Dev. Dyn. *238*, 1226–1248.

Bely, A.E., and Nyberg, K.G. (2010). Evolution of animal regeneration: re-emergence of a field. Trends Ecol. Evol. *25*, 161–170.

Bénazet, J.-D., and Zeller, R. (2009). Vertebrate limb development: moving from classical morphogen gradients to an integrated 4-dimensional patterning system. Cold Spring Harb. Perspect. Biol. *1*, a001339.

Billingham, R.E., and Russell, P.S. (1956). Incomplete wound contracture and the phenomenon of hair neogenesis in rabbits' skin. Nature *177*, 791–792.

Bishop, J.R., Schuksz, M., and Esko, J.D. (2007). Heparan sulphate proteoglycans fine-tune mammalian physiology. Nature *446*, 1030–1037.

Bodemer, C. (1958). The development of nerve-induced supernumerary limbs in the adult newt, Triturus viridescens. J. Morphol.

Bodemer, C. (1959). Observations on the mechanism of induction of supernumerary limbs in adult Triturus viridescens. J. Exp. Zool. *140*, 79–99.

Boilly, B., Cavanaugh, K.P., Thomas, D., Hondermarck, H., Bryant, S. V, and Bradshaw, R. (1991). Acidic fibroblast growth factor is present in regenerating limb blastemas of axolotls and binds specifically to blastema tissues. Dev. Biol. *145*, 302–310.

Borgens, R.B. (1982). Mice regrow the tips of their foretoes. Science *217*, 747–750.

Breedis, C. (1952). Induction of accessory limbs and of sarcoma in the newt (Triturus viridescens) with carcinogenic substances. Cancer Res. *12*, 861–866.

Breedis, C. (1954). Regeneration of hair follicles and sebaceous glands from the epithelium of scars in the rabbit. Cancer Res. *14*, 575–579.

Brockes, J.P., and Gates, P.B. (2014). Mechanisms underlying vertebrate limb regeneration: lessons from the salamander. Biochem. Soc. Trans. *42*, 625–630.

Bryant, S. V, and Baca, B.A. (1978). Regenerative ability of double-half and half upper arms in the newt, Notophthalmus viridescens. J. Exp. Zool. *204*, 307–323.

Bryant, S.V., and Gardiner, D.M. (1992). Retinoic acid, local cell-cell interactions, and pattern formation in vertebrate limbs. Dev. Biol. *152*, 1–25.

Bryant, S. V, French, V., and Bryant, P.J. (1981). Distal regeneration and symmetry. Science (80-.). *212*, 993–1002.

Bryant, S. V, Endo, T., and Gardiner, D.M. (2002). Vertebrate limb regeneration and the origin of limb stem cells. Int. J. Dev. Biol. *46*, 887–896.

Buckley, G., Wong, J., Metcalfe, A.D., and Ferguson, M.W.J. (2012). Denervation affects regenerative responses in MRL/MpJ and repair in C57BL/6 ear wounds. J. Anat. *220*, 3–12.

Bui, C., Ouzzine, M., Talhaoui, I., Sharp, S., Prydz, K., Coughtrie, M.W.H., and Fournel-Gigleux, S. (2010). Epigenetics: methylation-associated repression of heparan sulfate 3-O-sulfotransferase gene expression contributes to the invasive phenotype of H-EMC-SS chondrosarcoma cells. FASEB *24*, 436–450.

Campbell, L.J., and Crews, C.M. (2008). Wound epidermis formation and function in urodele amphibian limb regeneration. Cell. Mol. Life Sci. *65*, 73–79.

Campos, B., Wan, F., Farhadi, M., Ernst, A., Zeppernick, F., Tagscherer, K.E., Ahmadi, R., Lohr, J., Dictus, C., Gdynia, G., et al. (2010). Differentiation therapy exerts antitumor effects on stem-like glioma cells. Clin. Cancer Res. *16*, 2715–2728.

Campos-Xavier, A.B., Martinet, D., Bateman, J., Belluoccio, D., Rowley, L., Tan, T.Y., Baxová, A., Gustavson, K.-H., Borochowitz, Z.U., Innes, A.M., et al. (2009). Mutations in the heparan-sulfate proteoglycan glypican 6 (GPC6) impair endochondral ossification and cause recessive omodysplasia. Am. J. Hum. Genet. *84*, 760–770.

Carlson, B.M. (1974). Morphogenetic interactions between rotated skin cuffs and underlying stump tissues in regenerating axolotl forelimbs. Dev. Biol. *39*, 263–285.

Carlson, B.M. (1975). The effects of rotation and positional change of stump tissues upon morphogenesis of the regenerating axolotl limb. Dev. Biol. *47*, 269–291.

Chen, R.L., and Lander, A.D. (2001). Mechanisms underlying preferential assembly of heparan sulfate on glypican-1. J. Biol. Chem. *276*, 7507–7517.

Chen, E., Hermanson, S., and Ekker, S.C. (2004). Syndecan-2 is essential for angiogenic sprouting during zebrafish development. Blood *103*, 1710–1719.

Christen, B., and Slack, J.M. (1997). FGF-8 is associated with anteroposterior patterning and limb regeneration in Xenopus. Dev. Biol. *192*, 455–466.

Christensen, R.N., Weinstein, M., and Tassava, R. a (2001). Fibroblast growth factors in regenerating limbs of Ambystoma: cloning and semi-quantitative RT-PCR expression studies. J. Exp. Zool. *290*, 529–540.

Clark, L.D., Clark, R.K., and Heber-Katz, E. (1998). A new murine model for mammalian wound repair and regeneration. Clin. Immunol. Immunopathol. *88*, 35–45.

Cohn, M.J., Izpisúa-Belmonte, J.C., Abud, H., Heath, J.K., and Tickle, C. (1995). Fibroblast growth factors induce additional limb development from the flank of chick embryos. Cell *80*, 739–746.

Coolen, N.A., Schouten, K.C.W.M., Middelkoop, E., and Ulrich, M.M.W. (2010). Comparison between human fetal and adult skin. Arch. Dermatol. Res. *302*, 47–55.

Crawford, K., and Stocum, D.L. (1988). Retinoic acid coordinately proximalizes regenerate pattern and blastema differential affinity in axolotl limbs. Development *102*, 687–698.

Cregg, J.M., DePaul, M.A., Filous, A.R., Lang, B.T., Tran, A., and Silver, J. (2014). Functional regeneration beyond the glial scar. Exp. Neurol. *253*, 197–207.

Crickmore, M.A., and Mann, R.S. (2007). Hox control of morphogen mobility and organ development through regulation of glypican expression. Development *134*, 327–334.

Denis, J.-F., Lévesque, M., Tran, S.D., Camarda, A.-J., and Roy, S. (2013). Axolotl as a Model to Study Scarless Wound Healing in Vertebrates: Role of the Transforming Growth Factor Beta Signaling Pathway. Adv. Wound Care *2*, 250–260.

Dent, J.N. (1962). Limb regeneration in larvae and metamorphosing individuals of the South African clawed toad. J. Morphol. *110*, 61–77.

Ding, K., Lopez-Burks, M., Sánchez-Duran, J.A., Korc, M., and Lander, A.D. (2005). Growth factor-induced shedding of syndecan-1 confers glypican-1 dependence on mitogenic responses of cancer cells. J. Cell Biol. *171*, 729–738.

Douglas, B.S. (1972). Conservative management of guillotine amputation of the finger in children. Aust. Paediatr. J. *8*, 86–89.

Dow, K.E., Ethell, D.W., Steeves, J.D., and Riopelle, R.J. (1994). Molecular correlates of spinal cord repair in the embryonic chick: heparan sulfate and chondroitin sulfate proteoglycans. Exp. Neurol. *128*, 233–238.

Elenius, K., Vainio, S., Laato, M., Salmivirta, M., Thesleff, I., and Jalkanen, M. (1991). Induced expression of syndecan in healing wounds. J. Cell Biol. *114*, 585–595.

Endo, T., Bryant, S. V, and Gardiner, D.M. (2004). A stepwise model system for limb regeneration. Dev. Biol. *270*, 135–145.

Esko, J., and Lindahl, U. (2001). Molecular diversity of heparan sulfate. J. Clin. Invest. *108*, 169–173.

Esko, J.D., Kimata, K., and Lindahl, U. (2009). Proteoglycans and Sulfated Glycosaminoglycans. In Essentials of Glycobiology: 2nd Edition, A. Varki, R.D. Cummings, and J.D. Esko, eds. (New York: Cold Spring Harbor Laboratory Press),.

Fernández-Vega, I., García, O., Crespo, A., Castañón, S., Menéndez, P., Astudillo, A., and Quirós, L.M. (2013). Specific genes involved in synthesis and editing of heparan sulfate proteoglycans show altered expression patterns in breast cancer. BMC Cancer *13*, 24.

Ferris, D.R., Satoh, A., Mandefro, B., Cummings, G.M., Gardiner, D.M., and Rugg, E.L. (2010). Ex vivo generation of a functional and regenerative wound epithelium from axolotl (Ambystoma mexicanum) skin. Dev. Growth Differ. *52*, 715–724.

French, V., Bryant, P.J., and Bryant, S. V (1976). Pattern regulation in epimorphic fields. Science *193*, 969–981.

Gardiner, D.M. (2005). Ontogenetic decline of regenerative ability and the stimulation of human regeneration. Rejuvenation Res. *8*, 141–153.

Gardiner, D., and Bryant, S. (1989). Organization of positional information in the axolotl limb. J. Exp. Zool. *251*, 47–55.

Gardiner, D.M., and Holmes, L.B. (2012). Hypothesis: terminal transverse limb defects with “nubbins” represent a regenerative process during limb development in human fetuses. Birth Defects Res. A. Clin. Mol. Teratol. *94*, 129–133.

Gargioli, C., and Slack, J.M.W. (2004). Cell lineage tracing during Xenopus tail regeneration. Development *131*, 2669–2679.

Garza-Garcia, A., Harris, R., Esposito, D., Gates, P.B., and Driscoll, P.C. (2009). Solution structure and phylogenetics of Prod1, a member of the three-finger protein superfamily implicated in salamander limb regeneration. PLoS One *4*, e7123.

Ghosh, S., Roy, S., Séguin, C., Bryant, S. V, and Gardiner, D.M. (2008). Analysis of the expression and function of Wnt-5a and Wnt-5b in developing and regenerating axolotl (Ambystoma mexicanum) limbs. Dev. Growth Differ. *50*, 289–297.

Gilbert, S.F. (2013). Developmental Biology (Sinauer Associates, Inc.).

Gilbert, T.W., Sellaro, T.L., and Badylak, S.F. (2006). Decellularization of tissues and organs. Biomaterials *27*, 3675–3683.

Glim, J.E., Everts, V., Niessen, F.B., Ulrich, M.M., and Beelen, R.H.J. (2014). Extracellular matrix components of oral mucosa differ from skin and resemble that of foetal skin. Arch. Oral Biol. *59*, 1048–1055.

Guimond, J.-C., Lévesque, M., Michaud, P.-L., Berdugo, J., Finnson, K., Philip, A., and Roy, S. (2010). BMP-2 functions independently of SHH signaling and triggers cell condensation and apoptosis in regenerating axolotl limbs. BMC Dev. Biol. *10*, 15.

Guimond, S., Maccarana, M., and Olwin, B.B. (1993). Activating and inhibitory heparin sequences for FGF-2 (basic FGF). Distinct requirements for FGF-1, FGF-2, and FGF-4. J. Biol. *268*, 23906–23914.

Habuchi, H., Habuchi, O., and Kimata, K. (2004). Sulfation pattern in glycosaminoglycan: does it have a code? Glycoconj. J. *21*, 47–52.

Häcker, U., Nybakken, K., and Perrimon, N. (2005). Heparan sulphate proteoglycans: the sweet side of development. Nat. Rev. Mol. Cell Biol. *6*, 530–541.

Han, M., An, J.Y., and Kim, W.S. (2001). Expression patterns of Fgf-8 during development and limb regeneration of the axolotl. Dev. Dyn. *220*, 40–48.

Han, M., Yang, X., Lee, J., Allan, C.H., and Muneoka, K. (2008). Development and regeneration of the neonatal digit tip in mice. Dev. Biol. *315*, 125–135.

Hata, S., Namae, M., and Nishina, H. (2007). Liver development and regeneration: from laboratory study to clinical therapy. Dev. Growth Differ. *49*, 163–170.

Hirata, A., Gardiner, D.M., and Satoh, A. (2010). Dermal fibroblasts contribute to multiple tissues in the accessory limb model. Dev. Growth Differ. *52*, 343–350.

Hirata, A., Makanae, A., and Satoh, A. (2013). Accessory limb induction on flank region and its muscle regulation in axolotl. Dev. Dyn. *242*, 932–940.

Holder, N., Tank, P.W., and Bryant, S. V. (1980). Regeneration of symmetrical forelimbs in the axolotl, Ambystoma mexicanum. Dev. Biol. *74*, 302–314.

Huynh, M.B., Morin, C., Carpentier, G., Garcia-Filipe, S., Talhas-Perret, S., Barbier-Chassefière, V., van Kuppevelt, T.H., Martelly, I., Albanese, P., and Papy-Garcia, D. (2012). Age-related changes in rat myocardium involve altered capacities of glycosaminoglycans to potentiate growth factor functions and heparan sulfate-altered sulfation. J. Biol. Chem. *287*, 11363–11373.

Illingworth, C.M. (1974). Trapped fingers and amputated finger tips in children. J. Pediatr. Surg. *9*, 853–858.

Ito, M., Yang, Z., Andl, T., Cui, C., Kim, N., Millar, S.E., and Cotsarelis, G. (2007). Wnt-dependent de novo hair follicle regeneration in adult mouse skin after wounding. Nature *447*, 316–320.

Le Jan, S., Hayashi, M., Kasza, Z., Eriksson, I., Bishop, J.R., Weibrecht, I., Heldin, J., Holmborn, K., Jakobsson, L., Söderberg, O., et al. (2012). Functional overlap between chondroitin and heparan sulfate proteoglycans during VEGF-induced sprouting angiogenesis. Arterioscler. Thromb. Vasc. Biol. *32*, 1255–1263.

Kamimura, K., Maeda, N., and Nakato, H. (2011). In vivo manipulation of heparan sulfate structure and its effect on Drosophila development. Glycobiology *21*, 607–618.

Kang, J., Nachtrab, G., and Poss, K.D. (2013). Local Dkk1 crosstalk from breeding ornaments impedes regeneration of injured male zebrafish fins. Dev. Cell *27*, 19–31.

Kato, K., Orii, H., Watanabe, K., and Agata, K. (2001). Dorsal and ventral positional cues required for the onset of planarian regeneration may reside in differentiated cells. Dev. Biol. *233*, 109–121.

Kato, M., Wang, H., Bernfield, M., Gallagher, J.T., and Turnbull, J.E. (1994). Cell surface syndecan-1 on distinct cell types differs in fine structure and ligand binding of its heparan sulfate chains. J. Biol. Chem. *269*, 18881–18890.

Kawakami, Y., Rodriguez Esteban, C., Raya, M., Kawakami, H., Martí, M., Dubova, I., and Izpisúa Belmonte, J.C. (2006). Wnt/beta-catenin signaling regulates vertebrate limb regeneration. Genes Dev. *20*, 3232–3237.

Kawamata, H., Tachibana, M., Fujimori, T., and Imai, Y. (2006). Differentiation-inducing therapy for solid tumors. Curr. Pharm. Des. *12*, 379–385.

Kerszberg, M., and Wolpert, L. (2007). Specifying positional information in the embryo: looking beyond morphogens. Cell *130*, 205–209.

Kim, W.S., and Stocum, D.L. (1986). Retinoic acid modifies positional memory in the anteroposterior axis of regenerating axolotl limbs. Dev. Biol. *114*, 170–179.

Kim, H., Son, D., Choi, T.H., Jung, S., Kwon, S., Kim, J., and Han, K. (2013). Evaluation of an amniotic membrane-collagen dermal substitute in the management of full-thickness skin defects in a pig. Arch. Plast. Surg. *40*, 11–18.

Kligman, A.M., and Strauss, J.S. (1956). The formation of vellus hair follicles from human adult epidermis. J. Invest. Dermatol. *27*, 19–23.

Kobayashi, T., Habuchi, H., Nogami, K., Ashikari-Hada, S., Tamura, K., Ide, H., and Kimata, K. (2010). Functional analysis of chick heparan sulfate 6-O-sulfotransferases in limb bud development. Dev. Growth Differ. *52*, 146–156.

Kragl, M., Knapp, D., Nacu, E., Khattak, S., Maden, M., Epperlein, H.H., and Tanaka, E.M. (2009). Cells keep a memory of their tissue origin during axolotl limb regeneration. Nature *460*, 60–65.

Kramer, K.L., and Yost, H.J. (2002). Ectodermal Syndecan-2 Mediates Left-Right Axis Formation in Migrating Mesoderm as a Cell-Nonautonomous Vg1 Cofactor. Dev. Cell *2*, 115–124.

Kumar, A., Godwin, J.W., Gates, P.B., Garza-Garcia, A.A., and Brockes, J.P. (2007a). Molecular basis for the nerve dependence of limb regeneration in an adult vertebrate. Science *318*, 772–777.

Kumar, A., Gates, P.B., and Brockes, J.P. (2007b). Positional identity of adult stem cells in salamander limb regeneration. C. R. Biol. *330*, 485–490.

Kumar, A., Delgado, J.-P., Gates, P.B., Neville, G., Forge, A., and Brockes, J.P. (2011). The aneurogenic limb identifies developmental cell interactions underlying vertebrate limb regeneration. Proc. Natl. Acad. Sci. U. S. A. *108*, 13588–13593.

Laurencin, C.T., and Khan, Y. (2013). Regenerative Engineering (CRC Press).

Lawrence, R., Olson, S.K., Steele, R.E., Wang, L., Warrior, R., Cummings, R.D., and Esko, J.D. (2008). Evolutionary differences in glycosaminoglycan fine structure detected by quantitative glycan reductive isotope labeling. J. Biol. Chem. *283*, 33674–33684.

Lee, J., and Gardiner, D.M. (2012). Regeneration of limb joints in the axolotl (Ambystoma mexicanum). PLoS One *7*, e50615.

Leszczyniecka, M., Roberts, T., Dent, P., Grant, S., and Fisher, P.B. (2001). Differentiation therapy of human cancer: basic science and clinical applications. Pharmacol. Ther. *90*, 105–156.

Lévesque, M., Gatien, S., Finnson, K., Desmeules, S., Villiard, E., Pilote, M., Philip, A., and Roy, S. (2007). Transforming growth factor: beta signaling is essential for limb regeneration in axolotls. PLoS One *2*, e1227.

Levin, M. (2012). Morphogenetic fields in embryogenesis, regeneration, and cancer: non-local control of complex patterning. Biosystems. *109*, 243–261.

Levin, M. (2014). Endogenous bioelectrical networks store non-genetic patterning information during development and regeneration. J. Physiol. *592*, 2295–2305.

Lewandoski, M., Sun, X., and Martin, G.R. (2000). Fgf8 signalling from the AER is essential for normal limb development. Nat. Genet. *26*, 460–463.

Lheureux, E. (1977). [Importance of limb tissue associations in the development of nerve-induced supernumerary limbs in the newt Pleurodeles waltlii Michah (author's transl)]. J. Embryol. Exp. Morphol. *38*, 151–173.

Lin, X. (2004). Functions of heparan sulfate proteoglycans in cell signaling during development. Development *131*, 6009–6021.

Looso, M., Michel, C.S., Konzer, A., Bruckskotten, M., Borchardt, T., Krüger, M., and Braun, T. (2012). Spiked-in pulsed in vivo labeling identifies a new member of the CCN family in regenerating newt hearts. J. Proteome Res. *11*, 4693–4704.

Ludolph, D.C., Cameron, J.A., and Stocum, D.L. (1990). The effect of retinoic acid on positional memory in the dorsoventral axis of regenerating axolotl limbs. Dev. Biol. *140*, 41–52.

Maden, M. (1982). Vitamin A and pattern formation in the regenerating limb. Nature *295*, 672–675.

Maden, M., and Mustafa, K. (1982). Axial organization of the regenerating limb: asymmetrical behaviour following skin transplantation. J. Embryol. Exp. Morphol. *70*, 197–213.

Mak, K., Manji, A., Gallant-Behm, C., Wiebe, C., Hart, D.A., Larjava, H., and Häkkinen, L. (2009). Scarless healing of oral mucosa is characterized by faster resolution of inflammation and control of myofibroblast action compared to skin wounds in the red Duroc pig model. J. Dermatol. Sci. *56*, 168–180.

Makanae, A., Hirata, A., Honjo, Y., Mitogawa, K., and Satoh, A. (2013). Nerve independent limb induction in axolotls. Dev. Biol. *381*, 213–226.

Makarenkova, H.P., Hoffman, M.P., Beenken, A., Eliseenkova, A. V, Meech, R., Tsau, C., Patel, V.N., Lang, R.A., and Mohammadi, M. (2009). Differential interactions of FGFs with heparan sulfate control gradient formation and branching morphogenesis. Sci. Signal. *2*, ra55.

Mariani, F. V (2010). Proximal to distal patterning during limb development and regeneration: a review of converging disciplines. Regen. Med. *5*, 451–462.

Mariani, F. V, Ahn, C.P., and Martin, G.R. (2008). Genetic evidence that FGFs have an instructive role in limb proximal-distal patterning. Nature *453*, 401–405.

Martin, G.R. (1998). The roles of FGFs in the early development of vertebrate limbs. Genes Dev. *12*, 1571–1586.

Martin, P., and Leibovich, S.J. (2005). Inflammatory cells during wound repair: the good, the bad and the ugly. Trends Cell Biol. *15*, 599–607.

Martino, M.M., Briquez, P.S., Güç, E., Tortelli, F., Kilarski, W.W., Metzger, S., Rice, J.J., Kuhn, G. a, Müller, R., Swartz, M. a, et al. (2014). Growth factors engineered for super-affinity to the extracellular matrix enhance tissue healing. Science (80-.). *343*, 885–888.

Matsumoto, Y., Matsumoto, K., Irie, F., Fukushi, J., Stallcup, W.B., and Yamaguchi, Y. (2010). Conditional ablation of the heparan sulfate-synthesizing enzyme Ext1 leads to dysregulation of bone morphogenic protein signaling and severe skeletal defects. J. Biol. Chem. *285*, 19227–19234.

McCusker, C.D., and Gardiner, D.M. (2013). Positional information is reprogrammed in blastema cells of the regenerating limb of the axolotl (Ambystoma mexicanum). PLoS One *8*, e77064.

McCusker, C.D., and Gardiner, D.M. (2014). Understanding positional cues in salamander limb regeneration: implications for optimizing cell-based regenerative therapies. Dis. Model. Mech. *7*, 593–599.

McCusker, C., Lehrberg, J., and Gardiner, D. (2014). Position-specific induction of ectopic limbs in non-regenerating blastemas on axolotl forelimbs. Regeneration *1*, 27–34.

Melrose, J., Isaacs, M.D., Smith, S.M., Hughes, C.E., Little, C.B., Caterson, B., and Hayes, A.J. (2012). Chondroitin sulphate and heparan sulphate sulphation motifs and their proteoglycans are involved in articular cartilage formation during human foetal knee joint development. Histochem. Cell Biol. *138*, 461–475.

Menger, B., Vogt, P.M., Kuhbier, J.W., and Reimers, K. (2010). Applying amphibian limb regeneration to human wound healing: a review. Ann. Plast. Surg. *65*, 504–510.

Mescher, A.L. (1976). Effects on adult newt limb regeneration of partial and complete skin flaps over the amputation surface. J. Exp. Zool. *195*, 117–128.

Mescher, A.L., and Neff, A.W. (2006). Limb regeneration in amphibians: immunological considerations. ScientificWorldJournal. *6 Suppl 1*, 1–11.

Mitogawa, K., Hirata, A., Moriyasu, M., Makanae, A., Miura, S., Endo, T., and Satoh, A. (2014). Ectopic blastema induction by nerve deviation and skin wounding: a new regeneration model in Xenopus laevis. Regeneration *1*, 26–36.

Monaghan, J.R., and Maden, M. (2013). Cellular plasticity during vertebrate appendage regeneration. Curr. Top. Microbiol. Immunol. *367*, 53–74.

Morgan, T.H. (1901). Regeneration (London: Macmillan & Co, Ltd.).

Mullen, L.M., Bryant, S. V, Torok, M. a, Blumberg, B., and Gardiner, D.M. (1996). Nerve dependency of regeneration: the role of Distal-less and FGF signaling in amphibian limb regeneration. Development *122*, 3487–3497.

Muneoka, K., Holler-Dinsmore, G., and Bryant, S. V (1986). Intrinsic control of regenerative loss in Xenopus laevis limbs. J. Exp. Zool. *240*, 47–54.

Muneoka, K., Allan, C.H., Yang, X., Lee, J., and Han, M. (2008a). Mammalian regeneration and regenerative medicine. Birth Defects Res. C. Embryo Today *84*, 265–280.

Muneoka, K., Han, M., and Gardiner, D.M. (2008b). Regrowing human limbs. Sci. Am. *298*, 56–63.

Murali, S., Rai, B., Dombrowski, C., Lee, J.L.J., Lim, Z.X.H., Bramono, D.S., Ling, L., Bell, T., Hinkley, S., Nathan, S.S., et al. (2013). Affinity-selected heparan sulfate for bone repair. Biomaterials *34*, 5594–5605.

Murawala, P., Tanaka, E.M., and Currie, J.D. (2012). Regeneration: the ultimate example of wound healing. Semin. Cell Dev. Biol. *23*, 954–962.

Nachtrab, G., Czerwinski, M., and Poss, K.D. (2011). Sexually dimorphic fin regeneration in zebrafish controlled by androgen/GSK3 signaling. Curr. Biol. *21*, 1912–1917.

Nacu, E., Glausch, M., Le, H.Q., Damanik, F.F.R., Schuez, M., Knapp, D., Khattak, S., Richter, T., and Tanaka, E.M. (2013). Connective tissue cells, but not muscle cells, are involved in establishing the proximo-distal outcome of limb regeneration in the axolotl. Development *140*, 513–518.

Nakamura, T., Mito, T., Tanaka, Y., Bando, T., Ohuchi, H., and Noji, S. (2007). Involvement of canonical Wnt/Wingless signaling in the determination of the positional values within the leg segment of the cricket Gryllus bimaculatus. Dev. Growth Differ. *49*, 79–88.

Nizet, V., and Esko, J.D. (2009). Bacterial and Viral Infections. In Essentials of Glycobiology: 2nd Edition, A. Varki, R.D. Cummings, and J.D. Esko, eds. (New York: Cold Spring Harbor Laboratory Press),.

Nogami, K., Suzuki, H., Habuchi, H., Ishiguro, N., Iwata, H., and Kimata, K. (2004). Distinctive expression patterns of heparan sulfate O-sulfotransferases and regional differences in heparan sulfate structure in chick limb buds. J. Biol. Chem. *279*, 8219–8229.

Nurcombe, V., Ford, M.D., Wildschut, J.A., and Bartlett, P.F. (1993). Developmental regulation of neural response to FGF-1 and FGF-2 by heparan sulfate proteoglycan. Science (80-.). *259*, 103–106.

Ohuchi, H., Nakagawa, T., Yamamoto, A., Araga, A., Ohata, T., Ishimaru, Y., Yoshioka, H., Kuwana, T., Nohno, T., Yamasaki, M., et al. (1997). The mesenchymal factor, FGF10, initiates and maintains the outgrowth of the chick limb bud through interaction with FGF8, an apical ectodermal factor. Development *124*, 2235–2244.

Ojeh, N., Hiilesvuo, K., Wärri, A., Salmivirta, M., Henttinen, T., and Määttä, A. (2008). Ectopic expression of syndecan-1 in basal epidermis affects keratinocyte proliferation and wound re-epithelialization. J. Invest. Dermatol. *128*, 26–34.

Okolicsanyi, R.K., Griffiths, L.R., and Haupt, L.M. (2014). Mesenchymal stem cells, neural lineage potential, heparan sulfate proteoglycans and the matrix. Dev. Biol. *388*, 1–10.

Olwin, B.B., and Rapraeger, A. (1992). Repression of myogenic differentiation by aFGF, bFGF, and K-FGF is dependent on cellular heparan sulfate. J. Cell Biol. *118*, 631–639.

Paine-Saunders, S., Viviano, B.L., Economides, A.N., and Saunders, S. (2002). Heparan sulfate proteoglycans retain Noggin at the cell surface: a potential mechanism for shaping bone morphogenetic protein gradients. J. Biol. Chem. *277*, 2089–2096.

Peadon, A.M., and Singer, M. (1965). A quantitative study of forelimb innervation in relation to regenerative capacity in the larval, land stage, and adult forms of Triturus viridescens. J. Exp. Zool. *159*, 337–345.

Pecorino, L.T., Entwistle, A., and Brockes, J.P. (1996). Activation of a single retinoic acid receptor isoform mediates proximodistal respecification. Curr. Biol. *6*, 563–569.

Penc, S.F., Pomahac, B., Winkler, T., Dorschner, R.A., Eriksson, E., Herndon, M., and Gallo, R.L. (1998). Dermatan Sulfate Released after Injury Is a Potent Promoter of Fibroblast Growth Factor-2 Function. J. Biol. Chem. *273*, 28116–28121.

Poulin, M.L., and Chiu, I.M. (1995). Re-programming of expression of the KGFR and bek variants of fibroblast growth factor receptor 2 during limb regeneration in newts (Notophthalmus viridescens). Dev. Dyn. *202*, 378–387.

Poulin, M.L., Patrie, K.M., Botelho, M.J., Tassava, R. a, and Chiu, I.M. (1993). Heterogeneity in the expression of fibroblast growth factor receptors during limb regeneration in newts (Notophthalmus viridescens). Development *119*, 353–361.

Rai, B., Nurcombe, V., and Cool, S.M. (2011). Heparan sulfate-based treatments for regenerative medicine. Crit. Rev. Eukaryot. Gene Expr. *21*, 1–12.

Rajnoch, C., Ferguson, S., Metcalfe, A.D., Herrick, S.E., Willis, H.S., and Ferguson, M.W.J. (2003). Regeneration of the ear after wounding in different mouse strains is dependent on the severity of wound trauma. Dev. Dyn. *226*, 388–397.

Raman, R., Venkataraman, G., Ernst, S., Sasisekharan, V., and Sasisekharan, R. (2003). Structural specificity of heparin binding in the fibroblast growth factor family of proteins. Proc. Natl. Acad. Sci. U. S. A. *100*, 2357–2362.

Ramsbottom, S.A., Maguire, R.J., Fellgett, S.W., and Pownall, M.E. (2014). Sulf1 influences the Shh morphogen gradient during the dorsal ventral patterning of the neural tube in Xenopus tropicalis. Dev. Biol. *391*, 207–218.

Rapraeger, A., Krufka, A., and Olwin, B.B. (1991). Requirement of heparan sulfate for bFGF-mediated fibroblast growth and myoblast differentiation. Science (80-.). *252*, 1705–1708.

Reginelli, A.D., Wang, Y.Q., Sassoon, D., and Muneoka, K. (1995). Digit tip regeneration correlates with regions of Msx1 (Hox 7) expression in fetal and newborn mice. Development *121*, 1065–1076.

Reynolds, S., Holder, N., and Fernandes, M. (1983). The form and structure of supernumerary hindlimbs formed following skin grafting and nerve deviation in the newt Triturus cristatus. J. Embryol. Exp. Morphol. *77*, 221–241.

Rinkevich, Y., Lindau, P., Ueno, H., Longaker, M.T., and Weissman, I.L. (2011). Germ-layer and lineage-restricted stem/progenitors regenerate the mouse digit tip. Nature *476*, 409–413.

Rinn, J.L., Bondre, C., Gladstone, H.B., Brown, P.O., and Chang, H.Y. (2006). Anatomic demarcation by positional variation in fibroblast gene expression programs. PLoS Genet. *2*, e119.

Rinn, J.L., Wang, J.K., Liu, H., Montgomery, K., van de Rijn, M., and Chang, H.Y. (2008). A systems biology approach to anatomic diversity of skin. J. Invest. Dermatol. *128*, 776–782.

Roensch, K., Tazaki, A., Chara, O., and Tanaka, E.M. (2013). Progressive specification rather than intercalation of segments during limb regeneration. Science (80-.). *342*, 1375–1379.

Rollman-Dinsmore, C., and Bryant, S. V. (1984). The distribution of marked dermal cells from small localized implants in limb regenerates. Dev. Biol. *106*, 275–281.

Romero, R., and Bueno, D. (2001). Disto-proximal regional determination and intercalary regeneration in planarians, revealed by retinoic acid induced disruption of regeneration. Int. J. Dev. Biol. *45*, 669–673.

Rudd, T.R., Uniewicz, K.A., Ori, A., Guimond, S.E., Skidmore, M.A., Gaudesi, D., Xu, R., Turnbull, J.E., Guerrini, M., Torri, G., et al. (2010). Comparable stabilisation, structural changes and activities can be induced in FGF by a variety of HS and non-GAG analogues: implications for sequence-activity relationships. Org. Biomol. Chem. *8*, 5390–5397.

Salehi, Z. (2009). In vivo injection of fibroblast growth factor-2 into the cisterna magna induces glypican-6 expression in mouse brain tissue. J. Clin. Neurosci. *16*, 689–692.

Salley, J.D., and Tassava, R.A. (1981). Responses of denervated adult newt limb stumps to reinnervation and reinjury. J. Exp. Zool. *215*, 183–189.

Sandoval-Guzmán, T., Wang, H., Khattak, S., Schuez, M., Roensch, K., Nacu, E., Tazaki, A., Joven, A., Tanaka, E.M., and Simon, A. (2014). Fundamental differences in dedifferentiation and stem cell recruitment during skeletal muscle regeneration in two salamander species. Cell Stem Cell *14*, 174–187.

Sarrazin, S., Lamanna, W.C., and Esko, J.D. (2011). Heparan sulfate proteoglycans. Cold Spring Harb. Perspect. Biol. *3*.

Satoh, A., Gardiner, D.M., Bryant, S. V, and Endo, T. (2007). Nerve-induced ectopic limb blastemas in the Axolotl are equivalent to amputation-induced blastemas. Dev. Biol. *312*, 231–244.

Satoh, A., Bryant, S. V, and Gardiner, D.M. (2008a). Regulation of dermal fibroblast dedifferentiation and redifferentiation during wound healing and limb regeneration in the Axolotl. Dev. Growth Differ. *50*, 743–754.

Satoh, A., Graham, G.M.C., Bryant, S. V, and Gardiner, D.M. (2008b). Neurotrophic regulation of epidermal dedifferentiation during wound healing and limb regeneration in the axolotl (Ambystoma mexicanum). Dev. Biol. *319*, 321–335.

Satoh, A., Cummings, G.M.C., Bryant, S. V, and Gardiner, D.M. (2010a). Regulation of proximal-distal intercalation during limb regeneration in the axolotl (Ambystoma mexicanum). Dev. Growth Differ. *52*, 785–798.

Satoh, A., Cummings, G.M.C., Bryant, S. V, and Gardiner, D.M. (2010b). Neurotrophic regulation of fibroblast dedifferentiation during limb skeletal regeneration in the axolotl (Ambystoma mexicanum). Dev. Biol. *337*, 444–457.

Satoh, A., Makanae, A., Hirata, A., and Satou, Y. (2011). Blastema induction in aneurogenic state and Prrx-1 regulation by MMPs and FGFs in Ambystoma mexicanum limb regeneration. Dev. Biol. *355*, 263–274.

Schaller, S., and Muneoka, K. (2001). Inhibition of polarizing activity in the anterior limb bud is regulated by extracellular factors. Dev. Biol. *240*, 443–456.

Seifert, A.W., Kiama, S.G., Seifert, M.G., Goheen, J.R., Palmer, T.M., Maden, M., Monaghan, J.R., and Voss, S.R. (2012a). Skin regeneration in adult axolotls: a blueprint for scar-free healing in vertebrates. PLoS One *7*, e32875.

Seifert, A.W., Kiama, S.G., Seifert, M.G., Goheen, J.R., Palmer, T.M., and Maden, M. (2012b). Skin shedding and tissue regeneration in African spiny mice (Acomys). Nature *489*, 561–565.

Sell, S. (2006). Cancer stem cells and differentiation therapy. Tumour Biol. *27*, 59–70.

Sessions, S.K., and Bryant, S. V (1988). Evidence that regenerative ability is an intrinsic property of limb cells in Xenopus. J. Exp. Zool. *247*, 39–44.

Shimokawa, T., Yasutaka, S., Kominami, R., and Shinohara, H. (2012). Wound epithelium function in axolotl limb regeneration. Okajimas Folia Anat. Jpn. *89*, 75–81.

Da Silva, S.M., Gates, P.B., and Brockes, J.P. (2002). The newt ortholog of CD59 is implicated in proximodistal identity during amphibian limb regeneration. Dev. Cell *3*, 547–555.

Singer, M. (1946). The nervous system and regeneration of the forelimb of adult Triturus; the influence of number of nerve fibers, including a quantitative study of limb innervation. J. Exp. Zool. *101*, 299–337.

Singer, M. (1947). The nervous system and regeneration of the forelimb of adult Triturus; a further study of the importance of nerve number, including quantitative measurements of limb innervation. J. Exp. Zool. *104*, 223–249.

Slack, M.J. (1980). Morphogenetic properties of the skin in axolotl limb regeneration. J. Embryol. Exp. Morphol. *58*, 265–288.

Slack, J.M.W., Beck, C.W., Gargioli, C., and Christen, B. (2004). Cellular and molecular mechanisms of regeneration in Xenopus. Philos. Trans. R. Soc. Lond. B. Biol. Sci. *359*, 745–751.

Soo Kim, B., Ji Kim, E., Suk Choi, J., Hoon Jeong, J., Hyunchul Jo, C., and Woo Cho, Y. (2013). Human collagen-based multilayer scaffolds for tendon-to-bone interface tissue engineering. J. Biomed. Mater. Res. A.

Stepp, M. a. (2002). Defects in keratinocyte activation during wound healing in the syndecan-1-deficient mouse. J. Cell Sci. *115*, 4517–4531.

Stewart, S., and Stankunas, K. (2012). Limited dedifferentiation provides replacement tissue during zebrafish fin regeneration. Dev. Biol. *365*, 339–349.

Stewart, R., Rascón, C.A., Tian, S., Nie, J., Barry, C., Chu, L.-F., Ardalani, H., Wagner, R.J., Probasco, M.D., Bolin, J.M., et al. (2013). Comparative RNA-seq analysis in the unsequenced axolotl: the oncogene burst highlights early gene expression in the blastema. PLoS Comput. Biol. *9*, e1002936.

Stramer, B.M., Mori, R., and Martin, P. (2007). The inflammation-fibrosis link? A Jekyll and Hyde role for blood cells during wound repair. J. Invest. Dermatol. *127*, 1009–1017.

Summerbell, D. (1974). A quantitative analysis of the effect of excision of the AER from the chick limb-bud. J. Embryol. Exp. Morphol. *32*, 651–660.

Sun, X., Mariani, F. V, and Martin, G.R. (2002). Functions of FGF signalling from the apical ectodermal ridge in limb development. Nature *418*, 501–508.

Suzuki, M., Yakushiji, N., Nakada, Y., Satoh, A., Ide, H., and Tamura, K. (2006). Limb regeneration in Xenopus laevis froglet. ScientificWorldJournal. *6 Suppl 1*, 26–37.

Tabata, Y., Hijikata, S., Muniruzzaman, M., and Ikada, Y. (1999). Neovascularization effect of biodegradable gelatin microspheres incorporating basic fibroblast growth factor. J. Biomater. Sci. Polym. Ed. *10*, 79–94.

Takeo, S., Akiyama, T., Firkus, C., Aigaki, T., and Nakato, H. (2005). Expression of a secreted form of Dally, a Drosophila glypican, induces overgrowth phenotype by affecting action range of Hedgehog. Dev. Biol. *284*, 204–218.

Tamura, K., Ohgo, S., and Yokoyama, H. (2010). Limb blastema cell: a stem cell for morphological regeneration. Dev. Growth Differ. *52*, 89–99.

Tank, P.W. (1978). The failure of double-half forelimbs to undergo distal transformation following amputation in the axolotl, Ambystoma mexicanum. J. Exp. Zool. *204*, 325–336.

Tank, P.W., and Holder, N. (1978). The effect of healing time on the proximodistal organization of double-half forelimb regenerates in the axolotl, Ambystoma mexicanum. Dev. Biol. *66*, 72–85.

Tassava, R.A., and Olsen-Winner, C.L. (2003). Responses to amputation of denervated ambystoma limbs containing aneurogenic limb grafts. J. Exp. Zool. A. Comp. Exp. Biol. *297*, 64–79.

Taylor, G.G., Anderson, R., Reginelli, A.A., and Muneoka, K. (1994). FGF2 Induces Regeneration of the Chick Limb Bud. Dev. Biol. *163*, 282–284.

Thacker, B.E., Xu, D., Lawrence, R., and Esko, J.D. (2013). Heparan sulfate 3-O-sulfation: A rare modification in search of a function. Matrix Biol. *35*, 60–72.

Thoms, S.D., and Stocum, D.L. (1984). Retinoic acid-induced pattern duplication in regenerating urodele limbs. Dev. Biol. *103*, 319–328.

Thornton, C.S. (1960). Influence of an eccentric epidermal cap on limb regeneration in Amblystoma larvae. Dev. Biol. *2*, 551–569.

Tong, M., Tuk, B., Hekking, I.M., Vermeij, M., Barritault, D., and van Neck, J.W. (2009). Stimulated neovascularization, inflammation resolution and collagen maturation in healing rat cutaneous wounds by a heparan sulfate glycosaminoglycan mimetic, OTR4120. Wound Repair Regen. *17*, 840–852.

Tong, M., Tuk, B., Shang, P., Hekking, I.M., Fijneman, E.M.G., Guijt, M., Hovius, S.E.R., and van Neck, J.W. (2012). Diabetes-impaired wound healing is improved by matrix therapy with heparan sulfate glycosaminoglycan mimetic OTR4120 in rats. Diabetes *61*, 2633–2641.

Varki, A., Kannagi, R., and Toole, B.P. (2009). Glycosylation Changes in Cancer. In Essentials of Glycobiology: 2nd Edition, A. Varki, R.D. Cummings, and J.D. Esko, eds. (New York: Cold Spring Harbor Laboratory Press),.

Wallace, H. (1981). VERTEBRATE LIMB REGENERATION (Chichester: John Wiley & Sons Limited).

Wanek, N., Gardiner, D.M., Muneoka, K., and Bryant, S. V (1991). Conversion by retinoic acid of anterior cells into ZPA cells in the chick wing bud. Nature *350*, 81–83.

Wang, P.-Y., Chang, W.-L., and Pai, L.-M. Smiling Gurken gradient: An expansion of the Gurken gradient. Fly (Austin). *2*, 118–120.

Westerman, R.A., Carr, R.W., Delaney, C.A., Morris, M.J., and Roberts, R.G. (1993). The role of skin nociceptive afferent nerves in blister healing. Clin. Exp. Neurol. *30*, 39–60.

Wigmore, P., and Holder, N. (1985). Regeneration from isolated half limbs in the upper arm of the axolotl. J. Embryol. Exp. Morphol. *89*, 333–347.

Wilgus, T.A. (2008). Immune cells in the healing skin wound: influential players at each stage of repair. Pharmacol. Res. *58*, 112–116.

Wolpert, L. (1969). Positional information and the spatial pattern of cellular differentiation. J. Theor. Biol. *25*, 1–47.

Wolpert, L. (2011). Positional information and patterning revisited. J. Theor. Biol. *269*, 359–365.

Wong, J.W., Gallant-Behm, C., Wiebe, C., Mak, K., Hart, D.A., Larjava, H., and Häkkinen, L. (2009). Wound healing in oral mucosa results in reduced scar formation as compared with skin: evidence from the red Duroc pig model and humans. Wound Repair Regen. *17*, 717–729.

Xu, X., Weinstein, M., Li, C., Naski, M., Cohen, R.I., Ornitz, D.M., Leder, P., and Deng, C. (1998). Fibroblast growth factor receptor 2 (FGFR2)-mediated reciprocal regulation

loop between FGF8 and FGF10 is essential for limb induction. Development *125*, 753–765.

Yan, D., and Lin, X. (2009). Shaping morphogen gradients by proteoglycans. Cold Spring Harb. Perspect. Biol. *1*, a002493.

Yayon, A., Klagsbrun, M., Esko, J.D., Leder, P., and Ornitz, D.M. (1991). Cell surface, heparin-like molecules are required for binding of basic fibroblast growth factor to its high affinity receptor. Cell *64*, 841–848.

Yokoyama, H., Yonei-Tamura, S., Endo, T., Izpisúa Belmonte, J.C., Tamura, K., and Ide, H. (2000). Mesenchyme with fgf-10 expression is responsible for regenerative capacity in Xenopus limb buds. Dev. Biol. *219*, 18–29.

Yokoyama, H., Ide, H., and Tamura, K. (2001). FGF-10 stimulates limb regeneration ability in Xenopus laevis. Dev. Biol. *233*, 72–79.

Yokoyama, H., Tamura, K., and Ide, H. (2002). Anteroposterior axis formation in Xenopus limb bud recombinants: a model of pattern formation during limb regeneration. Dev. Dyn. *225*, 277–288.

Yokoyama, H., Maruoka, T., Aruga, A., Amano, T., Ohgo, S., Shiroishi, T., and Tamura, K. (2011). Prx-1 expression in Xenopus laevis scarless skin-wound healing and its resemblance to epimorphic regeneration. J. Invest. Dermatol. *131*, 2477–2485.

Yu, L., Han, M., Yan, M., Lee, E.-C., Lee, J., and Muneoka, K. (2010). BMP signaling induces digit regeneration in neonatal mice. Development *137*, 551–559.

Yu, L., Han, M., Yan, M., Lee, J., and Muneoka, K. (2012). BMP2 induces segment-specific skeletal regeneration from digit and limb amputations by establishing a new endochondral ossification center. Dev. Biol. *372*, 263–273.

ABBREVIATIONS

A, Ant	Anterior
AEC	Apical Epithelial Cap
AER	Apical Ectodermal Ridge
ALM	Accessory Limb Model
BMP	Bone Morphogenetic Protein
cDNA	Complementary DNA (synthesized from mRNA)
D	Dorsal
ECM	Extracellular Matrix
EST	Expressed Sequence Tag
FGF	Fibroblast Growth Factor
GAG	Glycosaminoglycan
KGFR	Keratinocyte Growth Factor Receptor
HepIII	Heparitinase I, also known as Heparinase III or Heparin Lyase III
HS	Heparan Sulfate
iPS	Induced Pluripotent
ND	Nerve Deviation
PI	Positional Information
P, Post	Posterior
PN	Postnatal (day)
RT-PCR	Reverse Transcription Polymerase Chain Reaction
V	Ventral
ZPA	Zone of Polarizing Activity

APPENDIX

Appendix A: Disaccharide heparan sulfate glycosaminoglycan compositional analysis of anterior and posterior axolotl limb skin by LCQ-MS

Through a collaboration with Roger Lawrence in the Jeffrey Esko laboratory at the University of California, San Diego and Glycotechnology Core, I attempted to measure the qualitative differences in heparan sulfate glycosaminoglycan chains. The Esko laboratory has developed a method for analyzing disaccharide subunit structure and non-reducing end of all glycosaminoglycan chains based on stable isotope tagging with aniline coupled with liquid chromatography-mass spectrometry (LC-MS) (Lawrence et al., 2008). The technique however required grams of starting material collected from hundreds of animals. To maximize sample collection from each animal, anterior and posterior skin samples spanned large proximal/distal ranges and overlapped with dorsal and ventral. Even with grams of starting material, we were unable to obtain 3-O sulfation analysis. Because of all these factors, I believe we were unable to see discernable differences between anterior and posterior by LC-MS. Since the LC-MS technique did not seem viable at the time. I decided to use the dimethylmethylene blue dye-binding Blyscan Assay for sulfated glycosaminoglycans.

Quantitative heparan sulfate disaccharide analysis by LCQ-MS (Lawrence et al., 2008) was done in collaboration with Roger Lawrence in the laboratory of Jeffrey Esko at the University of California San Diego and the Glycotechnology Core Resource.

Samples are digested overnight with Pronase/ Protease at 37°C and centrifuged at 14000rpm for 20min. The supernatant is passed through a DEAE column and the bound glycosaminoglycans (GAG) is eluted with 2M NaCl. The GAG is then desalted on PD10 size exclusion column and purified GAG is lyophilized. GAGs are then dissolved in buffer and a mixture of Heparinase I, II and III is added and the polysaccharide is digested at 37°C for 18hours. Following digestion, the mixture is fractionated using a 10,000 MWCO filter to remove enzyme and undigested GAG chains. The supernatant is dried.1 pmol to 10 nmol of HS disaccharides is transferred to 1.5 ml microcentrifuge tubes and dried down in a centrifugal evaporator. 15 µl of 12C6 aniline or 13C6 aniline and 15 µl of 1 M $NaCNBH_3$ (Sigma-Aldrich) freshly prepared in dimethyl sulfoxide: acetic acid (7:3, v/v) are added to each sample. Reactions are carried out at 65°C for 4 hours or, alternatively, at 37°C for 16 hours, and then dried in a centrifugal evaporator. The dried samples are resuspended in running buffer and used for LCQ-MS analysis.

An LCQ classic quadrupole ion trap mass spectrometer equipped with an electrospray ionization source, and a quaternary high-performance liquid chromatography pump (Thermo-Finnigan, San Jose, CA) is used for disaccharide analyses. Aniline isotopic and non-isotopic disaccharides are separated on a C18 reversed-phase column (0.46 cm x 25 cm, Vydac) with the ion pairing agent dibutylamine (DBA, Sigma-Aldrich). The solvent gradient used for eluting the samples are: 100% buffer A (8mM acetic acid, 5mM DBA) for 10 minutes, 17% buffer B (70% methanol, 8 mM acetic acid, 5 mM DBA) for 15 minutes; 32% buffer B for 15 minutes, 40% buffer B for 15 minutes, 60% buffer B for 15 minutes; 100% buffer B for 10 minutes; and 100% buffer A for 10 minutes. The most highly substituted disaccharides elute at 60% buffer B (42% methanol). Ions of interest are monitored in negative ion

mode, and signal intensity is optimized for a representative species of disaccharide. To minimize in-source fragmentation of sulfated disaccharides, the capillary temperature and spray voltage are kept at 140 °C and 4.75 kV, respectively.

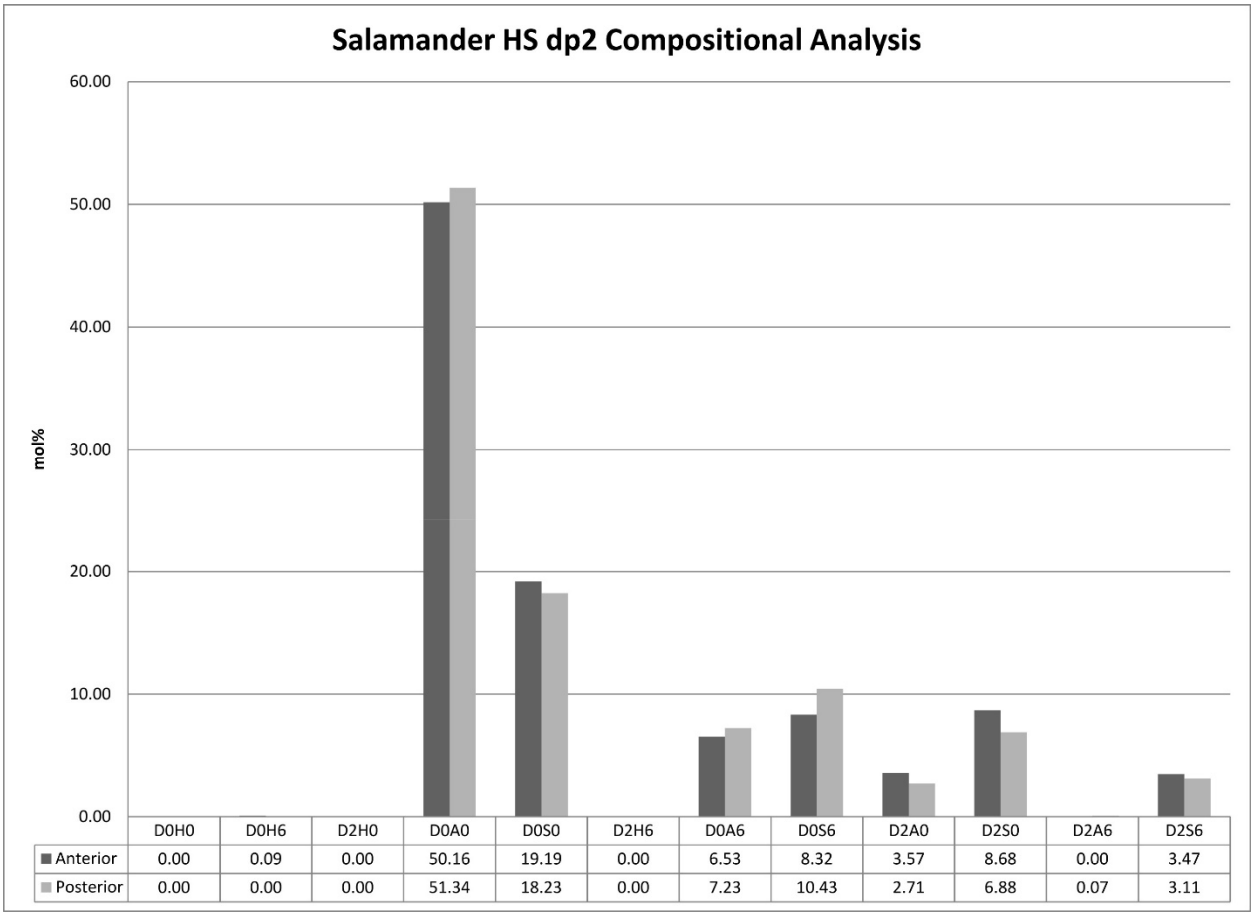

	D0H0	D0H6	D2H0	D0A0	D0S0	D2H6	D0A6	D0S6	D2A0	D2S0	D2A6	D2S6
Anterior	0.00	0.09	0.00	50.16	19.19	0.00	6.53	8.32	3.57	8.68	0.00	3.47
Posterior	0.00	0.00	0.00	51.34	18.23	0.00	7.23	10.43	2.71	6.88	0.07	3.11

Figure A. Disaccharide Heparan Sulfate GAG Compositional Analysis of N, 2-O and 6-O Sulfation in Anterior and Posterior Mature Axolotl Limb Skin. Y-axis = relative percentage, X-axis labels from left to right - D0A0: no sulfation, D0S0: N sulfation, D0A6: 6-O sulfation, D0S6: N and 6-O sulfation, D2A0: 2-O sulfation, D2S0: 2-O and N-sulfation, D2S6: 2-O, N and 6-O sulfation

Appendix B: Fat Inductive Mouse Wound ECM Grafts into Axolotl Wounds with Deviated Nerves Induces Dermal Glands and Disordered Nerve Overgrown

Large mouse skin wounds have the limited ability to regenerate hair follicles and fat. Since I found in Chapters 3 and 4 that axolotl regeneration-competent blastema cells can respond to specific differentiation signals to undergo osteogenesis rather than chondrogenesis, I hypothesized that ECM extracted from mouse wounds undergoing hair or fat induction may induce hair or fat in axolotl regenerative blastemas. Through a collaboration with Maksim Plikus and Raul Ramos, using the ALM, I grafted ECM from mouse wounds into axolotl wounds with deviated nerves (Figure B1).

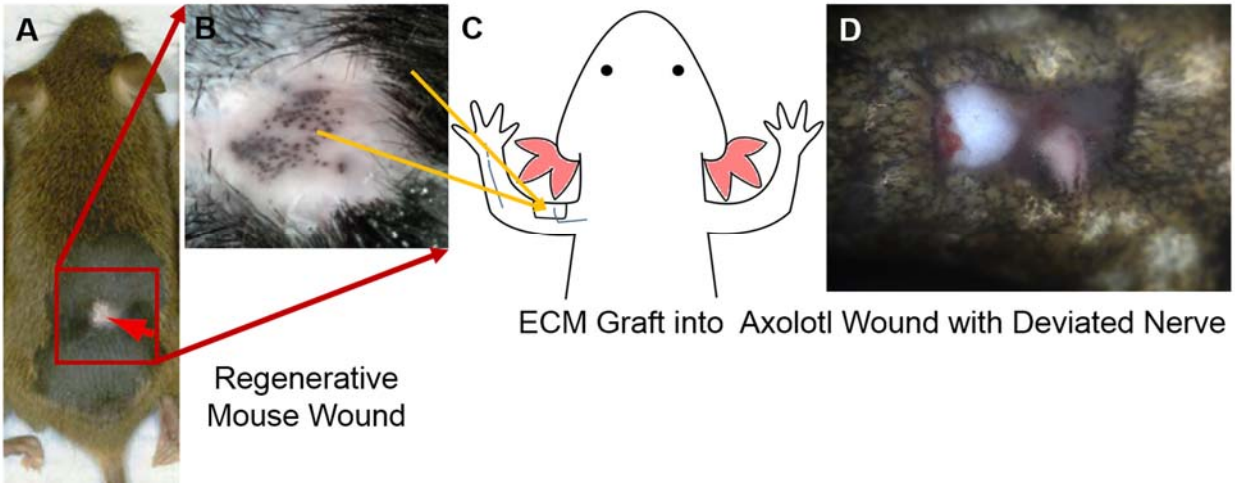

Figure B1. ECM from Mouse Wounds undergoing Hair or Fat Induction was Grafted into Sites of Nerve-Induced Axolotl Ectopic Regeneration. (A) Mouse with regenerative wound, (B) Mouse wound collected for ECM extraction and grafting into axolotl wound with deviated nerve (C) Both regenerative and nonregenerative wound areas were grafted. (D) Example of mouse wound ECM grafted into axolotl wound with deviated nerve.

ECM grafts from 21 day mouse wounds undergoing fat induction gave three interesting results: 1) Induction of increased dermal glands (Figure B2, B3), 2) Disordered nerve overgrowth (Figure B2, B4, B5), and 3) “Holes” that may adipocytes (Figure B2).

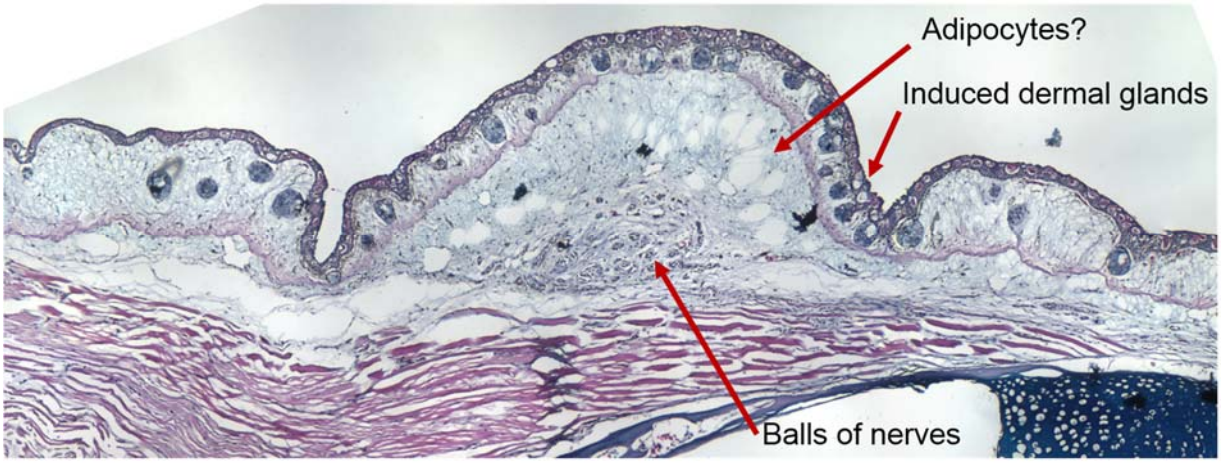

Figure B2. Fat Inductive Mouse Wound ECM Induces Dermal Glands and Nerve Overgrowth. Hemotoxylin, Eosin and Alcian Blue histological stain of section through regenerate from grafting fat inductive 21 day mouse wound ECM into axolotl wound with deviated nerve.

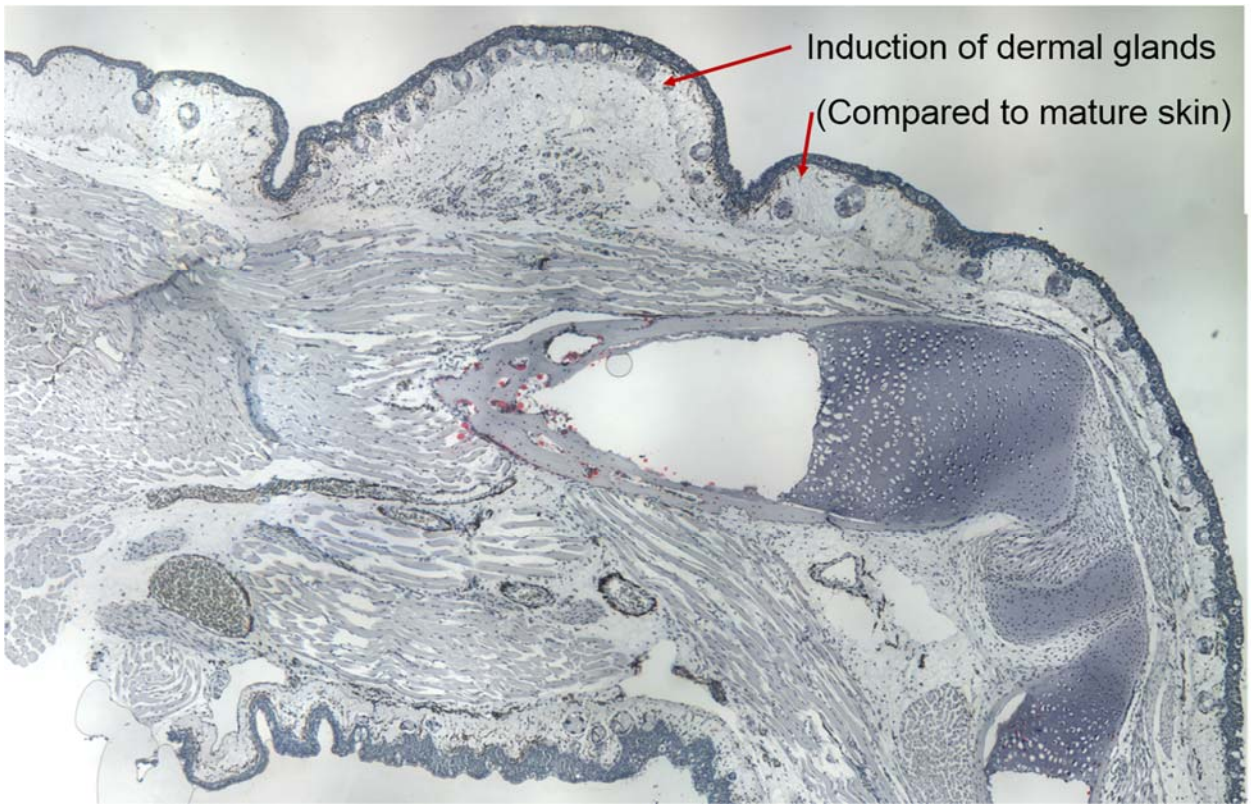

Figure B3. Fat Inductive Mouse Wound ECM Induces Dermal Glands.
Hemotoxylin and Oil Red O histological stain of section through regenerate from grafting fat inductive 21 day mouse wound ECM into axolotl wound with deviated nerve. Skin of regenerate has ~3x more dermal glands (blue circles) than normal skin.

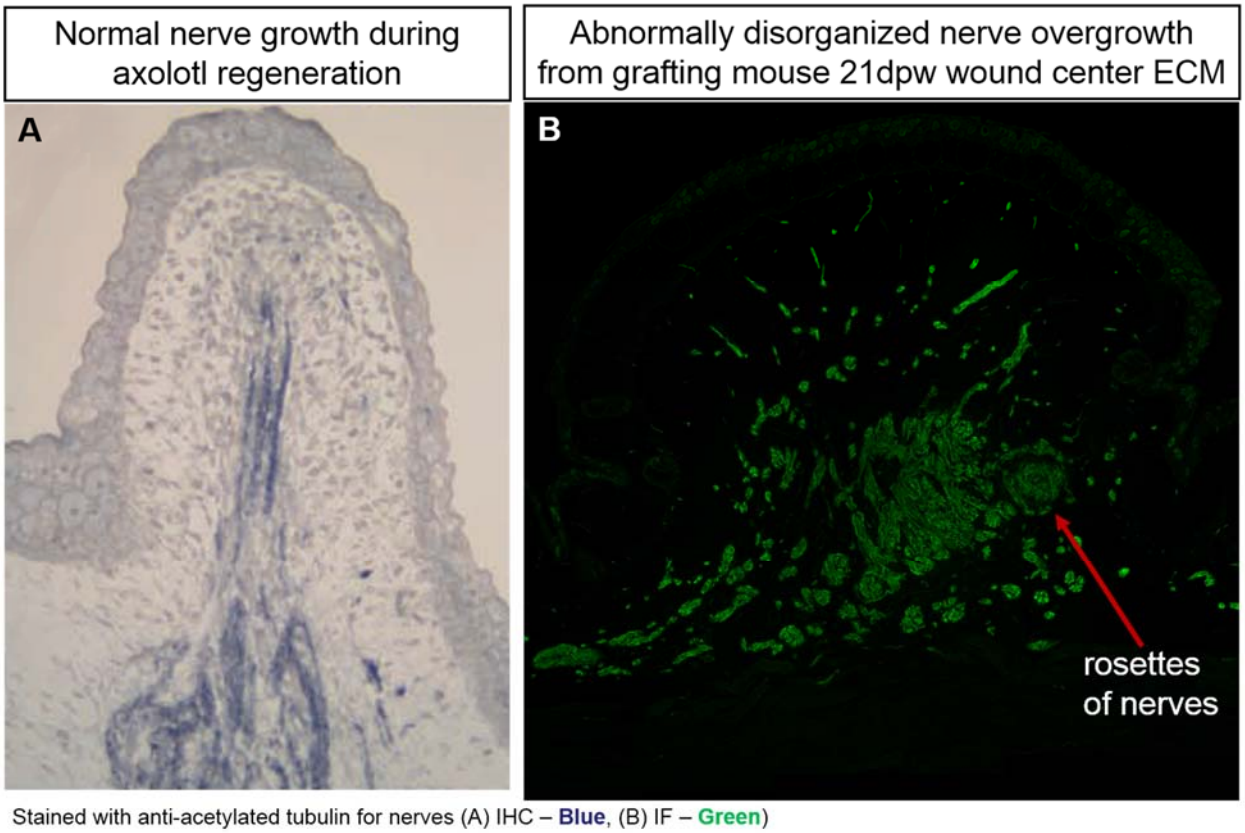

Figure B4. Fat Inductive Mouse Wound ECM Induces Disordered Nerve Overgrowth.
Nerve immunostaining of axolotl regenerations without mouse wound ECM graft (A) or with (B). Normal nerve growth is ordered and directional (proximal to distal). Mouse wound ECM grafts cause over growth and disorder. Nerves project back onto themselves forming rosettes.

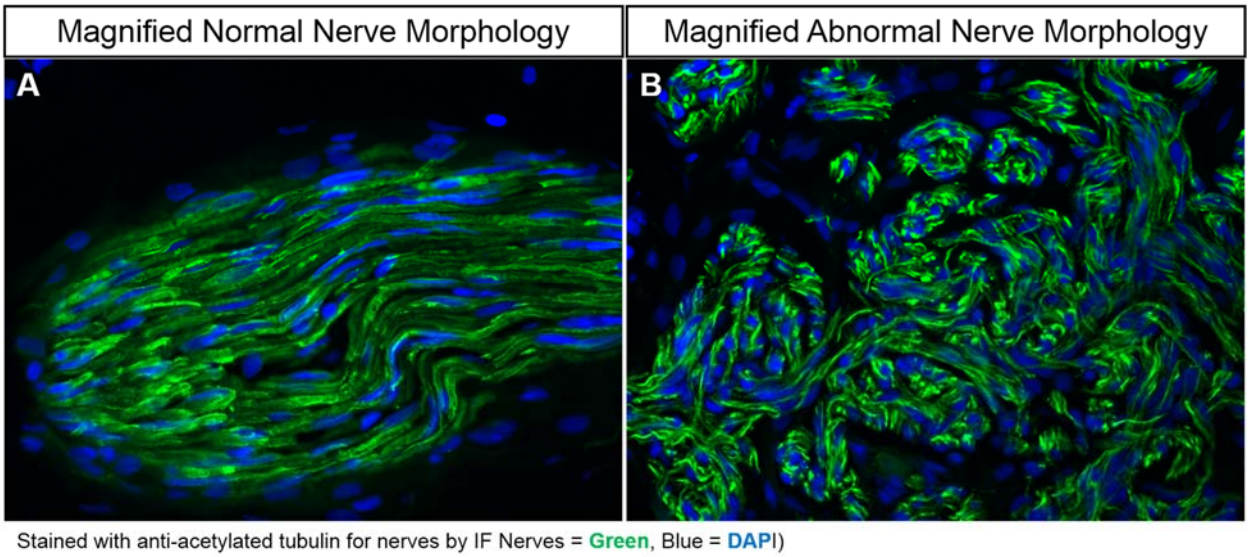

Figure B5. Fat Inductive Mouse Wound ECM Induces Disordered Nerve Overgrowth (Magnified).
Nerve immunostaining of normal axolotl nerves (A) mouse wound induced abnormal nerve overgrowth (B). Nerve over growth by mouse wound ECM does not have normal morphology, rather, the nerve fibers seem to project in random directions.

Appendix C: Axolotl Skin Grafts Contain Both Anterior/Posterior and Proximal/Distal Positional Information and Contribute to Their Original Location

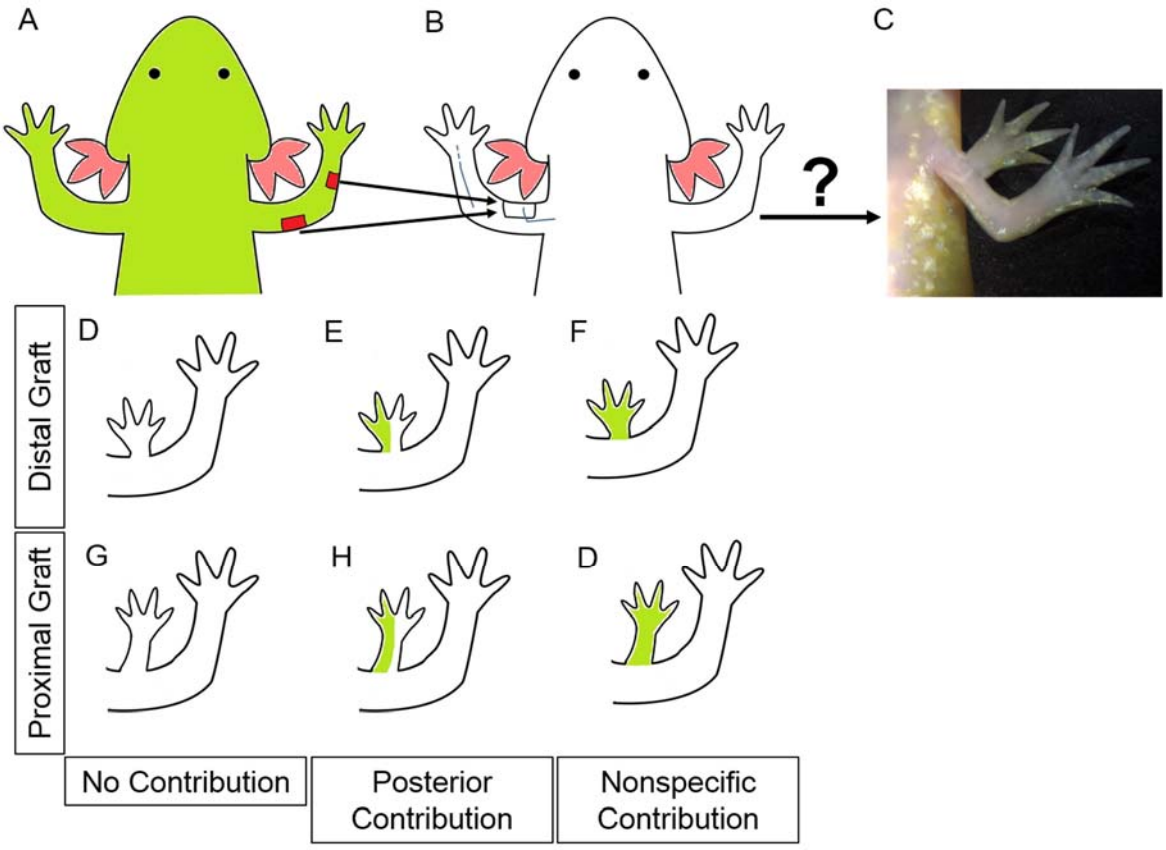

Figure C1. Schematic Diagram to Determine Proximal/Distal and Anterior/Posterior Contribution and Pattern Induction

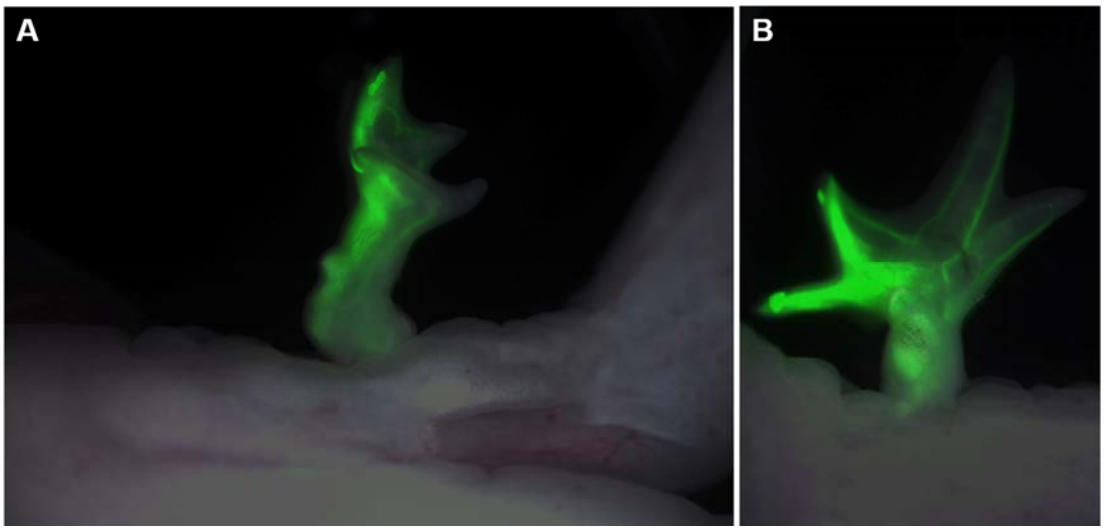

Figure C2. Axolotl Limb Skin Grafts have Proximal/Distal and Anterior/Posterior Positional Information to Determine Pattern Induction and Cell Contribution (B is alternate angle and magnification of A).

Appendix D: Heparitinase Injections Inhibit and Delay Axolotl Ectopic Blastema Formation

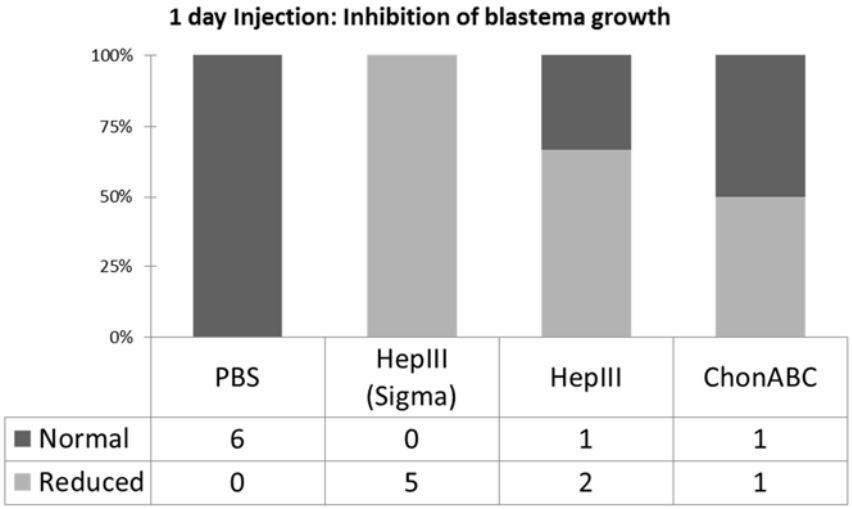

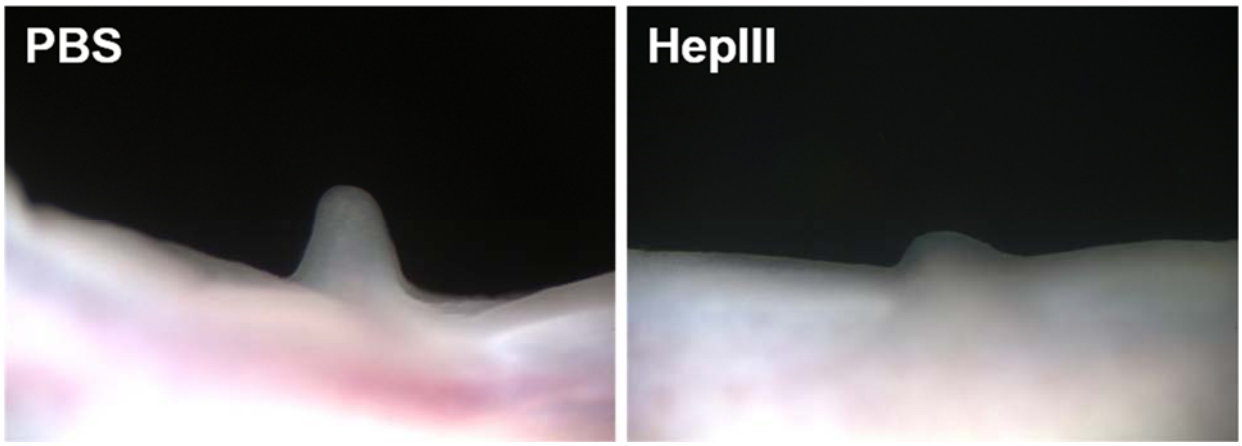

Figure D1. Injection of HepIII Inhibits and Delays Ectopic Blastema Formation in Axolotls